2017

Site Specific Sinkhole risk assessment in Central Florida using Cone Penetrometer Testing

Ryan Shamet
University of Central Florida

SITE SPECIFIC SINKHOLE RISK ASSESSMENT IN CENTRAL FLORIDA USING CONE PENETRATION TESTING

by

RYAN MICHAEL SHAMET

B.S. University of Central Florida, 2014

A thesis submitted in partial fulfillment of the requirements
for the degree of Master of Science
in the Department of Civil, Environmental, and Construction Engineering
in the College of Engineering and Computer Sciences
at the University of Central Florida
Orlando, FL

Spring Term
2017

ABSTRACT

As Florida's population is expanding and greater fluctuations in groundwater levels are being recorded, Central Florida has been experiencing a higher frequency of sinkhole occurrences than ever before in recorded history. Sinkholes in Central Florida are formed by a combination of bedrock weathering and overburden soil erosion due to the groundwater recharge and are a part of Florida's past and future geology. The initial stage of a sinkhole is referred to as soil raveling and is the most effective time to perform soil improvement measures, such as grouting, to mitigate further expansion of a subterranean void. Subsurface exploration tests, commonly implemented by geotechnical engineers for site characterization, have been shown to detect these sinkhole anomalies even when no signs of subsidence are evident on the ground surface. Secondary geophysical testing has also been proven to detect sinkhole raveling anomalies, but at the expense of additional time and money added to the specific project. In this study, current practices in detecting premature sinkholes were expanded upon with a primary focus on Cone Penetrometer testing data (CPT). Cone Penetrometer tests provide valuable high-resolution quantitative information regarding the discrete strength characteristics of relatively loose sandy and clayey subsoil. CPTs are also much quicker and cleaner to perform when compared to other subsurface testing procedures (e.g. Standard penetration tests). Therefore, CPTs were chosen for this study to understand how they can be implemented to assess risk of future sinkhole collapse, or other karst construction concerns, in Central Florida specific soils. By implementing the findings presented in this report, Geotechnical engineers and contractors in central Florida will be able to practically evaluate the size and severity of potential forming sinkhole without the use of additional

subsurface geophysical testing. The results of this study hope to eliminate extraneous testing costs, as well as maximize the efficiency of estimating mitigation products and procedures required all while still ensuring a safe design in Central Florida's highly karst areas.

To my fiancé and soon-to-be-wife “Cody”, my parents, brother, and friends. Thank you for your constant support and encouragement to continue doing what I love.

[23]Whatever you do, work heartily, as for the Lord and not for men, knowing that from the Lord you will receive the inheritance as your reward. You are serving the Lord Christ.

ACKNOWLEDGMENTS

I would like to express my sincerest appreciation and gratitude to my advisor and mentor, Dr. Boo Hyun Nam, for his patent guidance, continuous support, and countless cups of coffee discussion over these past several years while formulating and developing this study. I would also like to express special thanks to my committee members, Dr. Manoj Chopra and Dr. Ding-Bao Wang for their valuable time to review this paper.

I also want to expand a special thanks to the Florida Department of Transportation, State Materials Office and District 5, especially Dr. David Horhota, Ms Kathy Gray, Mr. Zachary Sullivan, and Mr. Kevin Hayden, for providing and supporting the Cone Penetrometer testing as well as for their valuable knowledge and insight of Central Florida sinkhole formation and detection.

Finally, I would like to thank the Department of Civil, Environmental and Construction Engineering for providing technical and financial support for this work.

TABLE OF CONTENTS

LIST OF FIGURES

LIST OF TABLES

LIST OF ABBREVIATIONS

CPT	-	Cone Penetration Test
FDOT	-	Florida Department of Transportation
FHWA	-	Federal Highway Administration
FSRI	-	Florida Sinkhole Research Institute
PCF	-	Pounds per cubic foot (lb/ft^3)
PSF	-	Pounds per square foot (lb/ft^2)
SBT	-	Soil Behavior Type
SPT	-	Standard Penetration Test
TSF	-	Tons per square foot (2000 lbs/ft^2)
USGS	-	United State Geological Survey

CHAPTER 1: INTRODUCTION

1.1 Problem Statement

Sinkholes risk assessment is no simple task and many times these events occur with only minutes of warning before the ground gives way. Central Florida sinkholes are a culmination of soil instability, geological formation and degradation, and hydrological extreme events and are more frequent in times following severe drought (Tihansky, 1999). Due to this combination of factors, exact sinkhole collapse processes are difficult to predict.

Subsurface exploration techniques such as standard penetration tests (SPTs) and cone penetrometer testing (CPTs) are commonly implemented in central Florida by geotechnical engineers for site characterization and to aid in foundation design for the structure or roadway design. These initial geotechnical tests have shown to be a viable way of predicting the initial formation of a sinkhole, called raveling. However, once these subsurface anomalies have been detected, secondary geophysical testing such as ground penetrating radar (GPR) and electro-resistivity mapping (ER) are commonly employed for further analysis of the potential risk of sinkhole formation at that specific site. Although these geophysical tests have been proven to detect subterranean voids (Bullock & Dillman, 2003), they have severe limitations in certain types of soils and loose resolution at deeper depths. Geophysical testing usually requires a specialized contractor and additional time for project completion which will add to the project costs and may not always be feasible for smaller scale projects.

With these disadvantages, there is an apparent need for further investigation of how the initial subsurface testing techniques (SPTs and CPTs) can be used to detect and assess potential sinkhole collapse risk for sites in central Florida. An in-depth study of testing data from actual

sinkhole sites was compared to sites suggesting sinkhole activity yet show no signs of subsidence on the ground surface. Also, through data processing, the severity of potential forming subterranean void can be estimated. Cone penetrometer testing was the primary method used to collect subsurface soil data in this study due to its high resolution of quantifiable data with depth. However, these data processing techniques can also be implemented for SPTs.

1.2 Research Objectives

The objectives of this research are to identify and establish trends in initial subsurface testing data which may suggest sinkhole formation. The results of this research can then be simplified through risk-charts, which can then help geotechnical engineers better understand the severity of potential sinkhole collapse on the specific site basis. By correlating these results to other sinkhole collapse factors, such as recharge rates or precipitation data, a more accurate assessment of sinkhole risk can then be performed. This research hopes to bridge the gap between the geomorphology study of sinkholes and the practicality of designing infrastructure in karst terrain, creating a better understanding of sinkhole risk from the geotechnical engineers' perspective.

1.3 Organization of Thesis

The chapters of this thesis are organized and described as follows:

- Chapter 1: Introduction - This chapter describes the project problem statement, description, methodology for conducting this project, and research scope. This chapter also presents a brief overview of Florida's geology and formation which is quintessential in understand the mechanism and formation of sinkholes found in central Florida.

- Chapter 2: Literature Review - This chapter reviews in greater detail the existing literature of karst terrain, Florida geology and hydrology, and classification of sinkhole types in central Florida. Also, reviewed in this chapter is the history and development Cone Penetrometer testing in geotechnical engineering. The current sinkhole mitigation techniques utilized by geotechnical engineer both before and after collapse
- Chapter 3: Methodology and discussion regarding the author's current research in identifying potential zones of sinkhole formation using Cone Penetration testing. Also discussed are methods on how to determine the severity of internal erosion (sinkhole formation).
- Chapter 4: Evaluation and assessment of sinkhole hazard using additional techniques formulated from the study presented in chapter 3. These additional techniques include point based, 2D profiling, and index comparison and contouring. A case study of sinkhole risk assessment using these tools is also performed for a specific project site in central Florida.
- Chapter 5: Summary and Conclusion – This chapter includes a summary of the project as well as discussion of limitations and plans for future research in this field.

CHAPTER 2: LITERATURE REVIEW

2.1 Karst Terrain

Geologically speaking, the Florida Peninsula is a relatively juvenile land mass. However, its formation process has consisted of many environmental changes contributing to its unique geology and consequent geotechnical engineering concerns. With each varying ice age, the landmass which we now call Florida has emerged and been submerged below the sea level. During times of submergence, shallow warm-water coral reefs form and die, depositing varying levels of calcium and magnesium carbonate on the sea floor. Meanwhile, ancient rivers rooted in the Appalachian Mountains, flow south and deposit alluvial sediment over the submerged Florida peninsula, creating deltas and salt marshes over.

As the sea level slowly recedes and the exposed Florida peninsula expands, varying sand deposits created from wave erosion start to accumulate over the carbonate deposits and alluvial sediment. Over time, the marine and river deposited matter, now with increased stresses from the sandy overburden, lithify to form carbonate-based sedimentary rock such as limestone, dolostone, and coquina. Repetition of this process, as the sea levels rise and fall, expose and conceal these layers of growing carbonate rock. In some areas, water traveling along the ground surface erodes the protective sandy overburden and river deposits (now consolidated into impermeable clay). The exposed carbonate rock experiences weathering both physically and chemically by the slightly acidic surface water. Cavities form within the soluble carbonate rock, and as the geological cycle repeats itself, water becomes trapped within the buried rock like a sponge. This process leads to the formation of what is known as Karst topography or terrain.

Although karst terrain can be found in many areas of the world (i.e the *Kraški rob*¸ a large limestone plateau located Slovenia in which the word "karst" is derived from), Florida's case of karst unique in fact that it creates the Floridan aquifer system (FAS). The fine-grained soil deposited by rivers and marine sediment, over time, compressed into a layer of silt and clay laying directly over the porous bedrock. This formation is known to geologists as the Hawthorne formation. Compared to the cavity ridden bedrock below it, the Hawthorne formation is widely considered 'impermeable' and it acts as an impedance for infiltrating groundwater. The result is a dual aquifer system: an unconfined, or surficial, aquifer of perched groundwater over the aquitard layer, and a confined aquifer located within the pores and cavities of the bedrock formations. The vertical travel of surface water through the surficial aquifer and impermeable layer filters the water allowing many Floridians to utilize the FAS as a reliable source of clean drinking water. Also, in areas where sections of the FAS is exposed near or at the ground surface, the crystal clear freshwater flows out of limestone fissures, forming springs. These springs not only create vast ecosystems which encourage sustainability of Florida's endangered species, but also they draw tourists in from all over the state/country, boosting the local economies.

2.2 Karst Features in Central Florida

Although there are great benefits resulting from karst geology, there are also many hazards. Arguably the most well-known geohazard resulting from karst geology are sinkholes. These concentrated instances of severe subsidence can wreak havoc on infrastructure supported on shallow foundations. As Florida's urban areas sprawl out to virgin karst terrain, sinkholes have been occurring more frequently and causing more damages than ever before (Florida Office of Insurance Regulation, 2010). Although sinkhole formation and mechanism has been thoroughly

studied by geologists and hydrologists (Tihansky, 1999) (Wilson & Beck, 1992), there is still a strong need for research in the field of sinkhole detection and risk assessment from a geotechnical engineering perspective.

2.2.1 Sinkhole Formation

2.2.1.1 Dissolution of bedrock

Most sinkhole occurrences in central Florida originate from the dissolution of the soluble limestone bedrock. The composition and height of overburden soils then governs the specific type of sinkhole which is most probable to form. Florida's bedrock formations consist of varying ages of limestone and dolomite; both rocks composed primarily of calcium carbonate ($CaCO_3$). The solution process begins as rainwater absorbs a slight amount of carbon dioxide. As water percolates, downward through the soil, the groundwater picks up even more carbon dioxide, generated by decaying organic matter. This results in a weak carbonic acid, which attacks the limestone as it seeps into fissures and recharges the Floridan aquifer. The following dissolution process is summarized in the below chemical equations.

$$H_2O + CO_2 \rightarrow H_2CO_3$$

(Rainwater absorbs carbon dioxide gas to form carbonic acid)

$$H_2CO_3 + CaCO_3 \rightarrow 2HCO_{3\,(aq)}^{-} + Ca_{(aq)}^{2+}$$

(carbonic acid reacts with limestone and yields dissolved bicarbonate ions and calcium ions)

The movement of water vertically through the rock medium follows the most favorable pathway, usually following a fissure or fracture. Over time, these pathways dissolve more rapidly than the surrounding areas because it carries more water. Because it is now larger, the favored

fissures can transmit water in even greater quantities, therefore self-accelerating the erosion process. Because of this process, it is more common to find fewer, yet larger, connected networks of cavities within the limestone with competent rock in between (i.e. the "swiss cheese block look"), rather than a vast plain of dissolved rock. These connected cavities allow sediment transport and erosion of the fine-grained soil above the limestone which is the starting mechanism for sinkhole formation.

2.2.1.2 Erosion of overburden soils

Due to the varying thickness of cover soils over the soluble bedrocks in central Florida, sinkhole formation type and collapse size is dependent on the type and formation of the finer-grained stratigraphy of the overburden soils. Although some areas in North Florida, where the limestone is exposed on the surface, experience rock ceiling collapse sinkholes, Central Florida sinkholes are almost always caused by downward migration of soil particles into the cavities within the bedrock. The thickness, types, and densities of the overburden soils greatly affect the type of sinkhole probable to form as shown in Figure 2-1. The vertical migration of soil sediment downwards into the limestone cavities can be caused by gravity or, expedited by seepage forces from groundwater recharging the deeper aquifers. These areas of higher recharge rates have also shown direct correlation to higher sinkhole occurrences (Gray, 1994). Degrading infrastructure, such as utilities lines or even leaking pools, can also play a major role in sinkhole formation; speeding up the natural erosive processes.

The average thickness of overburden soils varies greatly in the central Florida region, as presented in Figure 2-1. Generally, the thicker the overburden soil layer, the less likely a sinkhole is to occur. However, if a sinkhole does form, it is more likely to be much larger in diameter and

depth compared to other sinkholes in the state. This is evident by the numerous relic sinkholes in this region (Pink, Area IV, Figure 2-1). An example of such can be found underneath Deep Lake, just south of the town of Arcadia, Florida. This near perfect circular lake has been mapped by divers and discovered to be over 300 feet deep. The presence of a debris pile and distinct hour-glass shaped walls also suggests this mysterious lake was formed by a deep cover collapse. The type of overburden soils in a certain region play an imperative role in their susceptibility to erosion into the limestone voids thusly, affecting the type of sinkhole formed. The next section discusses the generalized classifications of sinkholes in Central Florida.

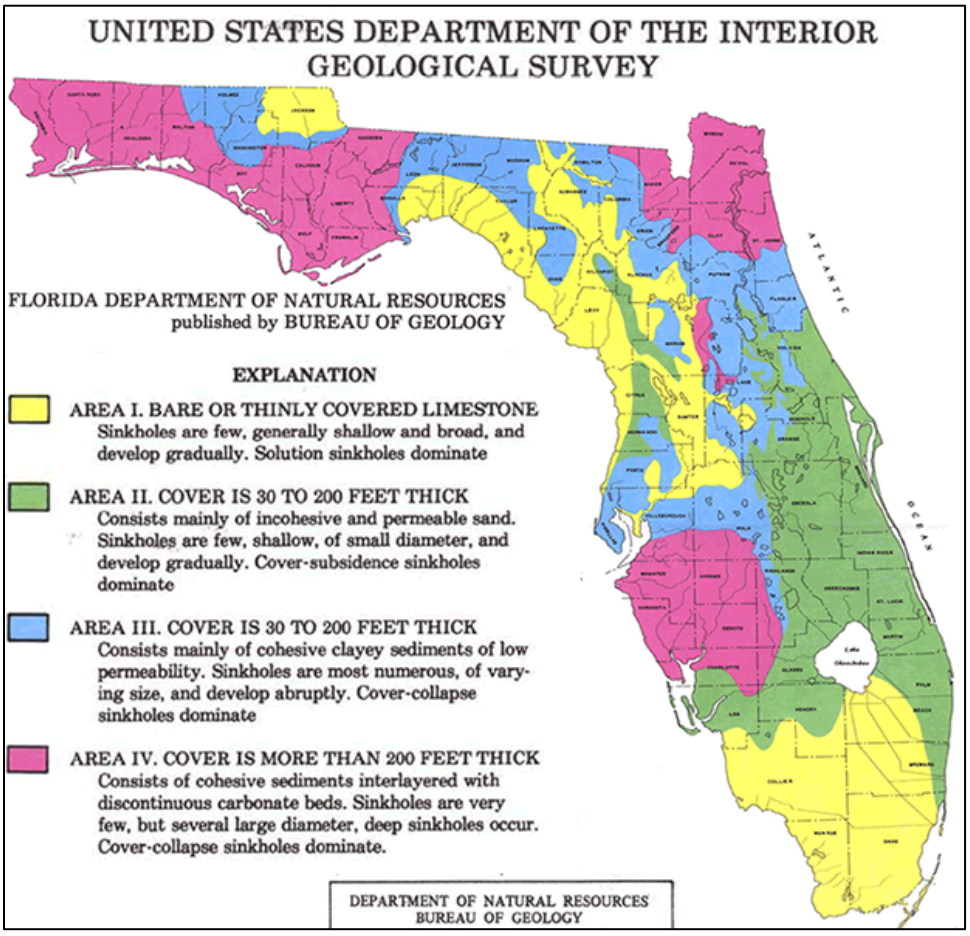

Figure 2-1: Florida Sinkhole type map

(Source: Department of Natural Resources Bureau of Geology, 1985)

2.2.2 Sinkhole Classifications

Sinkholes can be classified into general categories based on their formation type and typical landscape. These classifications are commonly referenced in engineering and geology literature. In Central Florida, where the bedrock is primarily limestone and the overburden soils are majority clayey or silty sands to clean sands, there are three general categories of sinkholes: Solution, Cover-subsidence, and Cover-collapse. A report published by the U.S.G.S in cooperation with the F.S.R.I., classified sinkholes the following way: (Beck & Sinclair, 1986)

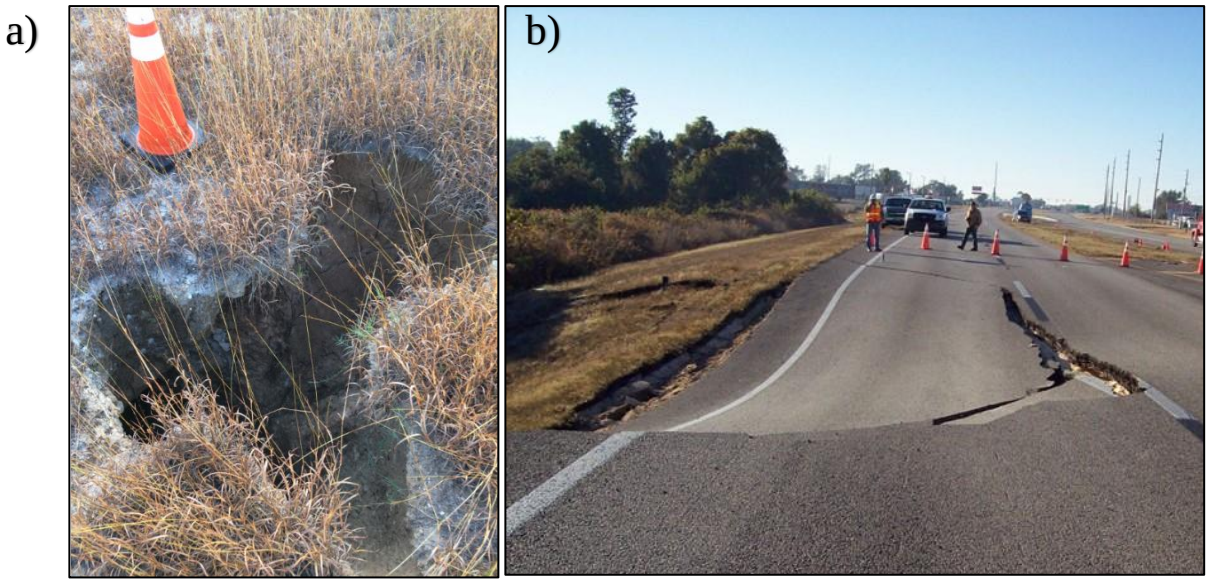

Figure 2-2: a) Solution Sinkhole. b) Cover subsidence sinkhole underneath roadway. (Source: FDOT)

2.2.2.1 Solution Sinkholes

In areas where limestone is exposed or thinly covered by permeable sands, solution sinkholes are most common. These sinkholes generally tend to be smaller in size but more frequent and easily triggered by rain events. In Central Florida, solution sinkholes are common just north-east of Tampa in a geomorphological structure known as the Ocala platform. In this area (Area 1

in Figure 2-1) the depth to water table is much greater than the surrounding area, therefore solution sinkholes often result in dry karst caves. Figure 2-2a shows a picture of an irregularly shaped solution sinkhole in Newberry Florida. This sinkhole formed after a large rain event eroded the thinly covered clayey sand into the pores of the underlain limestone. The depth of sinkhole measured about 6 feet, but the expanse was only a few feet wide. Large voids susceptible to devastating collapse commonly do not form because subsidence of the thin cover material, if any, occurs as the limestone surface dissolves. Detection of solution sinkholes is nearly impossible with subsurface testing since formation can occur relatively quickly during a severe rain event. However, during site development, grading and filling can usually trigger these sinkholes, allowing contractors to identify and fill before any structure is placed on the sensitive limestone area. Because these sinkholes often open into large interconnected cavities within the limestone, an isolated solution sinkhole on a site is a seldom occurrence, therefore a thorough due-diligence of the surrounding geology should be performed before developing in this area.

2.2.2.2 Cover-Subsidence Sinkholes

In areas where the limestone is covered by soil that are relatively non-cohesive and permeable, sinkholes develop by subsidence. Individual particles of sand move downwards in sequence, replacing the space formerly held by the dissolved limestone; like sand passing through an hour-glass. Since the overburden soils are non-cohesive, a structural arch is not able to develop, thus a subterranean void cannot fully form. Formation time for cover subsidence sinkholes can vary from hundreds of years, to a couple days depending on the overburden thickness and water movement within the stratigraphy. These types of sinkholes are most common in the eastern part central Florida (Area 2, Figure 2-1). Figure 2-2b shows an example of a cover subsidence sinkhole

forming underneath a US27 in Polk County. Much slower than a cover-collapse sinkhole, cover-subsidence can still result in extensive differential settlement cover large areas. Leaking utility lines or poorly design roadway drainage systems can also form cover-subsidence sinkholes by washing and eroding away the soil underneath.

2.2.2.3 Cover-Collapse Sinkholes

In west-central Florida, the sandy cover becomes gradually more cohesive with depth. A dense layer of slightly over-consolidated clayey sand or sandy clay overlaying the limestone surface (Hawthorne group) can act as a bridge over a developing cavity. The cohesion within this dense layer can develop and support arching effects with no noticeable signs of settlement on the surface. Once the stability of the soil arch is compromised either by extensive internal erosion, additional surcharge surface loading, or extreme seepage forces, a cover-collapse sinkhole will form.

Figure 2-3: Photos of devasting cover collapse sinkholes in central Florida

(Source: FDOT)

Cover-collapse sinkholes are generally the most devastating and can collapse with only minutes of warning. Figure 2-3 shows two photos of cover-collapse sinkholes occurring in west-central Florida. SPT borings performed near both collapses showed a thick clay layer overlaying the vuggy limestone. As the limestone cavity grew underneath, the cohesion within the clayey sand could hold up the soils above it; like a bridge. Eventually, collapse of the clay layer into the cavities occurred, resulting in the "throat" of the sinkhole (apparent in the left photo, highlighted by the dashed circle). The sandy sediment above then fails and collapses into the void, creating the larger diameter of collapse seen. Secondary collapse can continue as slope failure of the sandy soils continues, expanding the overall sinkhole size.

Although cover-collapse sinkholes provide little time for warning on the surface, the forming subterranean void can be detected using various subsurface exploration tests. However, a single test encountering an abnormally loose layer of cohesive soils directly above the weathered limestone does not necessarily mean a cover-collapse sinkhole is imminent. The information and findings presented in Chapters 3 and 4 of this thesis hope to provide further analysis techniques for subsurface testing (specifically CPT) to be used as a tool when evaluating sinkhole risk – especially risk of cover-collapse sinkhole formation.

2.3 Cone Penetration Testing

Cone penetration testing was developed from the need to quickly determine the strength of subsurface soils without the use of large scale, intrusive drilling equipment. Although pushing rods into the ground to determine soil strength is a very old practice, the first true static cone penetrometer tests were developed in 1931 in the Netherlands by P. Barentsen. In the early 1980s, porewater pressure measurement techniques were incorporated into the standard electric cone

penetrometer; allowing a single test to record cone tip resistance (q_c), sleeve friction (f_s), cone inclination (i), temperature and pore water pressure (u) as the probe is pushed through the soil strata (Sanglerat, 1972). These measurements are defined by the following equations (ASTM Standard D5778, 2012):

Cone Tip Resistance: $$q_c = \frac{Q_c}{A_c}$$

Sleeve Friction Resistance: $$f_s = \frac{Q_s}{A_s}$$

Friction Ratio: $$R_f = \frac{f_s}{q_c} * 100$$

Pore water pressure: $$u_0 = (z - z_w) * \gamma_w$$

Where: q_c = cone resistance (MPa)

Q_c = force on cone (kN)

A_c = cone base area = 10cm^2

f_s = sleeve friction resistance (kPa)

Q_s = force on friction sleeve element (kN)

A_s = area of friction sleeve = 150 cm^2

R_f = friction ratio (%)

u_o = hydrostatic water pressure (kPa)

z = depth of interest (m)

z_w = depth to groundwater table (m)

γ_w = unit weight of water = 9.81 (kN/m^3)

When using the electric cone, calibration of the measuring load cells should be performed prior to testing. The load cells consist of interconnected strain gauges rigidly attached to the shaft of the penetrometer tip. When a load is applied to the cone or to the friction sleeve, the shaft length changes, and gages are subjected to the identical deformation. The subsequent variation in length changes the resistance of the strain gages. The resistance is measured by applying a constant excitation signal to the load cells and recording the output voltage. Calibration is performed by taking a "zero" reading to measure the load cell voltage output when no loads are applied and when at a constant temperature. This process is imperative before performing penetration and is discussed in greater detail by Jean-Louis Riaund and Jerome Miran in their FHWA report (Riaund & Miran, 1992).

Figure 2-4 shows a schematic diagram of the standardized CPTU electric probe with location of piezo-element directly behind the cone tip. The cone probe shown samples data every 0.78 inches (2 cm) with a typical penetration rate of 0.787 in./s (2 cm/s), allowing the CPT to detect discrete soil horizons that would normally be missed using drive samples at specific depth intervals. Because of this accuracy with depth, cone penetrometer soundings are being employed with increasing regularity, especially when evaluating site susceptibility of certain geohazards such as soil liquefaction, landslides, or karst soil anomalies (Department of Geological Sciences & Engineering, 2006).

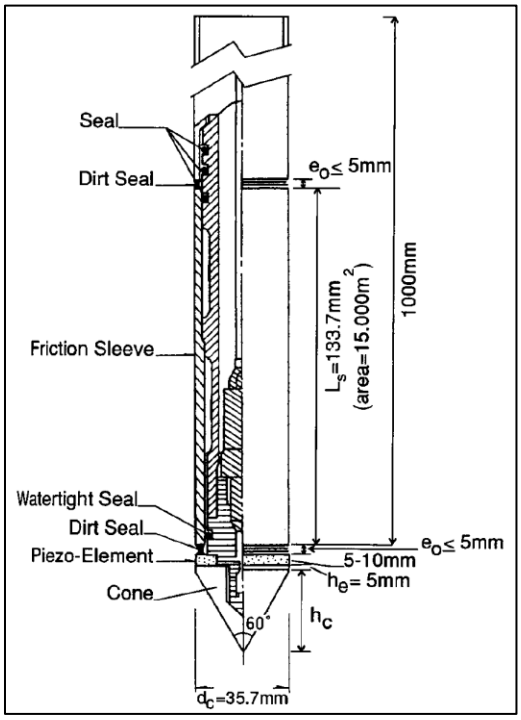

Figure 2-4: Schematic section through a CPTU probe.

(Source: ASTM D 5778-95)

2.3.1 CPT - correlations

A major limitation of CPTs is the inability to obtain soil samples for soil classification when stratifying a project site. Many researchers have established strong correlations between the CPT soil strength measurements (q_c and f_s) and SPT blow-count values (N) along with correlations to bearing capacity or settlement susceptibility (Meyerhof, 1956) (Douglas & Olsen, 1981) (Schmertmann, 1978). With the adaption of electronic cones – increasing the accuracy and reproducibility of the results—current research is being performed to correlate CPT results with soil classification and behavior type (Roberston P. , 1990) (2010) (2016). Using a wide database of experimental sites and soils from various geologic ages and formation throughout the world, Robertson developed, and is constantly updating, a Soil Behavior type (SBT) chart which

correlates values obtained from CPT (q_c, f_s and u_o) with the most probable type of soil the cone is penetrating through.

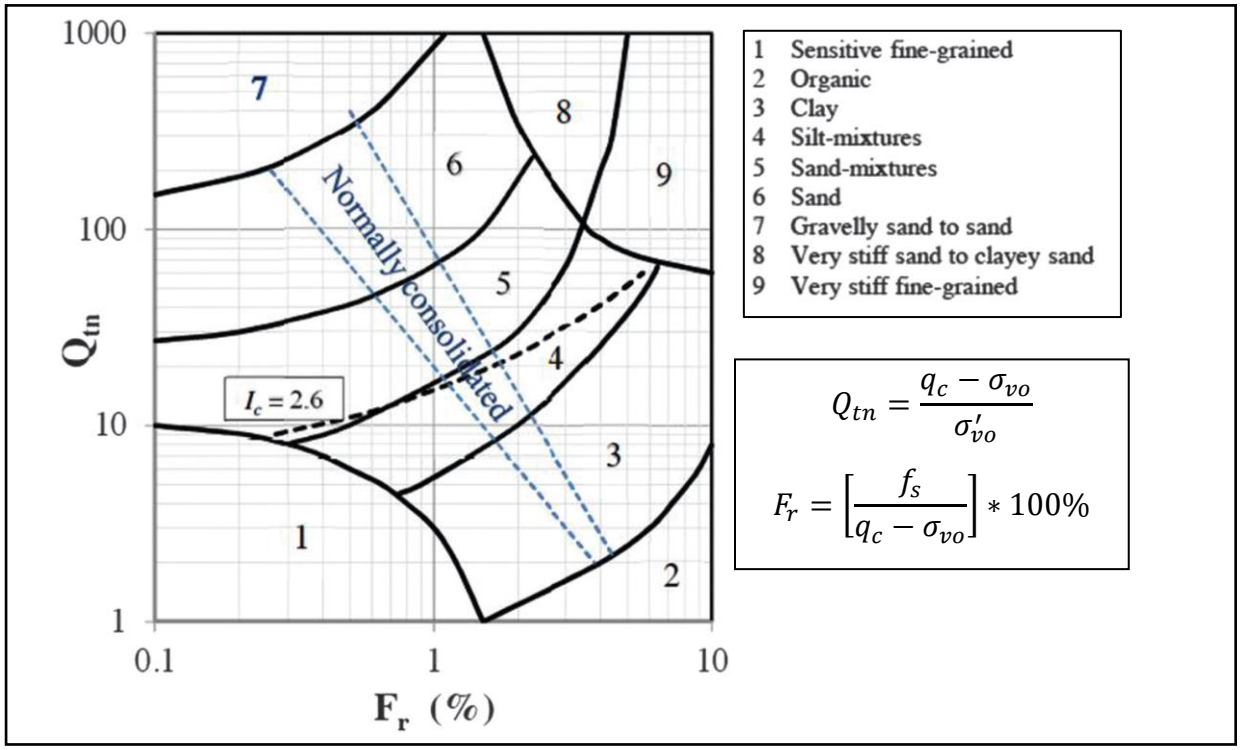

Figure 2-5: Soil Behavior Type Chart

(Source: Robertson, 1990)

Commercially available CPT data processing software uses these correlations to provide an estimated soil stratigraphy in "real-time" as the CPT is being performed. Robertson's newest SBT update provided a list of case-history sites which were used to create and validate his findings (see Table 1) (Robertson, 2016).

The database of CPT test sites used to empirically create the correlations, shown in Table 1, consist of a wide variety of soil types and location. Although this data shows strong correlation with SBT for specific soil types (i.e glacial clays with low organic content), there is an apparent absence of data obtained from test sites in karst terrain in the United States. Figure 2-5 presents a

map published by USGS of areas with karst or pseudo-karst geology within the contiguous United States. Each of the test site locations used for SBT validation, presented in Table 1, are also presented in Figure 2-5 (represented by red stars). It is clear from the figure that there is a lack of testing data performed in carbonate-based karst geology (represented by the blue colored area); let alone in Florida's unique karst geology which is spread through much of the state. Because of this lack of karst-calibration, CPT data analysis programs which reference the SBT system proposed by Robertson may provide inaccurate results when performed in Central Florida. The largest discrepancy between residual soils in Florida's karst geology and other non-karst geologic formations is the strength profile of soils. Because of the internal erosion and disturbance of sub soil layers near the limestone due to groundwater flow in karst areas, residual soils in central Florida often follow what is called an inverse soil profile (Sowers, 1996); that is, soil density and strength does increase with depth. Because of this occurrence, further investigation of CPT data should be performed in central Florida and analysis should not depend on correlations which are calibrated for subsoils formed through other natural processes differentiating from Florida's unique geology. This study present in greater detail the discrepancy between the currently used CPT-SBT system and the actual encountered soil type classification – especially in highly variable karst soils.

Table 1: List of sites used in CPT database Soil behavior type correlation

Taken from: (Robertson, 2016)

Reference No.	Site	Description	Geologic age	Q_{tn}	F_r (%)	U_2	I_G	K_G^*	Reference
1	San Francisco (USA)	Young Bay mud, NC–LOC clay	Holocene	4.0 (3.0–5.0)	1.0 (0.5–2.0)	2.0 (1.5–3.0)	30 (25–35)	85 (70–100)	P.K. Robertson (personal files)
2	Burswood Perth (Australia)	NC–LOC clay	Holocene	6.5 (5.5–8.0)	2.0 (1.0–3.0)	2.5 (1.5–3.5)	22 (18–30)	90 (75–122)	Randolph (2004)
3	Syncrude (Canada)	NC tailing sand	Recent	30 (20–65)	0.7 (0.4–1.0)	0	8 (6–10)	105 (100–110)	Wride et al. (2000)
4	Highmont (Canada)	NC tailing sand	Recent	40 (20–70)	0.3 (0.1–0.6)	0	8 (6–12)	130 (120–140)	Wride et al. (2000)
5	LL Dam (Canada)	NC tailing sand	Recent	45 (30–60)	0.4 (0.1–0.8)	0	8 (6–12)	140 (130–150)	Wride et al. (2000)
6	Holmen (Norway)	Drammen River, NC sand	Holocene	30 (20–60)	0.4 (0.2–0.7)	0	12 (10–18)	155 (125–205)	Lunne et al. (2003)
7	Onsoy (Norway)	NC–LOC clay	Holocene	4.5 (4.0–5.0)	1.8 (1.2–2.2)	3.0 (2.5–3.5)	60 (50–70)	185 (155–215)	Lunne et al. (1997)
8	Tabarao (Brazil)	NC–LOC clay	Holocene	4.0 (3.0–5.0)	1.3 (1.1–1.5)	1.7 (1.0–2.2)	65 (50–80)	185 (140–225)	Schnaid and Odebrecht (2015)
9	University of British Columbia, McDonald Farm (Canada)	Fraser River, NC sand	Holocene	100 (50–150)	0.3 (0.2–0.5)	0	5 (3–9)	200 (100–300)	Campanella et al. (1983)
10	KIDD (Canada)	Fraser River, NC sand	Holocene	80 (40–150)	0.6 (0.3–1.0)	0.1 (–0.1–0.5)	8 (5–12)	214 (130–310)	Wride et al. (2000)
11	J-Pit (Canada)	NC tailing sand	Recent	35 (20–50)	0.7 (0.6–1.0)	0	15 (9–25)	215 (170–270)	Wride et al. (2000)
12	KIDD (Canada)	Fraser River, NC–LOC clay	Holocene	3.5 (3.0–4.0)	1.1 (0.9–1.4)	3.0 (2.0–3.5)	85 (60–110)	215 (155–280)	Wride et al. (2000)
13	Bothkennar (UK)	LOC silty clay	Holocene	6.5 (5.5–8.0)	1.6 (1.0–2.5)	3.6 (2.5–4.5)	60 (50–70)	240 (205–290)	Hight and Leroueil (2003)
14	University of British Columbia, McDonald Farm (Canada)	Fraser River, NC–LOC clay	Holocene	4.0 (3.0–5.0)	1.8 (1.5–2.2)	2.5 (2.0–3.0)	100 (80–120)	280 (230–320)	Campanella et al. (1983)
15	San Francisco (USA)	Old Bay clay, OC clay	Late Pleistocene	12.0 (5–30)	2.5 (1.5–5.0)	2.5 (–1.5–5.0)	45 (30–100)	300 (195–600)	P.K. Robertson (personal files)
16	Venice (Italy)	NC–LOC clayey silt	Holocene	7.5 (5.0–10.0)	2.0 (1.3–2.8)	1.0 (0.1–1.8)	70 (60–80)	315 (270–350)	Simonini (2004)
17	Amherst (USA)	Varved clay	Late Pleistocene	7.5 (6.5–9.0)	1.5 (0.8–3.0)	5.0 (3.0–6.0)	70 (50–90)	325 (225–400)	DeGroot and Lutenegger (2003)
18	Ford Center (USA)	LOC clay	Pleistocene	7 (5.5–9.0)	3.0 (2.5–43.5)	3.8 (3.0–4.5)	78 (70–90)	330 (300–380)	Finno et al. (2000)
19	Madingley (UK)	HOC clay	Cretaceous	35 (30–45)	4.5 (3.0–6.0)	–1	25 (15–30)	360 (330–430)	Lunne et al. (1997)
20	Griffin (USA)	Dense sand	Pleistocene	150 (80–400)	0.6 (0.3–1.0)	0	9 (4–20)	380 (215–800)	Safner et al. (2011)
21	Tangiers (Morocco)	Calcareous sand	Recent	100 (60–200)	0.2 (0.1–0.8)	0	12 (7–20)	380 (215–560)	Debats et al. (2015)
22	Campinas (Brazil)	Residual soil	—	20 (15–25)	6.0 (5.0–8.0)	1 (0–4)	45 (40–60)	425 (375–565)	De Mio et al. (2010)
23	Dubai (United Arab Emirates)	Calcareous sand	Recent	70 (60–80)	0.2 (0.1–0.3)	0	18 (15–21)	435 (360–500)	P.K. Robertson (personal files)
24	Porto (Portugal)	Residual soil	—	40 (30–50)	5.0 (3.0–7.0)	0	30 (20–40)	475 (320–640)	De Mio et al. (2010)
25	Ledge Point (Western Australia)	Calcareous sand	Holocene	150 (80–300)	0.5 (0.2–0.8)	0	10 (5–20)	500 (330–800)	Schneider and Lehane (2010)
26	Houston (USA)	Beaumont, OC clay	Pleistocene	25 (20–30)	4 (3.5–4.5)	–0.5 (–1.0–0)	48 (35–50)	535 (425–640)	Mayne (2009)
27	Atlanta (USA)	Piedmont, residual soil	—	45 (25–65)	2.2 (1.2–3.0)	–0.5 (–1.0–0)	33 (25–40)	570 (470–640)	Mayne (2009)
28	Charleston (USA)	Cooper Marl, calcareous clay	Oligocene	12 (8–25)	0.6 (0.4–1.4)	6 (4.5–11)	90 (50–200)	580 (330–1200)	Camp et al. (2002)
29	Los Angeles (USA)	Fernando, siltstone	Miocene	75 (60–100)	1.5 (1.0–2.0)	33 (20–40)	30 (17–40)	635 (510–1020)	P.K. Robertson (personal files)
30	Anchorage (USA)	Bootlegger Cove, HOC clay	Pleistocene	20 (10–50)	1.3 (1.0–2.0)	1.7 (1.0–5.5)	80 (50–110)	750 (450–1400)	Mayne and Pearce (2005)
31	Windsor (USA)	Calcareous cemented clay	Miocene	45 (40–50)	2.5 (2.0–3.0)	12 (5–16)	48 (40–65)	830 (690–1150)	Ku et al. (2013)
32	Calgary (Canada)	Glacial clay till	Pleistocene	40 (35–50)	3.0 (2.5–3.5)	5 (0–7.0)	55 (40–70)	850 (600–1100)	Mayne and Woeller (2008)
33	Newport Beach (USA)	Monterey, sandstone–siltstone	Miocene	150 (50–400)	2.5 (0.8–5.0)	1 (0–15)	20 (8–200)	860 (350–4000)	Bastani et al. (2014)

Note: Values shown are mean values, with ranges in parentheses. NC, normally consolidated; LOC, lightly overconsolidated (OCR < 4); OC, overconsolidated; HOC, heavily overconsolidated (OCR >4).

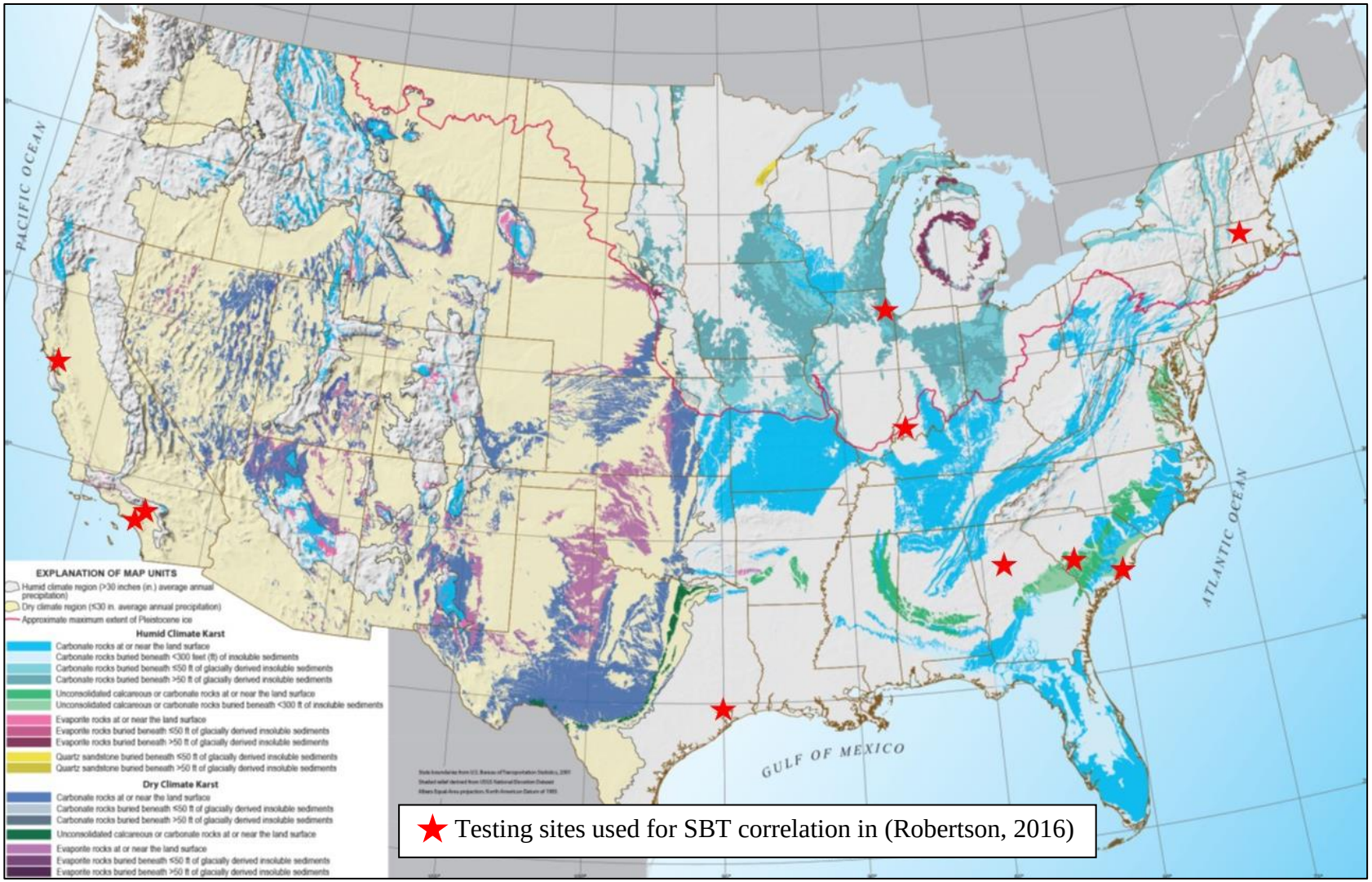

Figure 2-6: Karst and geology map in contiguous United States

(Source: USGS, 2014)

2.4 Sinkhole Detection in practice

Premature sinkhole detection is required to successfully mitigate a forming sinkhole before any structural damages occur to infrastructure; limiting the additional costs for repair. Figure 2-5 presents a theoretical project cost timeline for sinkhole mitigation/repair. In this timeline, we can see there is a crucial moment where mitigation becomes repair, causing the cost to increase substantially. This moment in time is the sinkhole collapse in a cover-collapse, or severe slope failure in a cover-subsidence sinkhole. Perhaps the largest uncertainty in the sinkhole cost timeline is, unfortunately, time itself. Sinkhole subterranean void growth and collapse is very difficult aspect to quantify. Complete collapse and opening of the sinkhole usually takes only a couple minutes or hours, however, the forming void underneath may be a result of hundreds or even million years of internal erosion at the rock-soil interface. Current techniques are being further developed to provide an early warning system of sinkhole collapse (Rizzo & Dettman, 2017), however the sinkhole risk assessment cannot be fully understood over time unless the rate of erosion is characterized. Research in this field is currently underway to estimate groundwater seepage forces measured from an array of *insitu* piezometers at sinkhole site in central Florida (Tu, 2016).

2.4.1 Subsurface exploration testing

A forming sinkhole may be detected using a single test showing very low strength soils at a certain depth at which does not agree with the surrounding soils comparable to the expected density from its original formation. Initial subsurface exploration tests, such as SPT and CPTs, can identify these anomaly soil layers which may suggest a forming sinkhole.

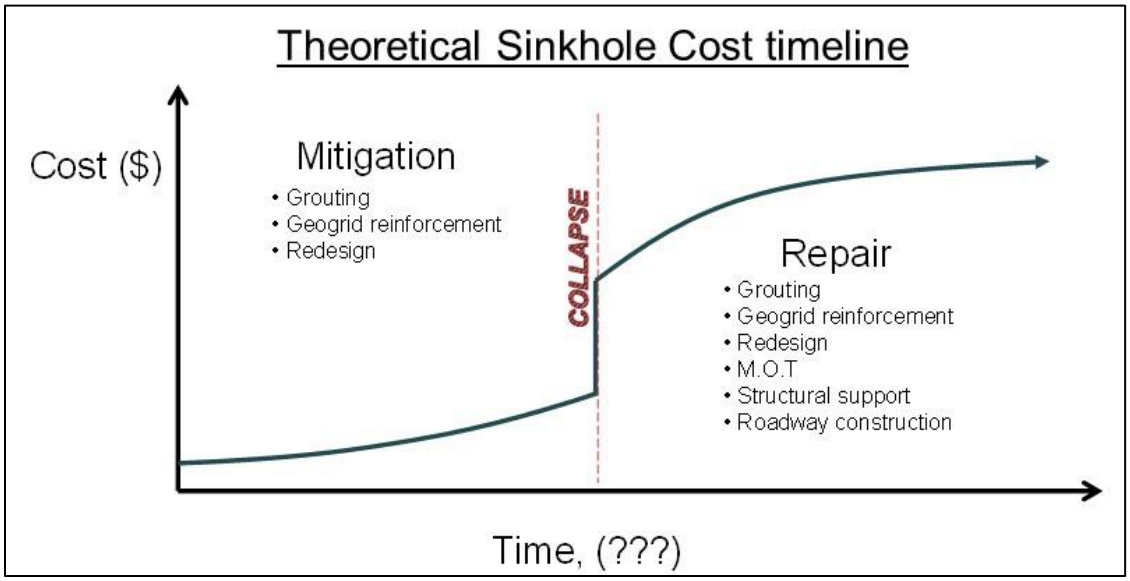

Figure 2-7: Conceptual cost timeline for sinkhole mitigation and repair

2.4.1.1 Standard penetration test (SPT)

SPTs are valuable in sinkhole detection because they can retrieve soil samples (although highly disturbed) from any depth. Laboratory testing and soil classification can then be performed when estimating the stratigraphy of the subsoil, allowing engineers to better estimate whether soils may be suggestive of sinkhole formation. SPTs also provide a penetration resistance data in the form of the number of blow counts (N) it takes to advance the sampling tip into the soil by a 140 lb hammer dropped 30 inches. In extremely loose sands or in soft clays, the drilling rods and sampling tip will advance into the soil under the self-weight of the rods or the hammer, without any additional forces being applied. These instances are labeled as “weight of hammer” or “weight of rod” conditions (WR/WH). When isolated cases of these conditions occur within a site, especially at reasonable depth directly above a refusal layer, sinkhole formation may be to blame. Further investigation is then commonly performed whether by additional SPTs or by geophysical

testing. However, many engineers believe WR/WH conditions may not be completely indicative of sinkhole formation because of the inaccuracy of N values at great depths (Edward D. Zisman, 2013). Figure 2-8 presents example soil boring logs from SPTs performed on the same project site in central Florida (Professional Services Industries, Inc. , 2014). The left boring shows a relatively normal soil stratigraphy consistent with the expected geology. The boring log on the right, however, encountered a significant region of very weak sandy soils at a depth of 60 feet below GSE—as shown by WR and the note that the rod fell from 63.5' to 78.5'. Another SPT sign of problematic loose soils includes the complete loss of drilling fluid (usually bentonite) that is circulated during the SPT to keep the bore-hole from collapsing. If loss of circulation occurs (denoted by the ←100% symbol), that means the drill tip progressed into a soil layer with similar characteristics to a void; that is, the soil is so loose that the viscous bentonite mud is able to breach and travel through that layer away from the bore-hole. The boring log on the right side of figure 2-8 presents an anomaly in which further investigation should be performed to ensure against a sinkhole hazard.

2.4.1.2 Cone Penetration Test (CPT)

CPTs can also be used to detect potential forming sinkhole under the same principle discussed above regarding SPTs. However, instead of the blow count value (N) obtained in SPT from a dynamic hammer, CPTs record penetration resistance in the form of tip resistance (q_c) and sleeve friction (f_s) by pushing a probe hydraulically at a steady rate. This method, is much more accurate at locating discrete horizons or discrepancies in the soil strata since the sampling per depth is much higher than that of SPT. However, the inability to obtain soil samples for lab testing or visual classification is a major limitation of CPT, especially when using a single test to estimate

site stratigraphy or geohazard potential. Therefore, "ground-truthing" is a common technique used when implementing CPTs for subsurface investigation. By conducting a CPT next to a conventional sampling boring (such as SPT), the CPT soil strength measurements (q_c and f_s) can be validated with actual soil type and index properties to provide a more accurate stratigraphy estimation. This technique is especially important when characterizing subsoil in a site with known karst geology. Figure 2-9 presents such an example of ground-truthing where a CPT tip resistance curve (q_c) with abnormally low values at a depth above the refusal layer, correlates strongly with the SPT suggesting sinkhole formation (see WH/WR conditions). The SPT blow count number (N) trends strongly correlate with the CPT tip resistance values (q_c) trends with depth. Once ground-truthing has been performed, CPTs can be performed throughout the site at a much quicker rate than that of SPTs, allowing for an efficient subsurface exploration and characterization (Department of Geological Sciences & Engineering, 2006).

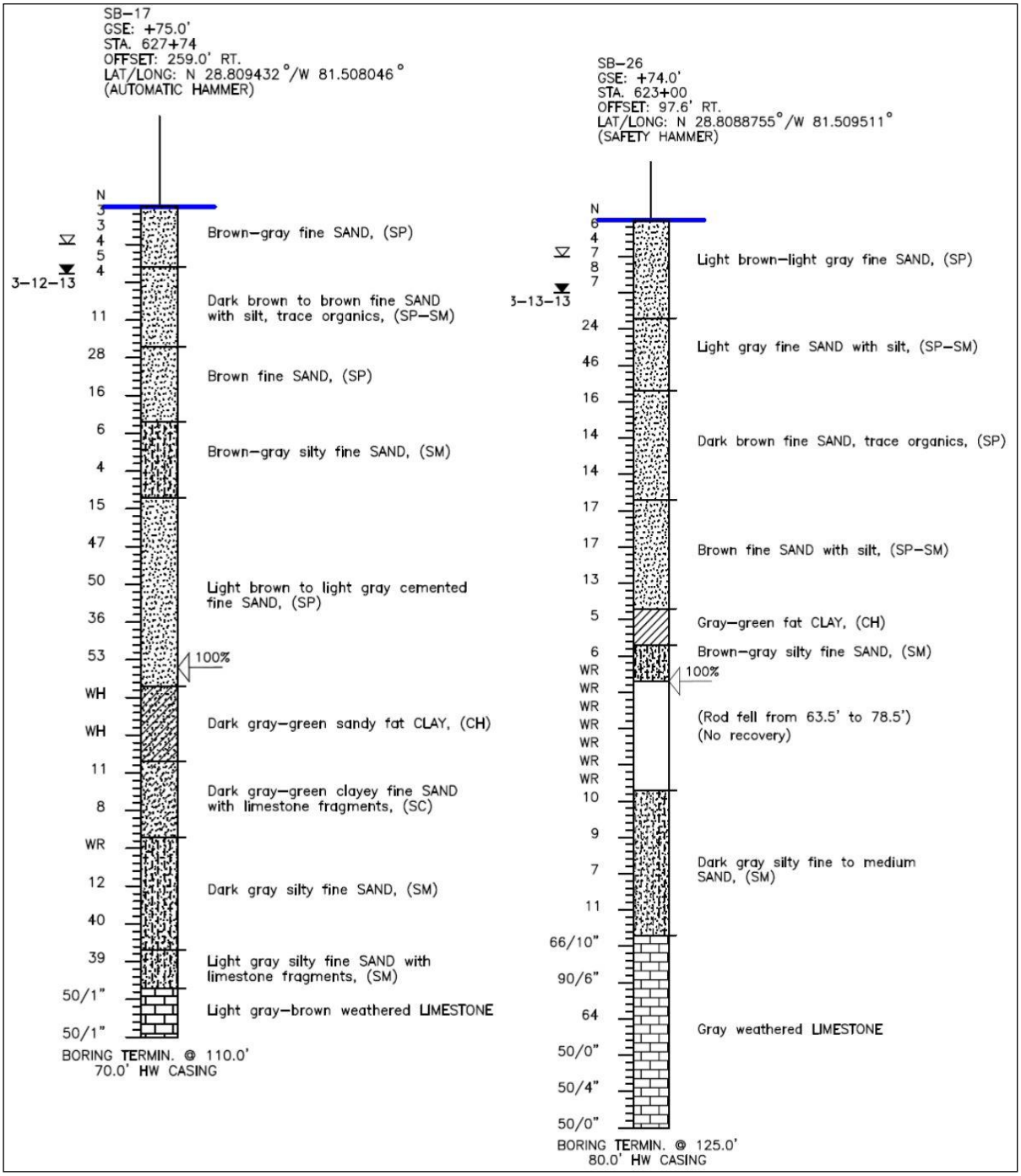

Figure 2-8: Example SPT boring logs in central Florida

(Source: Professional Services Industries, 2014)

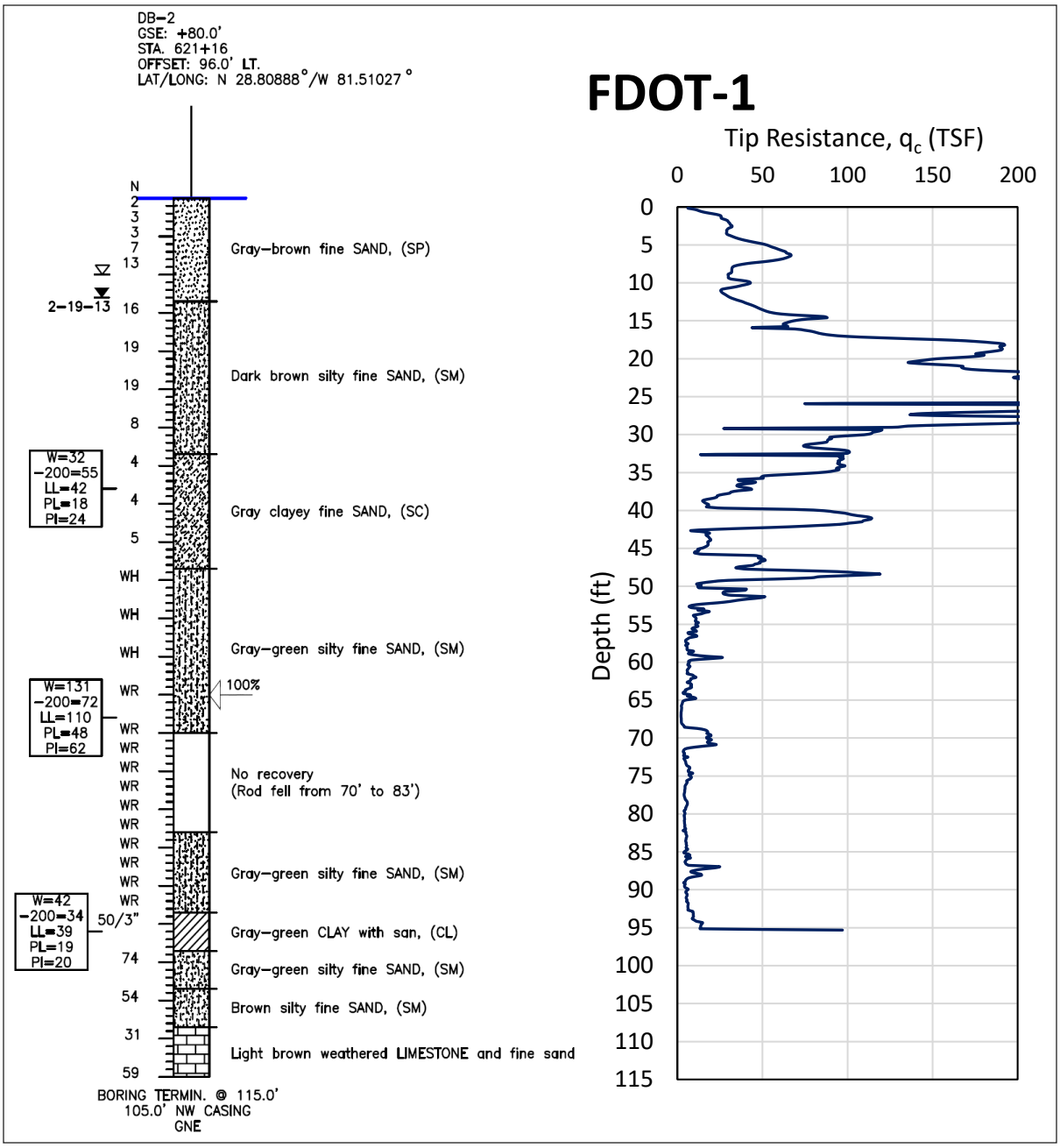

Figure 2-9: Example of "ground-truthing" between CPT q_c curve and SPT.

(Source: Professional Services Industries, 2014)

2.4.2 Geophysical testing

2.4.2.1 Ground Penetrating Radar (GPR)

Ground Penetrating Radar (GPR) is widely used as a non-intrusive technique to locate subterranean anomalies such as buried pipes or abrupt changes in soil density. GPRs emit and receive electromagnetic waves (10 to 3000 Mhz) and use the respective time-lag information between transmissions to survey and "map" a cross-section of soil. Although most effective at shallower depths, GPRs are being more commonly employed for sinkhole detection as lower-frequency antennas are being developed to retain resolution at larger depths. Specialized contractors and geophysicists have proven GPR is a functional method to detect a sinkhole anomaly (Professional Services Industries, Inc. , 2014), (Bullock & Dillman, 2003) but after detection, there is little information that can be obtained from the GPR data. Also, GPR data can be very difficult to interpret, especially when attempting to draw conclusions of potential sinkhole size or severity from the presented soil map. Figure 2-10 shows such ambiguity in a GPR transect plot. From the GPR plot, it is clear there is a localized change of soil density, or type, along the investigated tract (notice the coagulation of horizontal layers in the circled section), but there still lacks standardized methodology for characterizing the subsoil and correlating GPR results to soil strength parameters; severely limiting the GPR as an effective subsoil investigation technique.

2.4.2.2 Electrical Resistivity Testing (ER)

Electrical resistivity surveying is a geophysical method in which an electrical current is injected into the earth and the subsequent response is measured at the ground surface to determine the resistance of the underlying soil. Implanted electrodes read the electrical potential as volts and then, using Ohm's Law, are converted to resistivity values. Resistivity of earth materials is

controlled by several properties including composition, water content, and effective permeability (PSI, 2014). Through inversion modeling of the ER data, a resistance map of the sub soil along the investigated tract can be developed. Like GPR, ER has proven to be able to detect subterranean air-filled voids such as abandoned mine shafts (Sheets, 2002), however, the two techniques also share in limitations. Interpretation of ER data is a very specialized task and requires extensive experience and knowledge of statistical modeling, soil electrical conductivity parameters, local geology, and expected soil composition. Geophysical testing methods, such as GPR and ER, are more commonly implemented to identify potential sinkhole zones or anomalies within the karst subsoil and are used in conjunction with SPT and CPT for site characterization; never as a lone technique.

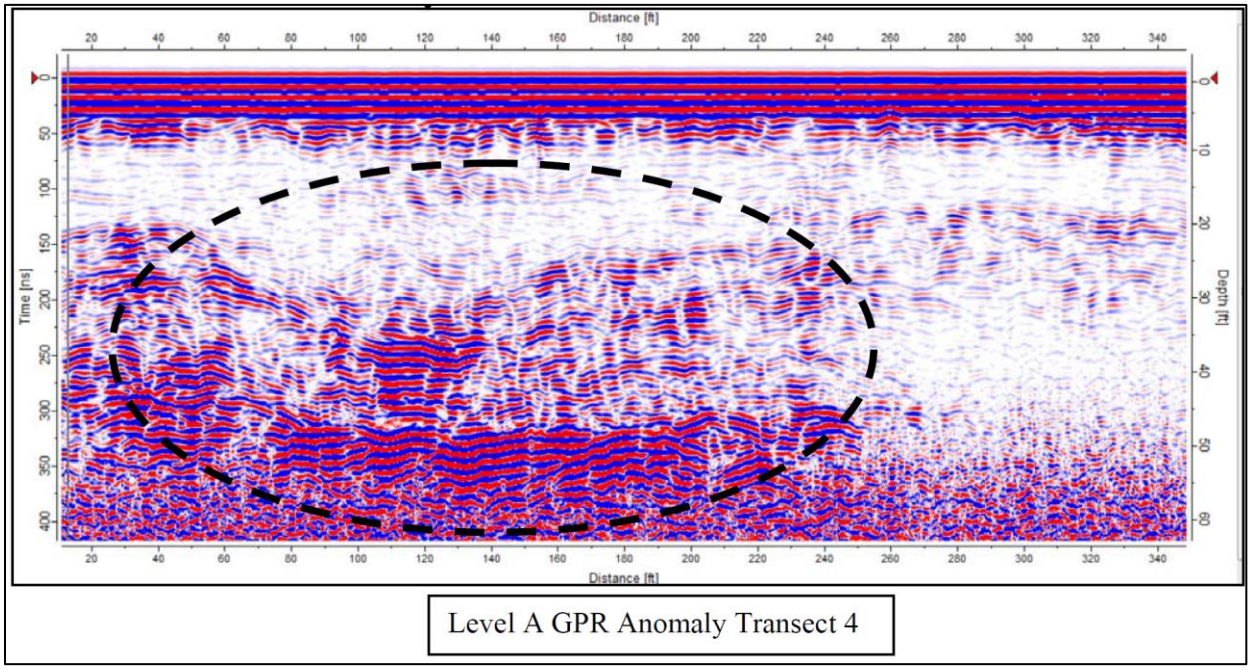

Figure 2-10: GPR transect of soil cross-section showing a potential sinkhole anomaly (Source: PSI, 2014)

CHAPTER 3: IDENTIFICATION OF SINKHOLE RAVELING AND DEVELOPMENT OF RAVELING CRITERIA IN CPT DATA

3.1 Introduction

Sinkholes have been occurring naturally in Florida for thousands of years. Much of Central Florida's circular ponds and lakes are attributed to karst geology and some type of sinkhole activity over the millennia. As Central Florida's urban areas expand, greater strains are placed on Florida's fragile aquifer systems from either over farming or potable water usage via deep water wells. Consequently, sinkholes have been forming more often and in more inconvenient locations creating a sharp increase in sinkhole related insurance claims over the past few years (Florida Office of Insurance Regulation 2010). The destructive outcome of sinkholes in central Florida is apparent (Figure 3-1) and can the result cause severe risk to the public and cost millions in infrastructure damages.

Figure 3-1: Photos of Central Florida sinkhole devastation
(left: Deltona road collapse 2010; right: Winter Park 1981)
(Source: FDOT)

Sinkholes are a geologic hazard that occur in areas underlain by soluble bedrock. Roughly 15% of the United States is underlain by rock susceptible to sinkhole development (Sinclair 1986), however, the discussion and methodology discussed in this chapter refers to sinkhole occurrence in areas with limestone bedrock, which underlays the bulk of Florida's Peninsula (Lane 1986).

In this chapter, the discussion focuses on the methodology of identifying possible developing sinkholes using data obtained from cone penetrometer tests performed in areas with either recent sinkhole formations or encountered sinkhole anomalies. Through proper data collection, processing, filtering, and analysis, a CPT-based raveling chart was developed as a tool for engineers to better understand the severity of sinkhole formation when developing in a location suggesting karst geology.

3.2 Raveling Mechanism and Criteria

Methods of detecting sinkhole anomalies tend to fall within the Geotechnical engineer's scope of work. Subsurface exploration tests such as Standard Penetration testing (SPT) and Cone Penetrometer testing (CPT) are commonly used by geotechnical engineers to determine soil engineering parameters at required depths depending on the type of structure being designed. In central Florida-- where the depth to encountered limestone varies greatly-- it is common for subsurface exploration tests to be performed completely through the overburden (or soil overlaying the bedrock) and terminate when the bed rock is encountered. This is beneficial for sinkhole detection since natural sinkholes in Florida originate at the bedrock-soil interface and propagate towards the surface over time (Gray 1994), (Rupert et al. 2004), (Sinclair 1986). The internal erosion and migration of the overburden soil into the cracks and cavities of the limestone bed rock creates a zone of loose, or disturbed, soil usually found above the weathered limestone interface. The main driving mechanism for this internal soil erosion in central Florida soils is vertical

groundwater seepage. The Floridan aquifer system (FAS) is a deep semi-confined aquifer which underlays most the state. Separating the FAS and the surficial groundwater table aquifer is a group of generally impermeable silty and clayey soil known as the Hawthorne formation. In certain areas in Central Florida, the Hawthorne formation can vary greatly in thickness and permeability and can even be non-existent from the soil strata (Figure 3-2). In these areas, vertical flow of groundwater between the surficial and Floridan aquifers is less impeded and the recharge rate (infiltration of water into the Floridan aquifer) is high. As shown in the highlighted red section in Figure 3-2, these areas coincide with the central Florida region. When cavities in the limestone bedrock are abundant, the vertical flow of groundwater between aquifers can cause soil migration and further erosion of the cavities. The soil migration and erosion of overburden, overtime, expands further into the overburden strata. This process is known as soil raveling, and is the main mechanism of sinkhole formation in central Florida.

Identifying any possible soil raveling is the primary method of detecting a forming sinkhole before any evidence may be present on the ground surface. The sinkhole formation due to the process of soil raveling is presented in Figure 3a. Here we see the vuggy, soluble bedrock overlain by a relatively thinner confining unit and then undifferentiated sands above that. The breach in the confining unit (hawthorne group soils) acts almost like a funnel which magnifies the seepage forces in that area, thus causing the concentrated internal erosion. Figure 3-3c presents the raveling concept over time, on a magnified scale at the Hawthorne-limestone interface. It is important to note that the raveling erosion does not necessarily form a complete void or subterranean cavern. Rather, the soil in that specific area becomes extremely loose and its unit weight drastically decreases. This is evident in multiple standard penetration test (SPT) borings performed in sinkhole active sites.

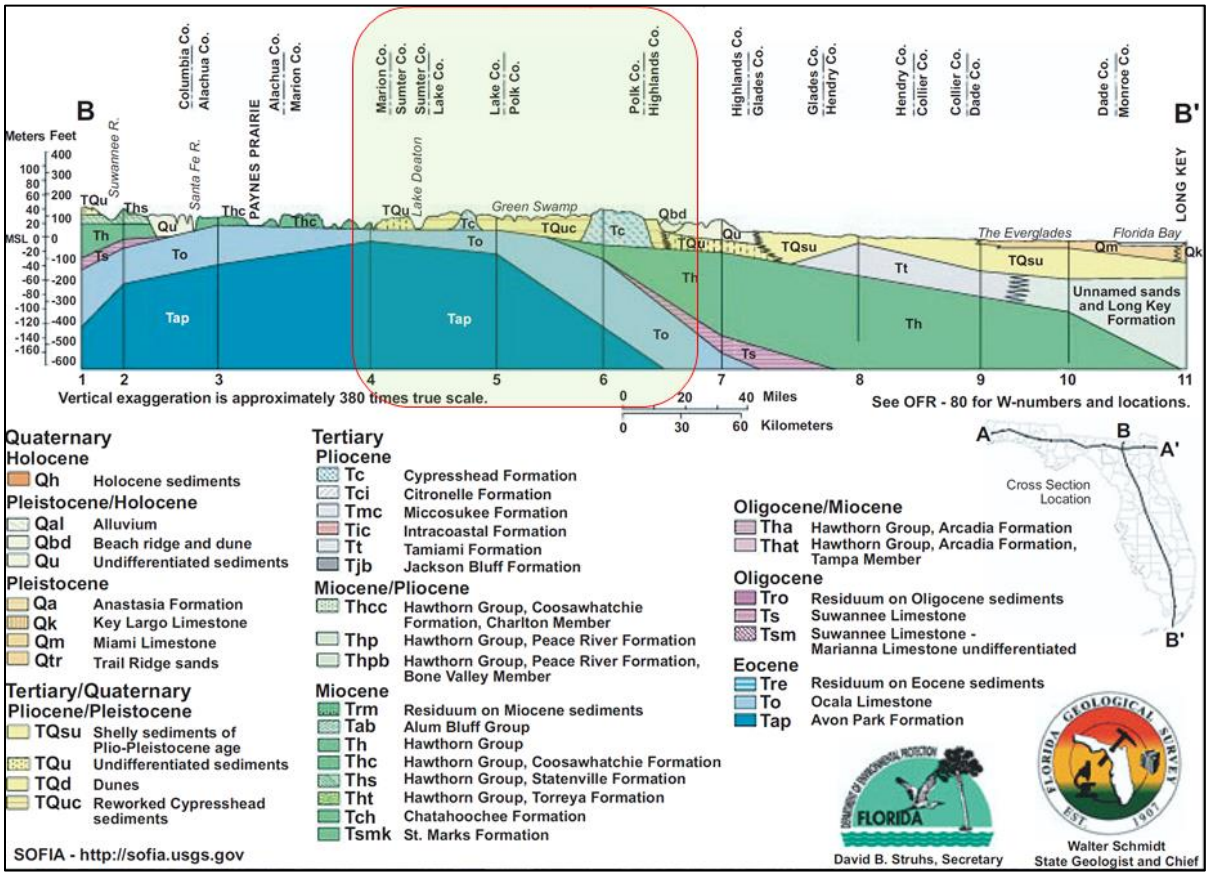

Figure 3-2: Geologic cross section of Florida Peninsula -- North to South

Source: (Florida Geological Survey, 2001)

Figure 3-3b presents such a SPT boring showing that at the depth one would expect to find the dense to medium dense silty and clayey fine sands of the hawthorn group, the blow counts (N-value) suggests very loose material as the drill tip begins to fall under its own weight of hammer or weight of the rods (WH or WR). However, the split spoon sampler is still able to recover some soil samples in these zones, suggesting –although extremely loose and disturbed—there is still granular material present in this specific region.

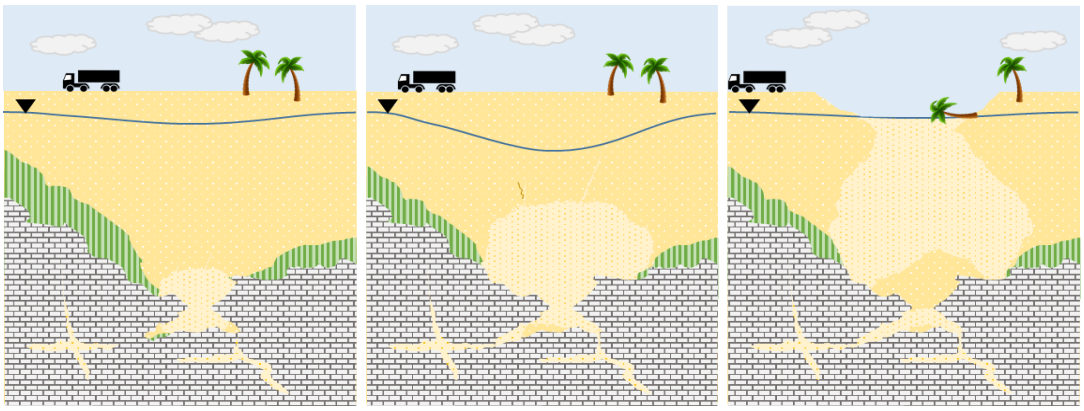

(a) Cover collapse sinkhole progression

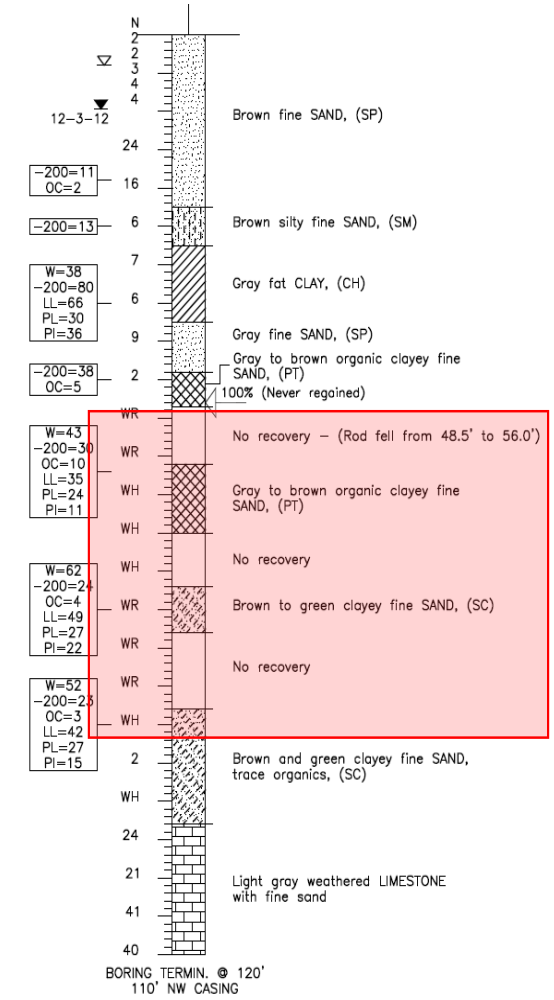

(b) SPT boring log suggesting raveling

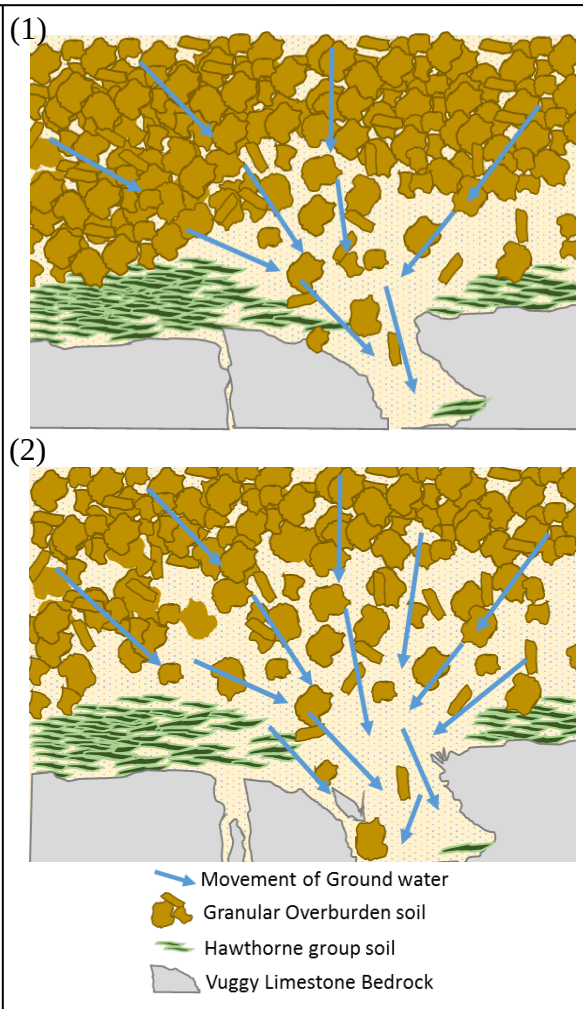

(c) Raveling mechanism over time

Figure 3-3: Soil raveling process.

3.3 Raveling Index

First suggested by in 1994 by Foshee and Bixler, the Raveling index (RI) is a tool used by many geotechnical engineers in central Florida to evaluate sinkhole risk by using a single CPT or SPT boring. The index is defined as the thickness of the raveled soil layer (t_r) divided by the depth to the top of the encountered raveled zone (d_r). This ratio gives a relative indication of the degree of soil erosion taken place in the overburden sandy soil. The smaller the ratio, the less deterioration of soil and the lower the risk of future sinkhole activity. Raveled soils are identified by abnormally low tip resistance values (q_c < 10 TSF) encountered above the weathered limestone (Foshee & Bixler, 1994). Although RI is a useful tool for understanding and comparing site investigation techniques, it is limited from the fact that only q_c is input for analysis.

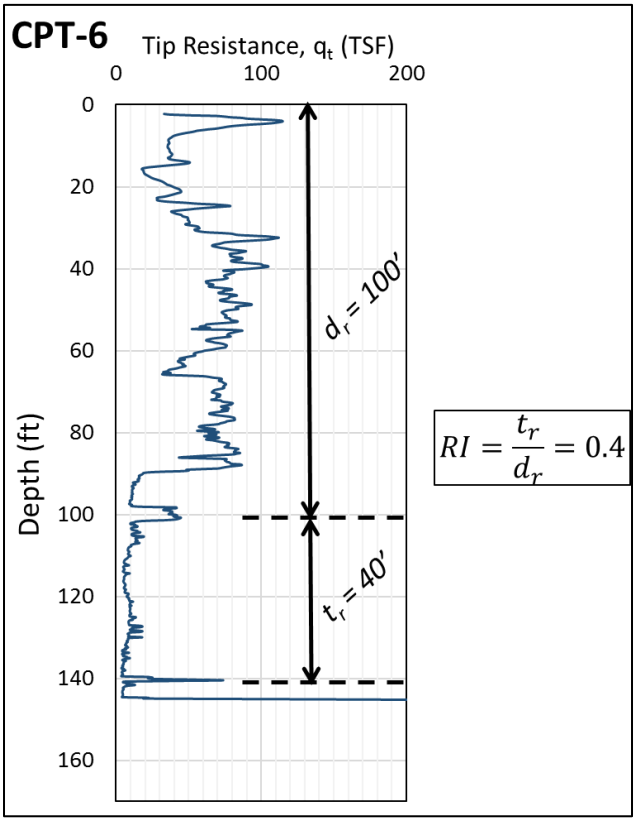

Figure 3-4: Raveling Index example from CPT

3.4 Methodology

The objective of this chapter is to understand how CPTs performed in karst geology in central Florida measure soil stiffness parameters such as cone tip resistance, sleeve friction resistance, and frictional ratio (q_c, f_s, and R_f). The end goal is to develop a processing method geotechnical engineers can use when analyzing CPTs performed in central Florida which suggest a potential sinkhole anomaly. The popular CPT soil behavior type programs, which correlate CPT measurements to soil classifications, are believed to not best represent soil in karst landscapes, especially when raveling may be present. For example, a soil horizon which possesses very low penetration resistance may be falsely represented as sensitive fine grained, organic material, or a fat clay if classified using the latest SBT procedures presented in Robertson 2016 (see Figure 2-5) With hopes to understand and identify trends in how CPTs measure, subsurface data was collected from several known sinkhole active sites in central Florida within the same geotechnical and hydrogeological conditions.

3.4.1 Data collection and preparation

A historical CPT database from central Florida's active sinkhole project sites was graciously provided by FDOT district 5. The database consisted of subsurface data for 12 sinkholes occurring in or near central Florida's highways within the last 15 years. Extensive subsurface exploration test data was also provided for the Wekiva Parkway project, showing large areas of soft soil anomalies; suggesting possibility of sinkhole formation. By developing a CPT data analysis criteria based on the documented sinkhole site data, a sinkhole risk assessment for Wekiva parkway was performed. These criteria in CPT data was developed using all three CPT

data outputs [tip resistance (q_c), sleeve friction (f_s), and friction ratio (R_f)] to identify severely raveled soils; rather than only using q_c as a basis for raveling.

It is important to note that geology in Central Florida, although relatively similar in age and lithology, varies greatly over even a couple miles. For convenience, USGS and FGS have characterized Florida into different geologic categories and present the information on color-coded maps, called Geologic Maps. These categories are created by grouping soils together based on their bedrock age, residual soil formation, depth to bedrock, majority soil types, and permeability. Therefore, when comparing residual soil condition data between different project sites, analysis only was performed between the sites within the similar geologic formation category near the land surface. Out of the 12 total sinkhole occurrence sites provided by FDOT with CPT data, 3 were located within the same geological formation as the Wekiva parkway project. Figure 3-5 presents a map of Central Florida with the three sinkhole sites, the Wekiva parkway site, and the similar residual soil geologic formation – the cypress head formation.

The Cypress head formation (represented by Tc) is composed primarily of siliciclastics and occurs only in the Florida peninsula and eastern parts of Georgia. This formation originates from the upper Pliocene epoch (~ 5.3 to 2.5 million years before present) and consists of reddish brown, unconsolidated to poorly consolidated, fine to very course, clean to clayey sands (FGS, 2001). The cypress head formation is also considered to be very permeable and its sands form part of the surficial aquifer system. In central Florida, the Cypress head formation is underlain by the Hawthorne groups (Th) and Ocala limestone formation (To). (Shown in Figure 3-2)

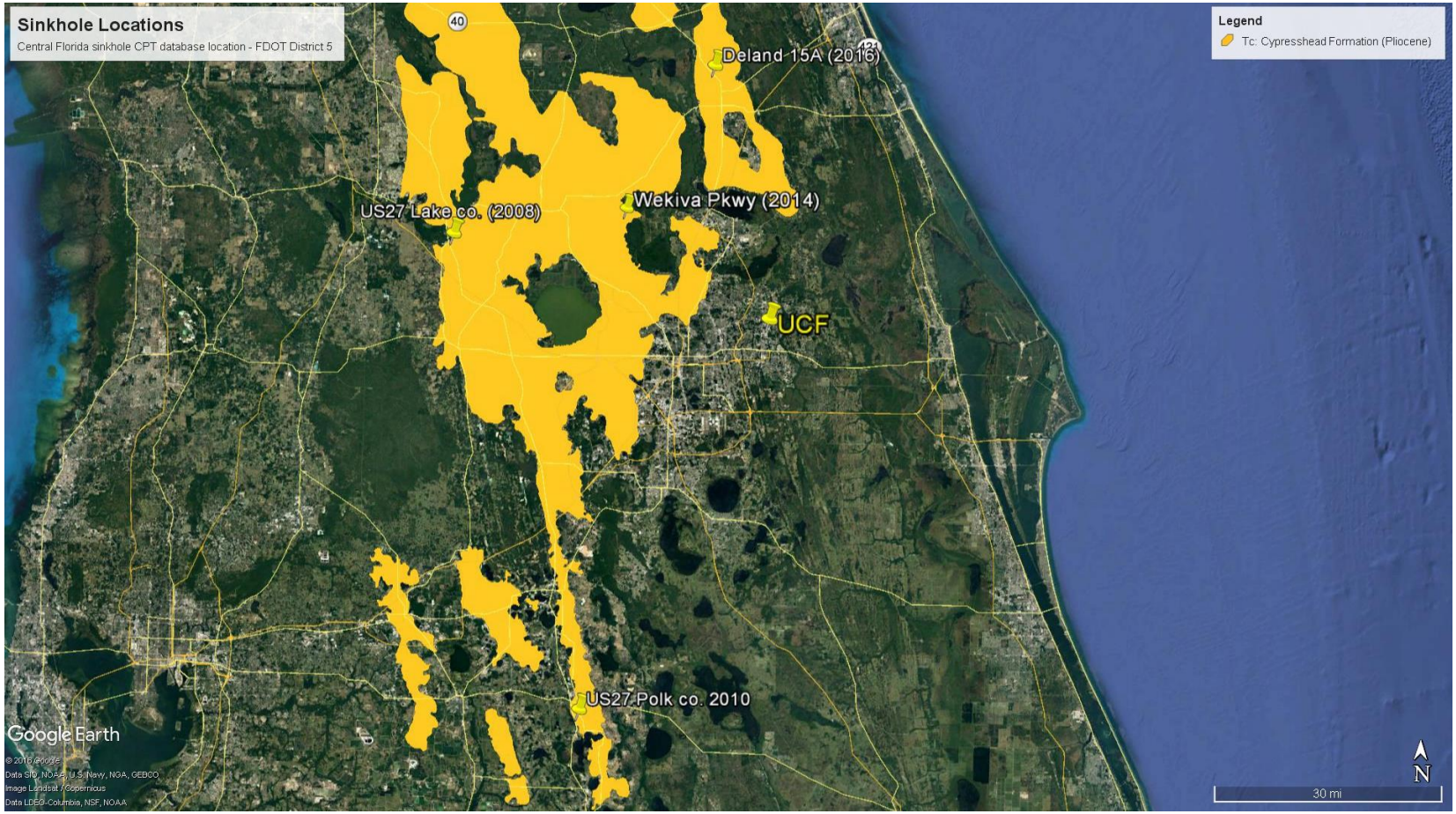

Figure 3-5: Map of Central Florida sinkhole sites within Cypresshead formation geology

3.4.2 Data processing

3.4.2.1 Normalization of tip resistance and friction ratio

Even though we are comparing data obtained in similar geological conditions, the suspected raveling zones are located at varying depths above the limestone. To correct for overburden stresses, a normalization procedure was performed on all CPTs analyzed. Normalization of CPT data to correct for overburden stresses, pore water pressures, and lateral earth pressures is a common procedure in CPT-SBT research (Riaund & Miran, 1992) (Robertson, 2010) (Moss, Seed, & Olsen, 2006). The normalization equations used in this study follow the procedure outlined by Robertson and Wride (1998); presented below:

$$Normalized\ Cone\ Resistance: Q_{tn} = \left(\frac{q_c - \sigma_{vo}}{P_a}\right)\left(\frac{P_a}{\sigma'_{vo}}\right)^n$$

$$Normalized\ Friction\ Ratio: F_R = \frac{f_s}{q_c - \sigma_{vo}} * 100\%$$

Where q_c is the measured cone tip resistance; f_s is the measured sleeve friction resistance; P_a is the atmospheric pressure in the same units as q_c; and σ_{vo} and σ'_{vo} are the total and effective overburden stresses, respectively. The value *n* is the stress exponent and varies from 0.5 in sands to 1.0 in clays (Olsen & Malone, 1988). Since the objective of this research is to simply compare data from each site to each other, an assumed value of 0.65 was used for the stress exponent value of *n* since the encountered soils at the four project sites consisted primarily of sands and silty to clayey sands. To determine the stress variables, an assumption on soil unit weight must be made. An original assumption of γ_{sat} = 110 lb/ft^3 for the entire soil column was made, and a sensitivity analysis (see chapter 3.6.1) showed the ranges of expected unit weight soils at each site would produce

negligible differences in Q_{tn} and R_f in the suspected raveled zones. It should also be noted that the measured sleeve friction value (f_s) was not normalized or corrected for overburden stresses. Normalization of f_s is a highly debated topic and is not well established in the literature.

Groundwater elevations are also needed prior to applying the Normalization equations to determine the effective stress, σ'_{vo}. Most groundwater information for each CPT was obtained from nearby SPT boring logs; which provided an encountered depth to water table. If no nearby SPT was present, an assumed depth to water table was set as 10 feet; which was congruent with the average encountered water table for most analyzed central Florida sites in this study.

3.4.2.2 Filtering "spikes"

CPT is an ideal test for sinkhole detection because it can detect the slightest strength change in the soil strata during penetration due to the high sampling rate. Also, the CPT records tip resistance (q_c) and sleeve friction (f_s) at a constant rate with depth. Consequently, this results in approximately 140 data points for every ten feet of penetration test. In this study, 125 individual CPTs were analyzed; with an average penetration depth of 90 feet. This results in an immense amount of data with an incomprehensible range of scatter (shown in Figure 3-6). To identify trends in the CPT data relating to sinkhole activity only, a simple filtering procedure was performed for each test. The procedure listed below was used to limit the amount of q_c, f_s, and R_f data in obtained CPT data:

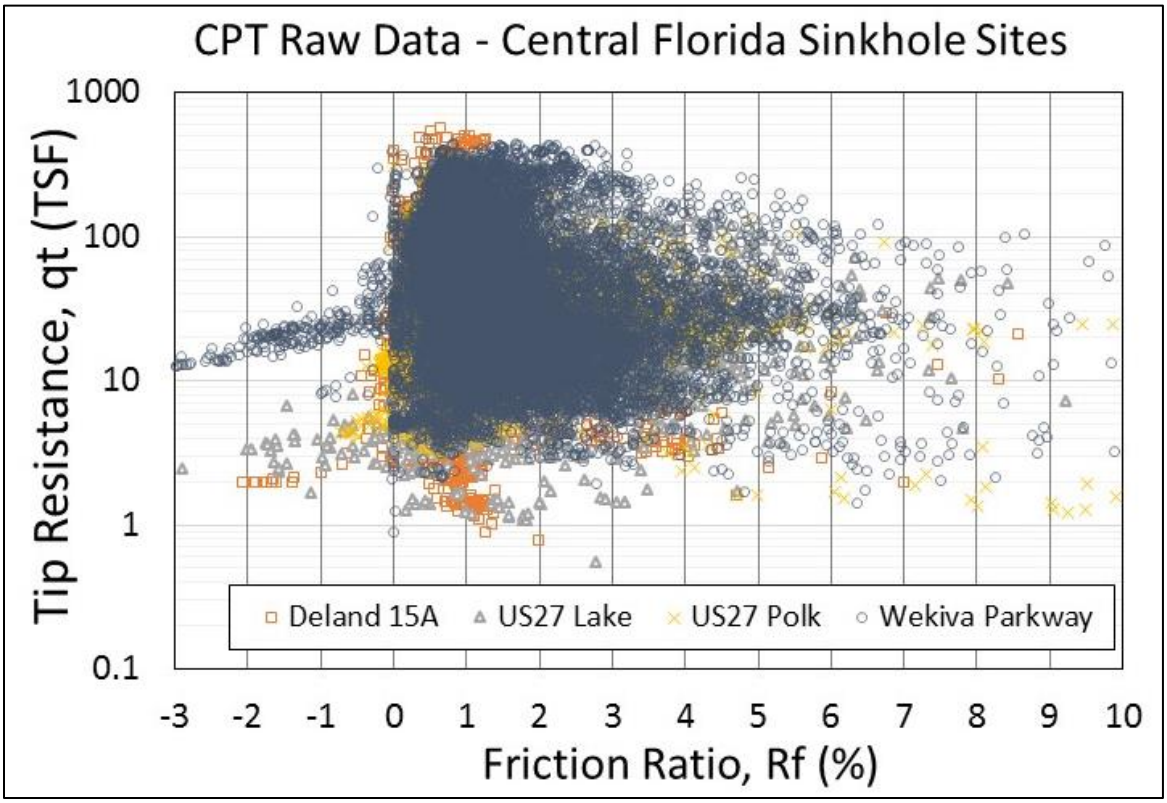

Figure 3-6: SPT-CPT comparison in raveling anomaly with highlighted transitional (yellow) and raveling (red) layers

- First, for CPTs performed within proximity to SPT borings suggesting raveling conditions, an expected depth-of-raveling was established and only data within that window was kept. For most CPTs, this window was around the 50 to 100 feet in depth-mark, although there were some outlier CPTs with much shallower or deeper raveling zones. Figure 3-7 shows an example of such determination using a nearby SPT to filter the non-sinkhole forming soil data out. In this figure, we see specifically how the CPT q_c and f_s curves show similarities between the indication of sinkhole formation provided in the SPT boring log (WH/WR, no recover of sample, and 100% loss of circulation).

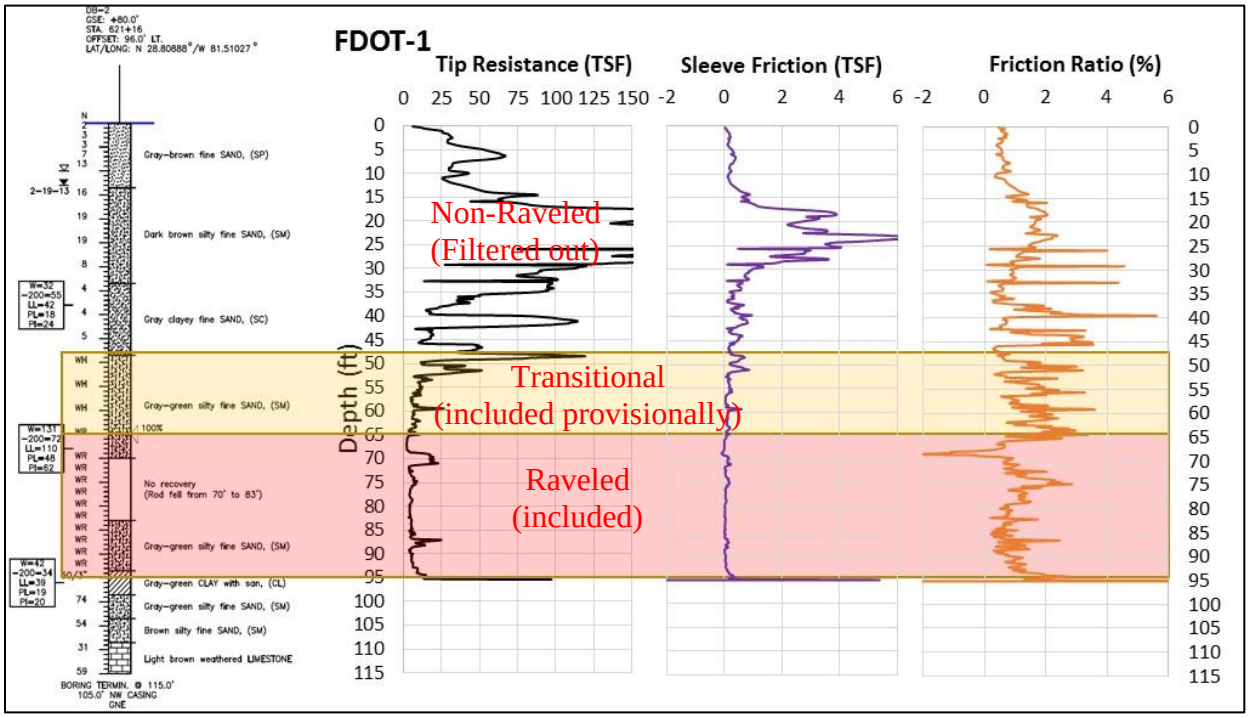

Figure 3-7: Example of SPT- CPT comparison used to filter overburden non-raveled soils

- For CPTs performed without any nearby SPT borings available for validation, the raveled soil zone was assumed to be the abnormally low q_c values directly above the refusal layer. Luckily, the only project sites analyzed which did not have validation SPT borings were those which a had a sinkhole collapse occur. Therefore, the assumption that the encountered soft soils are indicative of sinkhole activity is validated by the nearby collapsed sinkhole.
- Once the raveled soils were determined, further filtered was performed to account for the heterogeneity of the soil. The goal of this filtering process was to identify the data in which only raveled soils is encountered. Even in the raveled soil zones, the penetrating cone sensor can push into interbedded planes of harder material such as limestone lenses

or phosphates. Since the penetrating cone sensor is only roughly 1.5 inches in diameter, even the slightest inconsistency in material density can skew the q_c and f_s curves. This is even more common in central Florida since the raveling of soil originates within the Hawthorne group formation. This geological formation consists of silty or clayey sand interbedded with abundant phosphates minerals; which can range from a couple millimeters to a couple inches in diameter. Any penetration through an intact phosphate mineral can create a "spike" in the CPT q_c curves within the raveled zone, which may give false identification of an actual soil horizon covering more than just a couple millimeters spatially. Therefore, to account for this uncertainty, any abnormal "spikes" in q_c measured within the raveled zone were filtered out. The respective sleeve friction and friction ratios were also filtered out at that specific depth corresponding to the spikes of q_c. Figure 3-8 provides an example of such q_c spikes within the raveling zone.

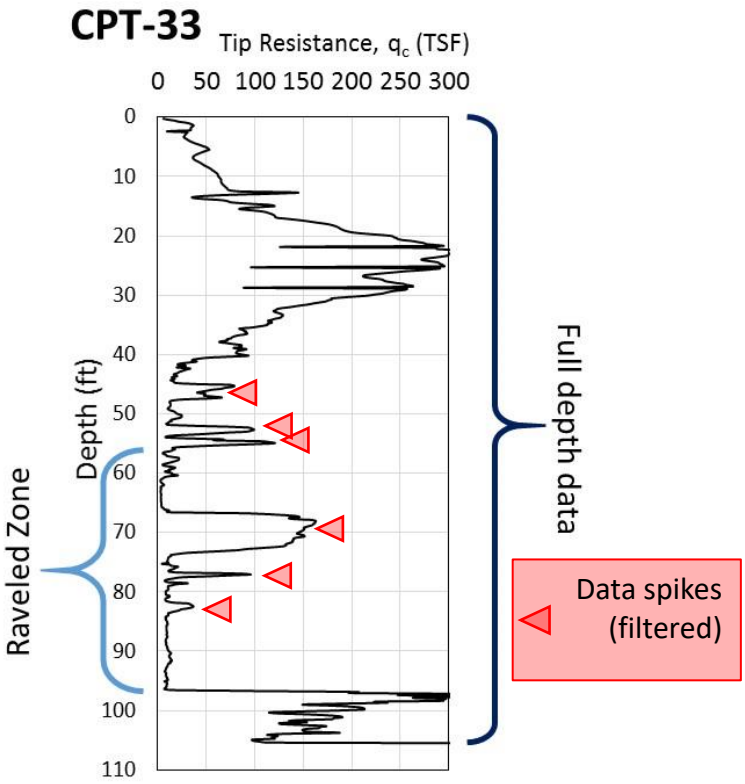

Figure 3-8: Example of CPT q_c with "spikes" in raveling zone

Filtering the CPT data allowed for trends within the q_c, f_s, and R_f parameters to become apparent. This process was performed for each CPT test for corrected values (Q_{tn} & F_R) and for the measured data (q_c, f_s, & R_f).

3.5 Project site Descriptions

The data filtering and processing techniques discussed in the earlier sections were all performed on CPT sounding data obtained from various projects in Central Florida which exhibit karst geology. A total of four sites were used in this study due to their similarities in geology and CPT data. Information and data from all four sites were provided by FDOT district 5 and each involve a state roadway system with either a recent sinkhole collapse or highly variable soil conditions suggesting a potential forming sinkhole.

3.5.1 Wekiva Parkway – SR 46 Connector

Perhaps the most quintessential present example of roadway design within central Florida's karst geology is the currently ongoing Wekiva Parkway Project (expected completion 2022). This project will not only be widening, rebuilding, and averting over 15 miles of existing state and county roads, but when finished, it will connect and complete central Florida's beltway around downtown Orlando. The planned construction of over 25 miles of toll road will pass through East Orange, Lake, and Seminole Counties. Sections of the Wekiva Parkway project cut straight through areas with abundant springs, relic sinkholes, and other signs of karst geology. Standard geotechnical tests for the roadway showed signs of raveled soils at numerous locations. Extensive subsurface exploration testing was performed in certain areas with low settlement thresholds or areas where testing exhibited extensive raveled zones. One of these locations is located just north of the Wekiva Springs State Park near State Road 46 in Lake County. Within this specific section of roadway, over 94 CPTs were performed with all terminating at refusal layer. Over 20 SPTs were also performed, in this specific ½ mile section of roadway, 11 of which performed adjacent to CPTs for ground truthing (an example of such shown in Figure 2-9). Due to the extensive amount of suspected soil raveling encountered, multiple sinkhole mitigation techniques were used for this specific project; even though no visible signs of recent sinkhole activity were apparent on the ground surface. These methods include: deep soil grout injection to fill the suspected subterranean raveled zones, geogrid tension support underneath the roadway to delay subsidence if sinkhole collapse does occur, and complete redesign of planned earth embankment to a bridge. Where each of these methods were employed, a greater density of CPTs were performed to allow for the most efficient design of mitigation type. These mitigation areas are apparent in Figure 3-9, where we see clusters of testing points on the layout. CPT data was grouped during the

normalization and filtering procedures by the type of mitigation technique performed for ease of processing.

3.5.2 Deland State Road 15A

Early January 2016, a sinkhole opened in the north bound lanes of state road 15A, about 0.5 miles south of U.S highway 17, just north of the central Florida city of Deland. Once stabilized, the sinkhole was measured to be about 18 feet in diameter. A total of nine CPTs were performed around the collapsed zone to measure the extent of any subterranean raveling which may have not collapsed. One of such tests performed lost the penetrating cone sensor when the CPT rods fell unexpectedly at a depth of around 12 feet, never to be recovered.

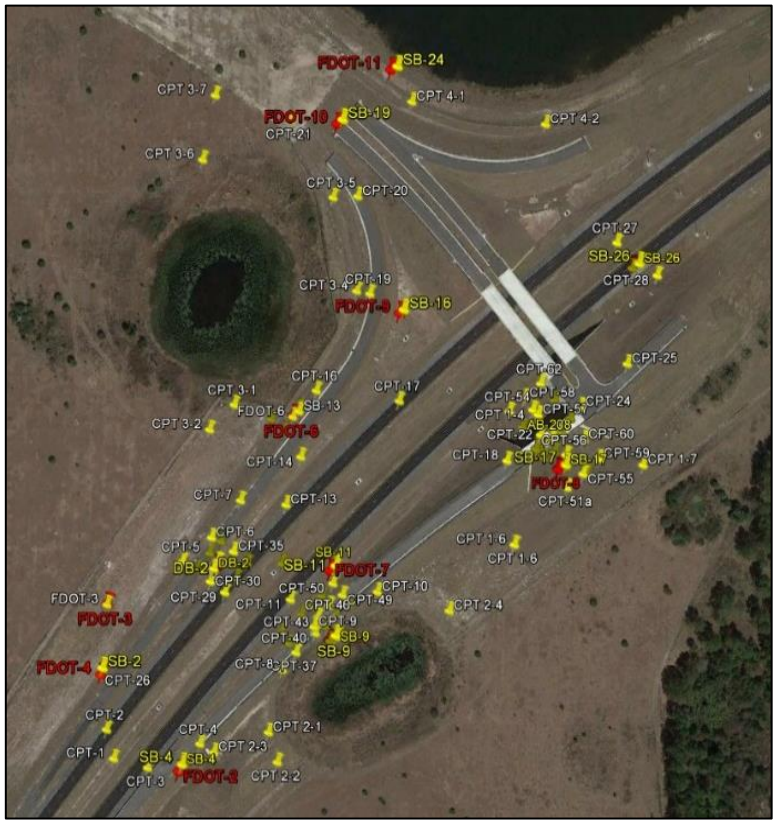

Figure 3-9: Layout of CPTs for Wekiva SR 46 connector project

Once another cone sensor was obtained, an additional test nearby was performed –with greater precaution of extremely loose material— and recorded a large layer of extremely low measured tip resistance (q_c) values between 0 and 2 TSF from a depth of 12 feet to around 75 feet. This specific CPT suggested a significant amount of the sinkhole void did not contribute the collapse on the surface. Therefore, injection grouting was performed for this sink before backfilling to protect against future collapse. The other CPTs performed all showed similar signs of encountered loose material directly above the refusal layer located between 90 – 120 feet in depth. An SPT performed in this location verified the expected penetration depth for weathered limestone was near 100 feet, allowing us to assume the CPTs were terminated at the limestone interface.

3.5.3 US 27 Lake County

On the evening of February 27, 2008, a sinkhole was found at a construction site on U.S. 27 about 0.5 miles north of State Road 48, near Leesburg, Florida. The sink opened in a turn lane under construction adjacent to the northbound lanes of U.S. 27. It was approximately four feet in diameter and extended about seven feet in depth at an angle. No utilities were located within the proximity of the sink, ruling out formation and collapse caused by leaking pipes. A total of 16 CPTs were performed around the collapsed zone. One CPT, located closest to the sink, encountered a layer of abnormally soft soil conditions between the depths of 16 to 82 feet, directly above the refusal layer. CPTs performed further away from the collapse found significantly better soil conditions with the thickness of soft soils only between 0 and 16 feet. All CPTs performed showed similar trends in q_c curves with a refusal layer at a depth between 65 and 85 feet with varying thicknesses of soft soils directly above. The result of investigation indicated a relatively

small area was affected, however stabilization with cement pressure grouting was still performed to minimize the risk of future subsidence.

3.5.4 US 27 Polk County

On January 11th, 2010, a sink hole opened in the median of US 27 in Polk County, approximately 2.6 miles south of state road 60. An initial SPT boring performed in the southbound lane just west of the sink showed weight of hammer (WH) conditions in a silty fine sand layer from 85 to 120 feet in depth with limestone encountered at 133 feet. An additional SPT boring performed in the NB lanes, just east of the sink, showed no WH/WR conditions and limestone was encountered at a depth of 100 feet. An additional six CPTs were also performed around the sink; each of which showing varying degrees of soft material directly above the refusal layer between 110 and 160 feet in depths. All six CPT q_c curves showed similar trends when compared to the SPT blow count (N) values with respect to depth. Cement injection grouting was also performed to repair sinkhole and lessen the likelihood of future collapse.

3.6 Results and Discussion

3.6.1 Normalizing CPT Data

Trends in the Q_{tn} data curves were consistent throughout each test: that is, lower values of q_c encountered at shallower depths resulted in larger values of Q_{tn}, and adversely, lower values of q_c found at deeper depths resulted in much lower values of Q_{tn} (shown in Figure 3-10) This is expected since as depth increases, so will the total and effective stress values. Further trends of

normalization data within sinkhole active sites were noticed and discussion of such implications to sinkhole detection are presented in Chapter 4 of this thesis. The normalization equations for tip resistance and friction ratio require knowledge of soil densities to determine the effective and total stresses at each depth increment. For this study, the assumption of a saturated soil unit weight of 110 lb/ft^3 was used.

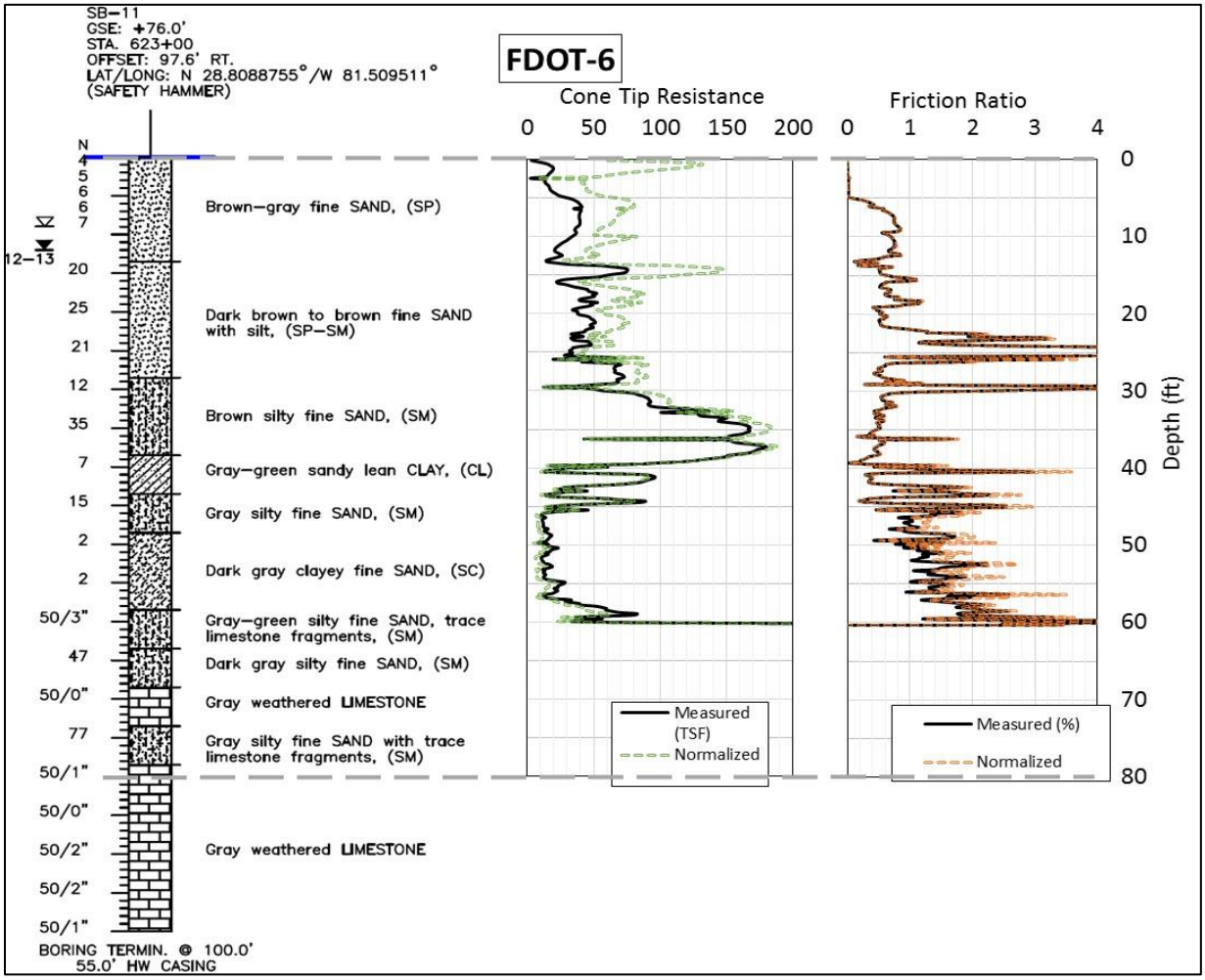

Figure 3-10: SPT-CPT correlation boring showing effects of normalization in CPT data.

A sensitivity analysis was performed to identify the range of calculated Q_{tn} with depth when various unit weights are used to determine the needed stress inputs. Figure 3-11 presents an example CPT from the Wekiva parkway project in which Q_{tn} was calculated using three different saturated unit weights. The three saturated unit weights (90, 110, and 130 lb/ft^3) represent the typically encountered range of soil densities found within the cypresshead formation's sandy soils. Shown in Figure 3-11, the range Q_{tn} corresponding to the range of saturated soil unit weights was found to be relatively small in the soil raveling zones. Also, the resulting normalized friction ratio (F_R) seems to have less of a dependence on soil unit weight at all depths.

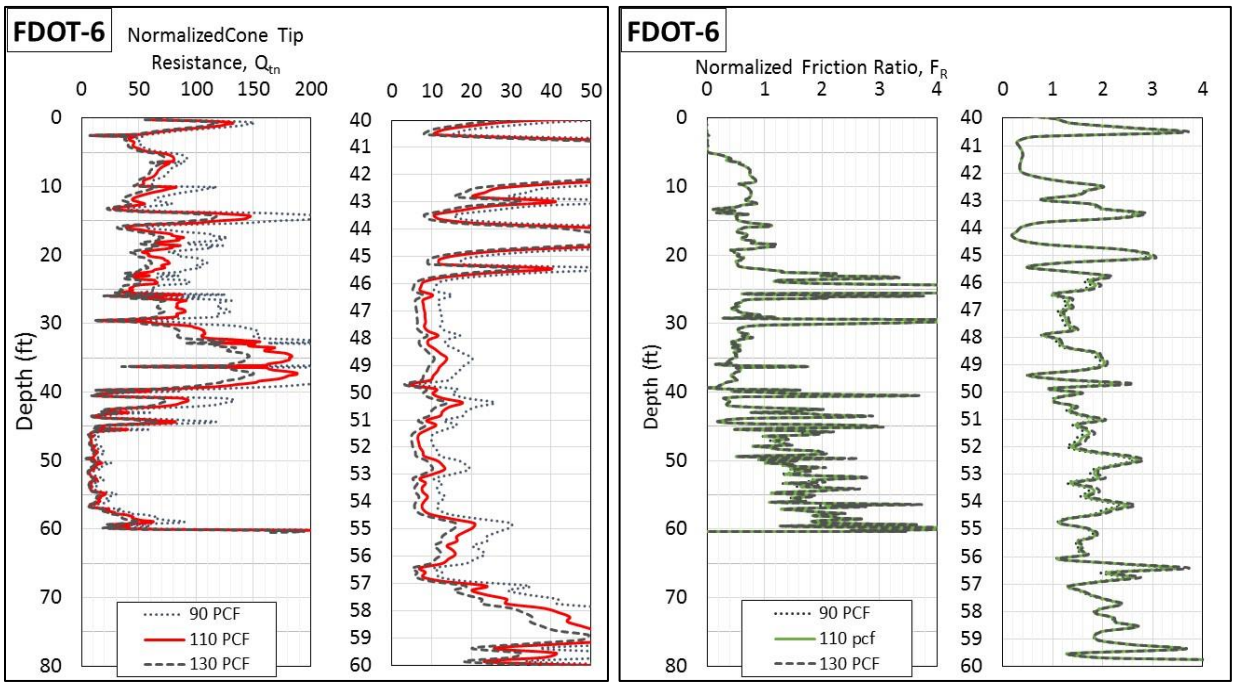

Figure 3-11: Effects of estimating unit weight on values of Q_{tn} and F_R; focus on suspected raveled zone

3.6.2 Filtered CPT Data

The filtering procedure performed on the CPT data greatly decreased the amount of unwanted data in the raveling analysis. Figure 3-12 shows the resulting data histograms before and after filtering. A result of normalization within tip resistance is also apparent when comparing part (a) and part (b) in Figure 3-12. Within the raveled zones, there is a much higher frequency of low Q_{tn} values than in the measured tip resistance values (q_c) in the same tests. All three histograms show the CPT data performed within these sinkhole sites follow a log-normal distribution. After filtering of non-raveled soils, and of any encountered "spikes" in the raveled zone, the typical range of q_c and Q_{tn} values have shown to be within the values of [2 – 32 TSF] and [0 – 26], respectively. This finding suggests that raveled soils may produce tip resistances (q_c) larger than 10 TSF, which is the current practice for detecting raveled material in central Florida, as suggested by Gray (1994). Likewise, an identified range of encountered sleeve friction (f_s) values, within raveled soils, is shown to be within approximately [-0.5 – 1.0 TSF]; which has yet to be established for central Florida soils.

By viewing the histograms of data, CPT data parameters can be compared on a more precise scale within the raveled soils at known active sinkhole sites. Comparison between Q_{tn} and their respective f_s and F_R values can be viewed on a scatter plot, shown in Figures 3-13 and 3-14. Since the values of Q_{tn} are normalized with encountered depth (z), comparison can be made regardless of raveling zone thickness or depth to encountered raveling.

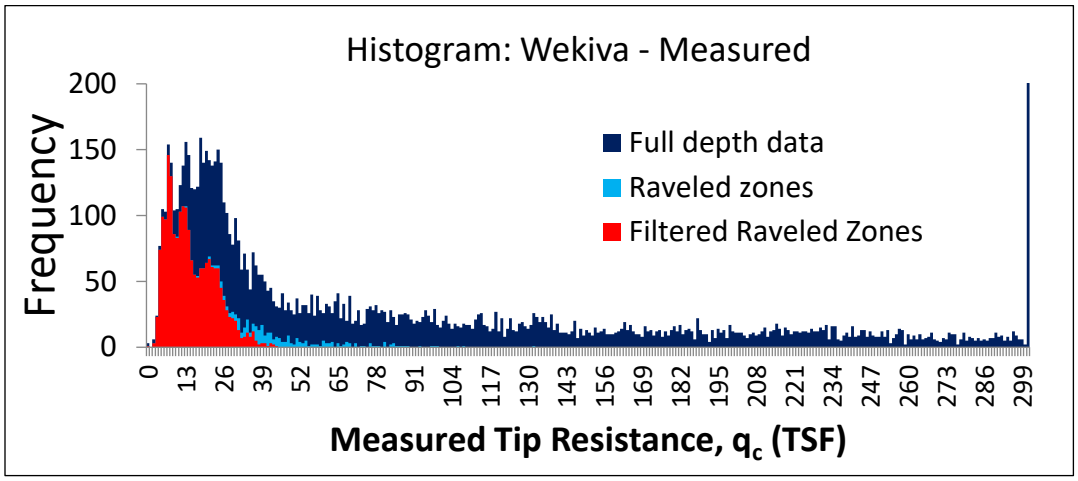

(a) Histograms of CPT measured tip resistance (q_t) data after filtering

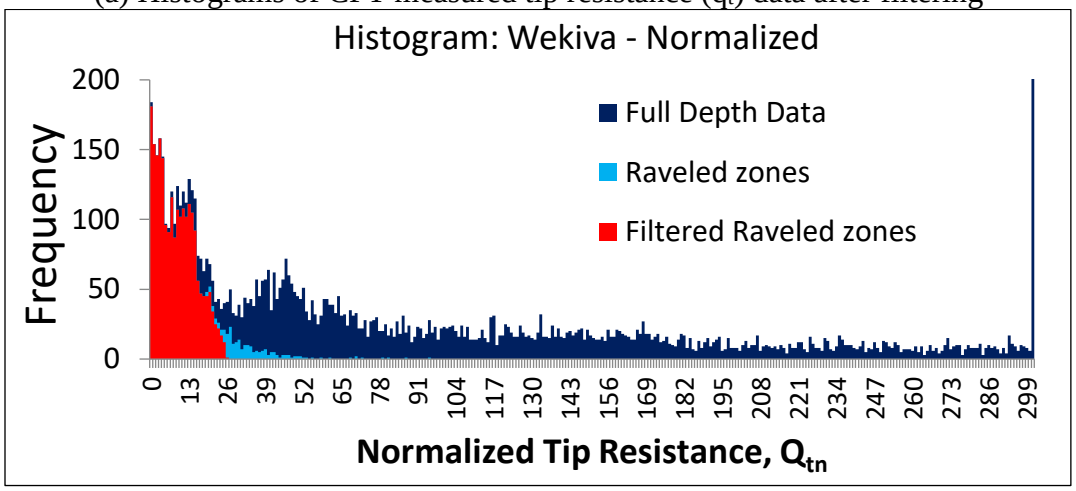

(b) Histograms of CPT normalized tip resistance (Q_{tn}) data after filtering

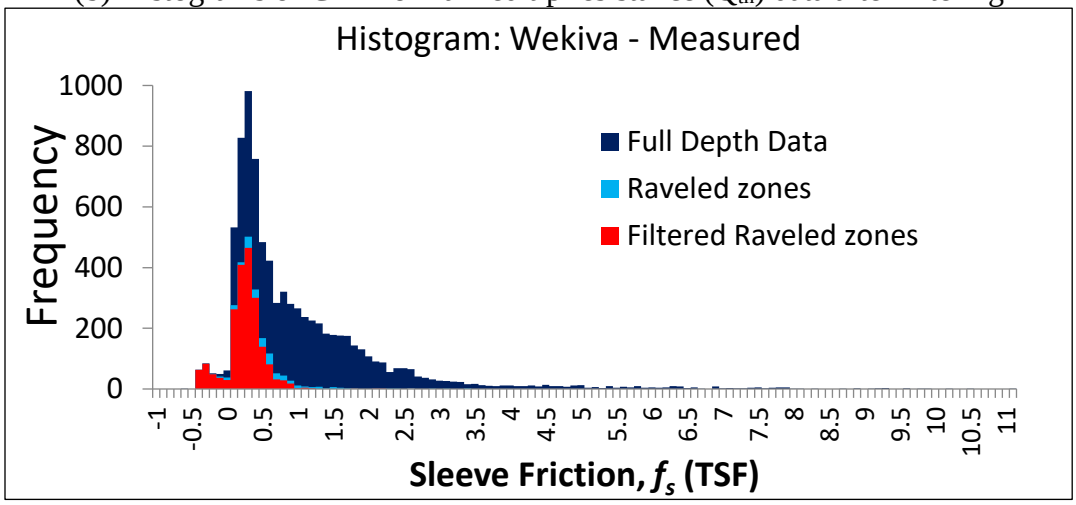

(c) Histograms of CPT measured sleeve friction (f_s) data after filtering

Figure 3-12: Effects of normalization and filtering of CPT data at Wekiva Parkway

Figures 3-13 and 3-14 show the filtered CPT data obtained from the three verified sinkhole sites (left), as well as the filtered CPT data obtained from the suspected sinkhole active site at the Wekiva Parkway (right). From the figures, we see strong comparisons between the collapse site data and the Wekiva Parkway data for both Q_{tn}, f_s, and F_R. The only noticeable discrepancy between the Wekiva data and the sinkhole collapse site data is the negative sleeve friction values measured at the bridge area within the Wekiva Parkway. The negative sleeve friction data was measured at a certain depth within several CPTs performed close to each other; suggesting it is a result of an isolated soil horizon found at the Wekiva Parkway. Further conclusions regarding the negative f_s values were unclear due to the lack of case histories showing this CPT anomaly in the literature. Practicing engineers in central Florida and CPT operators were both uncertain why there exists such large layers of negative skin friction values in central Florida. Both agree that it could be a result of calibration issue within the cone sensors, but also agree that further investigation should be performed to identify if there are any correlations of negative skin friction layers with sinkhole formation/raveling.

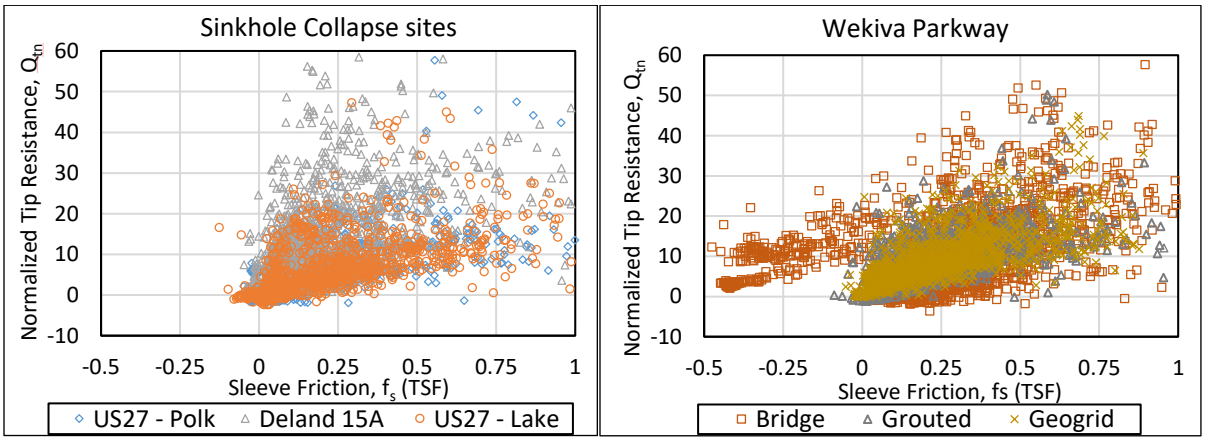

Figure 3-13: CPT raveled data after filtering at study sites (Q_{tn} vs f_s)

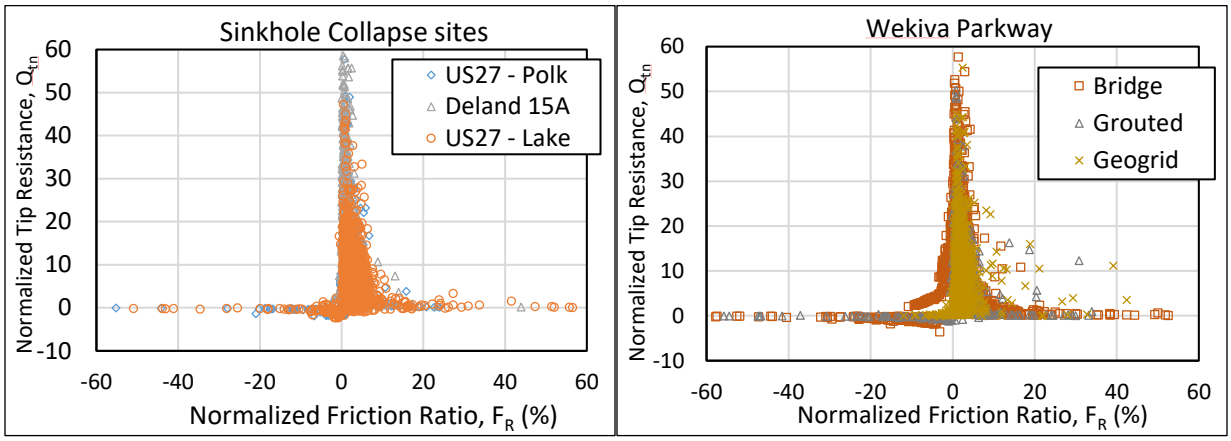

Figure 3-14: CPT raveled data after filtering at study sites (Q_{tn} vs F_R)

Normalizing the friction ratio for soils with very low tip resistance was determined to problematic due to the resultant large number outliers. This result is shown in Figure 3-14 by the large scatter of F_R values as Q_{tn} approaches zero. The normalization equation used for friction ratio has the measured tip resistance (q_c) in the denominator. Therefore, when q_c decreases, the resulting F_R value will increase, especially when q_c is less than one. These outliers within the F_R data never encountered within SBT correlation and CPT data normalization literature review. Therefore, the charts developed in this study to identify raveled soils exclude F_R values and are only developed using Q_{tn} and f_s data. However, the presence of a large-number "spikes" within the normalized friction ratio was found to be congruent with SPT data suggesting sinkhole formation; discussed in further detail in Chapter 5.

The similarity of CPT data between the known raveled soils at the sinkhole active sites and the suspected raveling zones within the Wekiva Parkway project allowed the author to combine all the sites as whole "raveled data-set". Now, out of the 125 total CPTs in which were included in this study, 107 show signs of raveling soils which suggest sinkhole activity is being encountered.

Therefore, 18 CPTs performed (all at the Wekiva parkway site) did not encounter any soft soil anomalies. These CPTs still showed similar stratigraphy trends within the competent layers of soil, however, at depths where the raveling would start, the "safe" CPTs would either hit a refusal layer or a layer exhibiting q_c values of larger values. Figure 3-15 presents such an example of two CPTs performed at Wekiva site with similar curves in the competent soils yet a drastic decrease in q_c for one of the tests at a depth where the hawthorn group should be encountered (CPT-55). The normalized tip resistance and sleeve friction data from the 18 "safe" CPTs was plotted over the respective data from the filtered "Raveled" CPTs that from both Wekiva, and sinkhole active sites. No filtering was performed on the "safe" CPTs since there was no defined raveling zone within these tests.

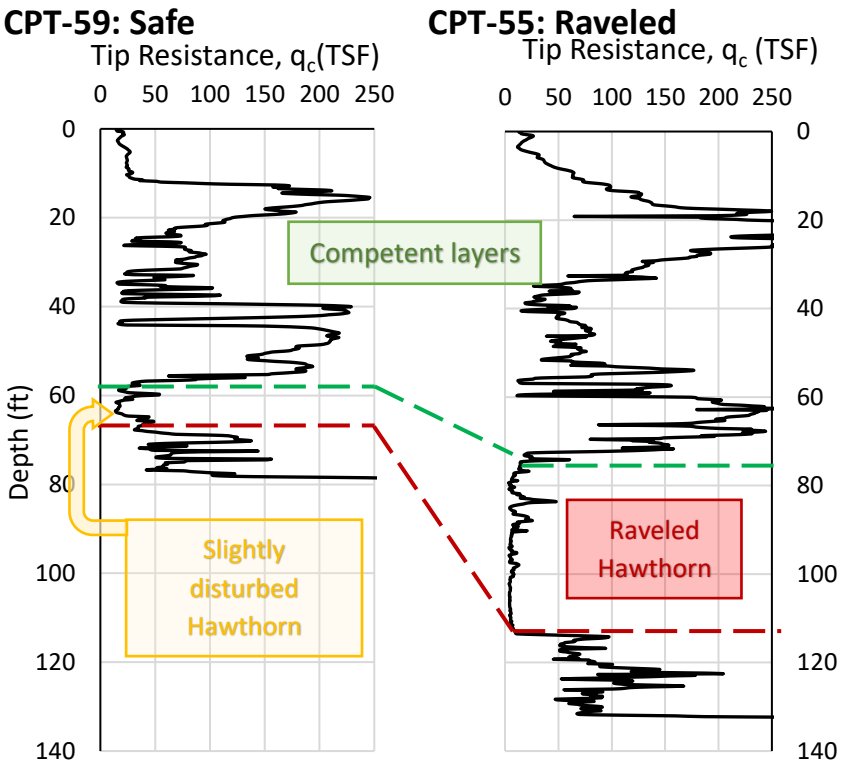

Figure 3-15: Example of "safe" CPT and "Raveled" CPT q_c curves

A clear distinction between the two data groups is apparent in both the Normalized tip resistance (Q_{tn}) and the sleeve friction (f_s) values. The normalized tip resistance data was plotted in log scale since most of the data was within the values of 1 to 5. As shown in Figure 3-16, there is a significant amount of overlapping scatter between the two groups for f_s in the approximate range of [0 – 0.5 TSF] and Q_{tn} in the approximate range of [5 -12]. These ranges are believed to be data collected in the partially disturbed hawthorn group of soils. Verified by SPTs and CPTs performed at sinkhole collapse sites, it is common to find a transitional zone of partially raveled material with decreasing q_c values tapering into the raveled zone. This area is believed to be the "front lines" of internal erosion and is held intact by residual cohesion forces. Physical sinkhole modeling performed in the lab has shown similar results when re-creating a cover-collapse sinkhole (Perez, Nam, Chopra, & Sallam, 2017).

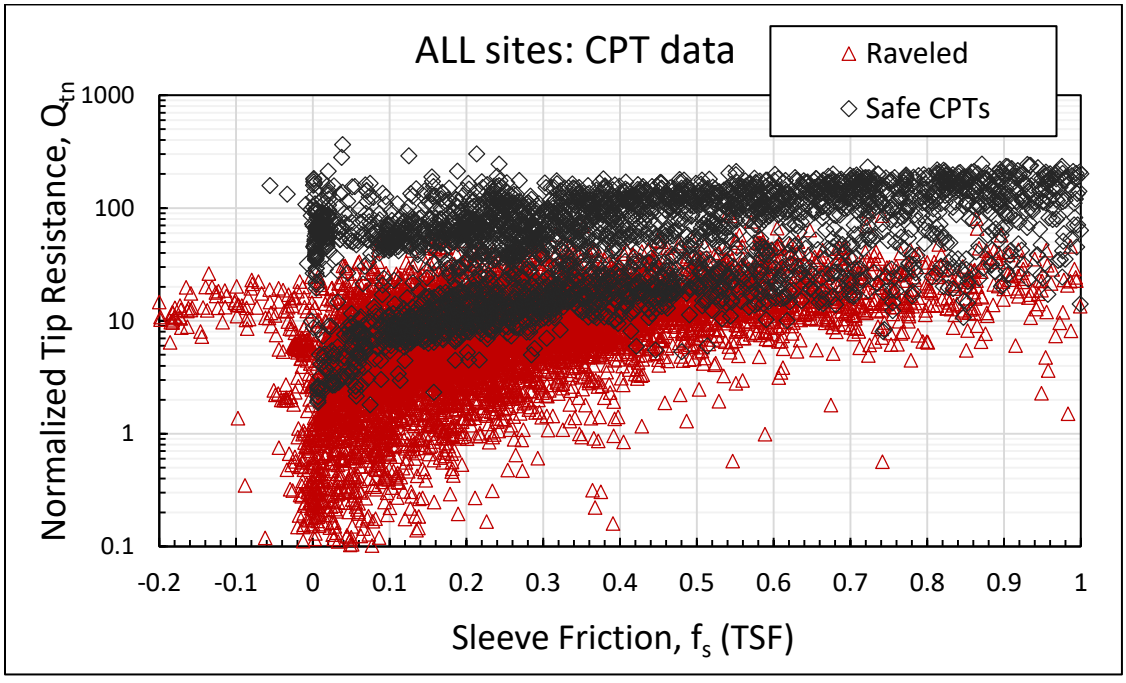

Figure 3-16: CPT data scatter from all sites of both raveled and "safe" tests (Q_{tn} vs f_s)

Figure 3-17 presents an example CPT performed approximately ten feet north of a collapsed sinkhole opening at the US27 Lake County site. Extremely low resistance soils were encountered at a depth of 60 feet with a gradual decrease in q_c starting at approximately the 30-foot mark. A conceptual 2D profile of the sinkhole is shown as well in the figure with approximate location of CPT performed.

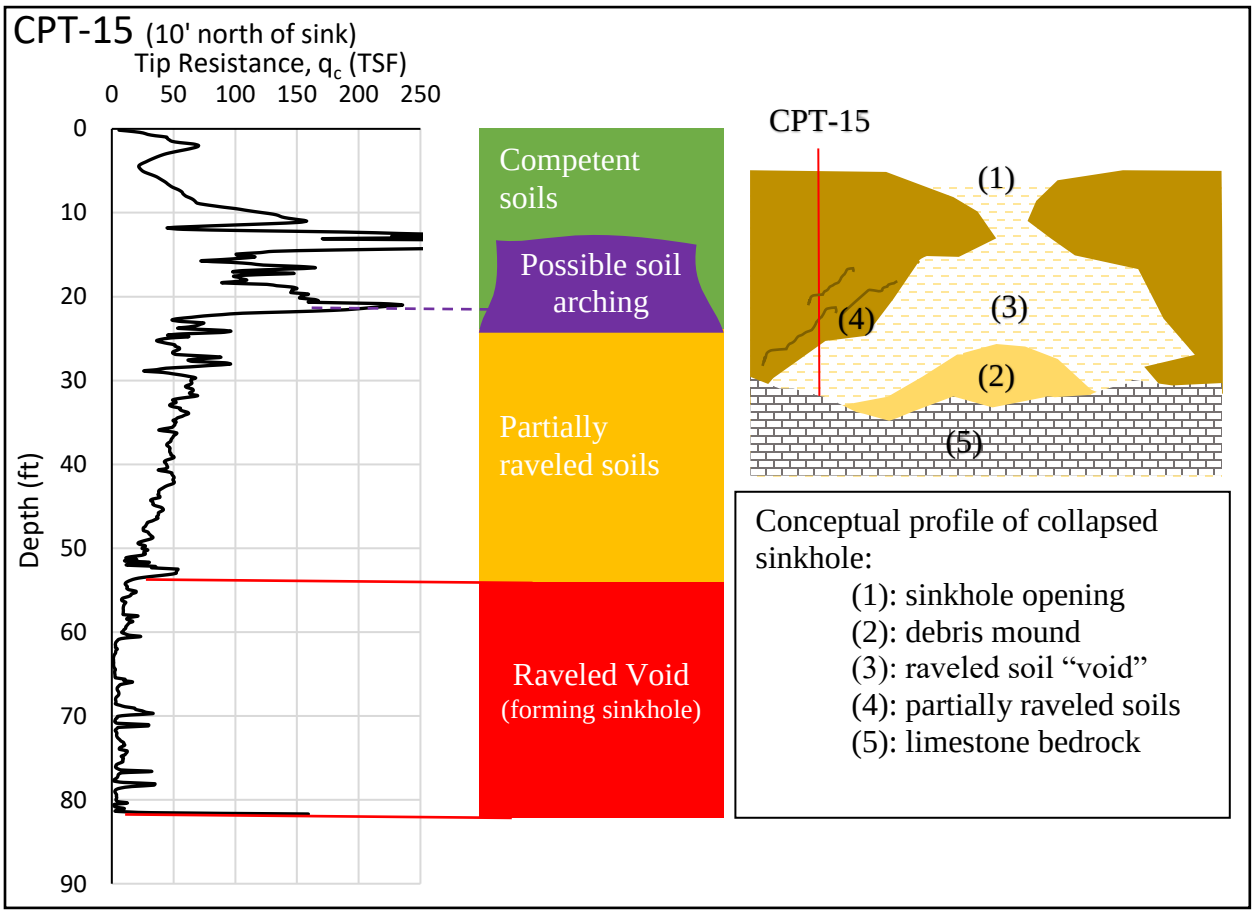

Figure 3-17: CPT performed near collapses sinkhole showing raveling stages within the q_c curve.

3.6.3 CPT-based raveling Chart

The comparison of raveled and safe CPT data shown in Figure 3-16 was used to develop a CPT-based raveling chart for central Florida sites existing within the Cypress head formation of residual soils. This chart, shown in Figure 3-18, was developed as a tool to identify potential raveled soils from Q_{tn} and f_s values obtained from CPT tests. The category envelope lines were created by approximating the ranges of data scatter from the "safe" CPTs and "raveled" CPTs and the overlapping section believed to be partially raveled (or transitional) soils.

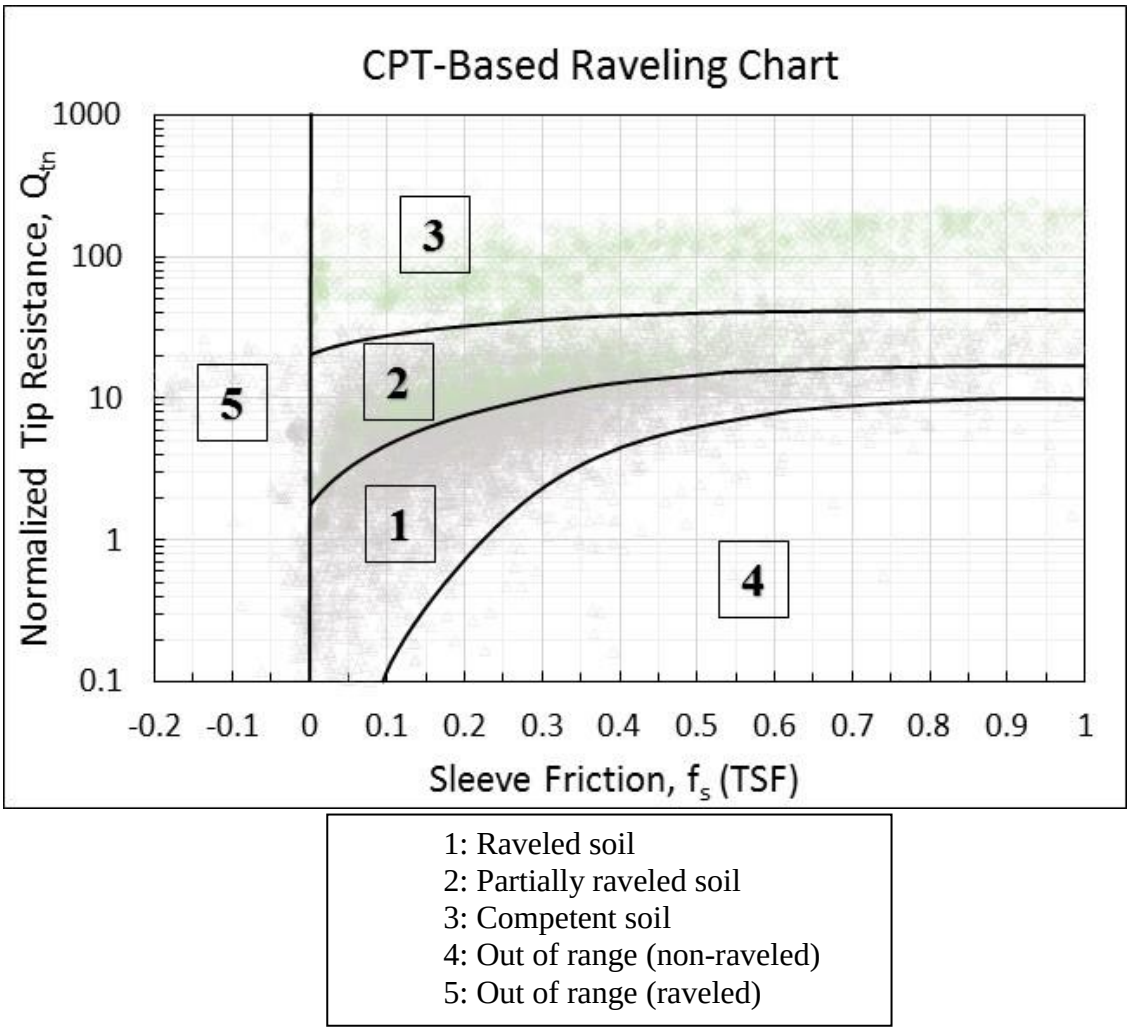

Figure 3-18: Proposed raveling chart using CPT data (Q_{tn} vs f_s) in cypresshead formation (Central Florida)

CPT data within stage 4 is believed to be non-raveled silty clay soils based on review of CPT soil correlation literature (Schmertmann, 1978) (Riaund & Miran, 1992). Stiff, over consolidated clayey soils are not encountered in the central Florida geology which the study sites were located in. Therefore, no data was obtained within these Q_{tn}, f_s ranges. Further investigation should be performed in other geologic conditions to better establish a soil type in this category.

Like stage 4, stage 5 is also out of the range of our data set. Although some negative skin friction values were encountered, the exact origin of the negative skin friction could not be correlated to sinkhole formation with complete certainty due to the lack consistent data in this range. However, any encounter of significant ranges of negative skin friction values, especially if testing in central Florida's karst regions, should warrant additional investigation to determine if the anomalous data is caused by an internal void or by improper cone calibration.

3.7 Conclusions

The information presented within this chapter provides an extensive look into the specific CPT data collected within known sinkhole active sites and suspected sinkhole active sites. CPTs performed in response to three separate sinkhole occurrences in central Florida were analyzed and correlated to a project site, also in central Florida, which had several potential sinkhole anomalies identified by subsurface testing. Although no subsidence or collapse has been detected at the Wekiva parkway site, the suspected raveled soils encountered there showed strong resemblance in CPT data to the verified raveled soils at the collapsed sinkhole sites. After normalization and filtering of raveled soil CPT data, further conclusions could be established regarding methods to identify raveled soils using CPT.

A summary of finding from this chapter are as follows:

- The criteria of identifying raveled soil zones using the CPTs was updated by incorporating values of sleeve friction along with tip resistance. Table 2 compares the current practice for identifying raveled soils and the proposed raveling identification criteria based on CPT data. Further investigation should be performed in other geological formations within central Florida to validate these findings. Also, additional CPTs performed within known sinkhole sites should also be incorporated to this study as they occur in the future. Correlations between measured and normalized friction ratios can also be established with further investigation.
- A CPT based raveling chart was created from trends in the Q_{tn} and f_s values measured within raveled soils in Central Florida's cypresshead soil formation. Plotting scatter CPT data of Q_{tn} vs f_s values from questionable CPTs performed within this specific geology can be used as a tool to identify potential raveled soils. This chart can help assess a risk of future sinkhole during site characterization by correlating any soft soils at a potential sinkhole site, with those obtained from a site with known sinkhole activity (i.e historical collapse)

Table 2: Summary of current and proposed raveled soil detection criteria using CPT parameters.

Source:	Region	CPT Parameters		
		Measured cone resistance, qc	Normalized Cone Resistance, Qtn	Measured sleeve friction, fs
Foshee & Bixler (1994)	Karst Central Florida	< 10 TSF	-	-
This study	Karst Central Florida (cypresshead formation)	-	< 26	< 1.2 TSF

CHAPTER 4: ASSESSMENT OF SINKHOLE HAZARD BY CONE PENETRATION TEST

4.1 Introduction

The object of this chapter is present techniques of assessing risk of sinkhole formation by analysis of CPT data performed in central Florida. Much of central Florida exhibits signs of karst geology in which soluble, porous limestone underlays varying layers of sand and silts. During the subsurface exploration at project sites in central Florida, SPTs and CPTs commonly exhibit layers of abnormally loose or soft soil directly above the limestone interface. As discussed in detail in Chapter 2, these soil layers are suspected to be eroded due to soil migration downward into the cavities of the bedrock. This internal erosion is identified as raveling by many engineers in central Florida. CPTs and SPTs performed in and around collapsed sinkholes in the past have shown this similar trend in data, suggesting raveling identification could be a method of identifying a forming sinkhole before any subsidence may be prevalent on the surface. However, simply identifying areas with soil raveling does not provide enough information for engineers to fully assess the risk of sinkhole collapse on a specific site. In this chapter, specific data analysis tools are presented which will allow geotechnical engineers in central Florida to better understand the severity of raveling and subsequent sinkhole risk by only using cone penetration data. Such tools discussed include both single testing procedures, and group or cluster of CPTs to better understand the expanse or shape of problematic soils.

4.2 CPT-Based Sinkhole Assessment

4.2.1 Point-based Method (1D profile)

The presented in this portion is a method of analyzing a single CPT tip resistance curve to identify the severity of encountered soil raveling. As discussed earlier in this thesis, a normalization procedure was imposed on all CPT q_c and R_f data to allow for comparison between the project sites with different overburden soil thicknesses. Normalized tip resistance (Q_{tn}) and normalized Friction ratio (F_r) were obtained by following the equations below and are both corrected for total and effective stresses assumed at the depth data was collected. Further discussion on assumptions and normalization technique can be found in chapter 3.4.2.1.

Normalized cone resistance,

$$Q_{tn} = \left(\frac{q_c - \sigma_v}{\sigma_v'}\right)^{0.65} \quad (1)$$

Normalized friction ratio,

$$F_r = \left(\frac{f_s}{q_c - \sigma_v}\right) * 100 \quad (2)$$

When applying equation (2) to CPTs exhibiting large raveled zones, an obvious anomaly was noted within the F_r values within the raveled ranges. As shown in Figure 4-1, the normalized friction ratio (F_R) curve spikes drastically in CPT-55 at a depth of about 80 feet, whereas the measured friction ratio (R_F) curve does not. The "positive to negative" spiking trend remains steady until the approximately 110 feet in depth; coincidently the same depth the raveled material stops. The reason behind this is noticeable trend can be seen in equation (2).

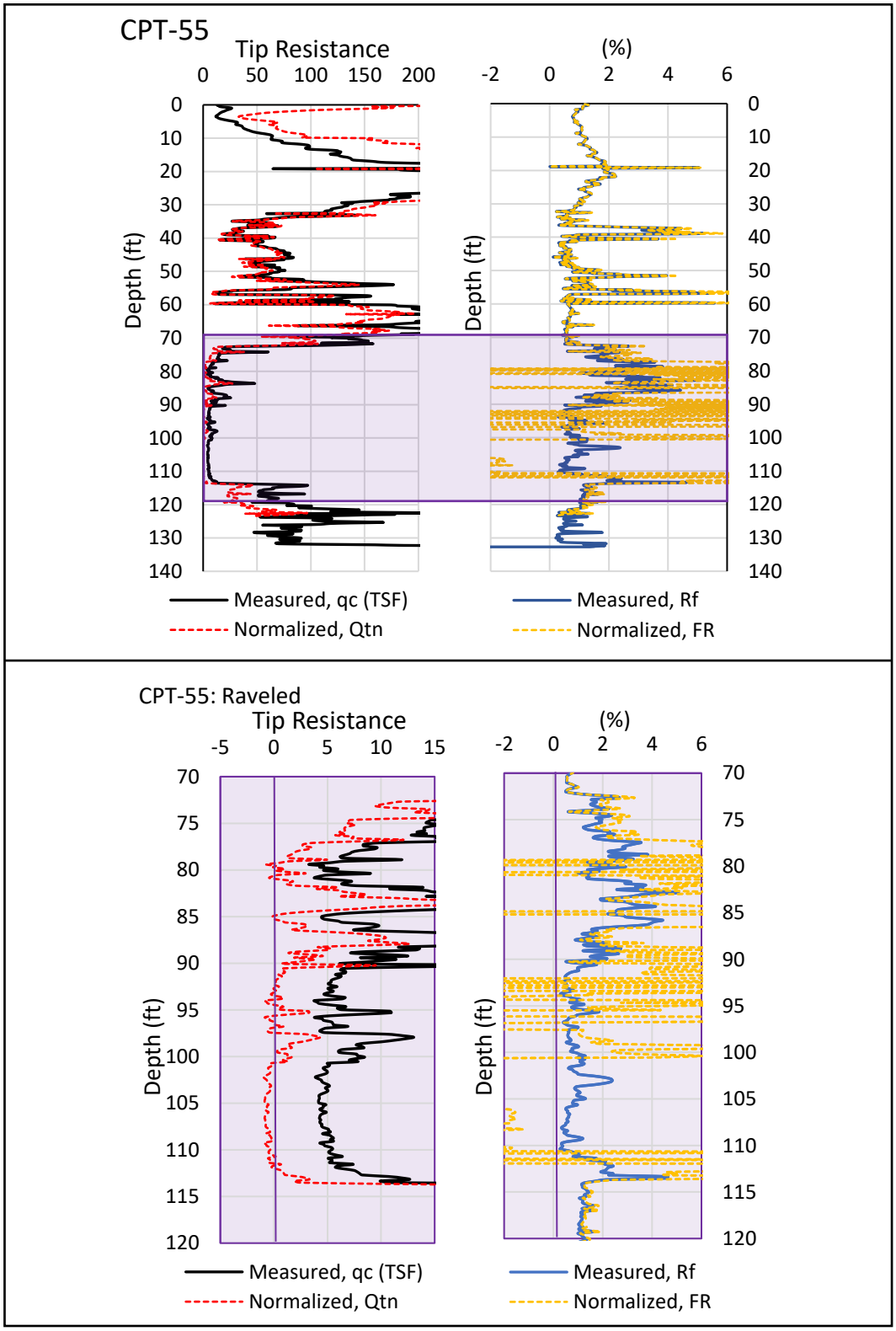

Figure 4-1: CPT showing drastic spiking in F_R data within raveled zone.

At these depths, the total vertical stresses (σ_v) estimated are larger, or near in value, to the measured cone resistance values (q_c); thus, creating a negative value for F_R. The change in data from positive to negative values, and vice-versa, are then accentuated by the denominator in Equation (2) being much smaller than the measured friction ratio so that $q_t - \sigma_v \ll f_s$.

The important thing to note here, is that at a depth, and at a certain measured tip resistance, equations (1) and (2) will yield negative values for Q_{tn} and F_R, respectively. If we assume all soil stresses are in equilibrium, in theory, the measured tip resistance should not be less than the total vertical stress created by the overburden soil column, at that depth. Although the shearing behavior created by the 60^o cone tip is not fully understood, we are still able to assume that given a typical stress profile of soil, the measured resistance value (q_c) should be greater than or equal to some unknown function of the summation of the horizontal and vertical *insitu* stresses; that is $q_c \geq f(\sigma_v + \sigma_h)$. If these values of normalized tip resistance yield negative values, there is a strong possibility that the encountered soil is being eroded and the vertical stresses are being transmitted through the soil plane through an arching effect in order to maintain equilibrium. This conceptual phenomenon was proposed by Terzaghi et. al (1943) and detection of such by CPT-q_c curves was first presented by Schmertmann (1978). Figure 4-2 presents this theory by showing the conceptual stress profiles in typical undisturbed soils, and in soil with arching. Arching will transmit the vertical stresses (σ_v) laterally through the soil, increasing the experienced horizontal stresses (σ_h) directly above the loose zone of soil. Further study into the shearing behavior caused by the cone tip would help verify this assumption of stress behavior correlation to q_c values.

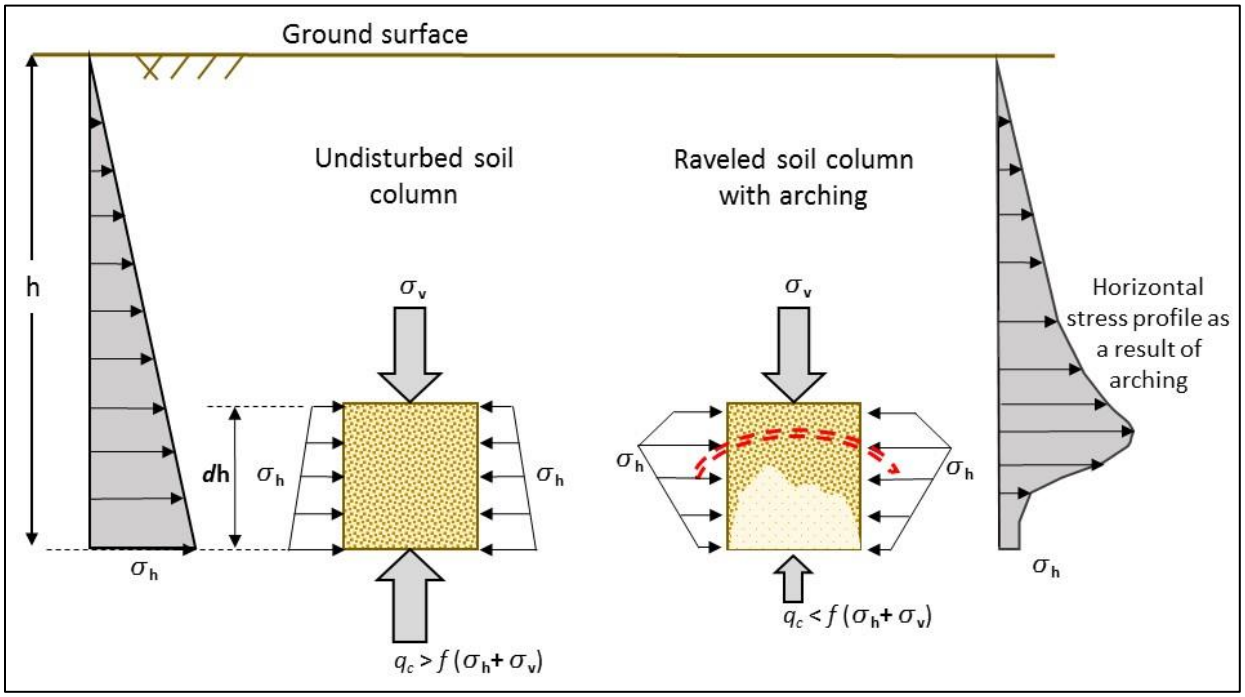

Figure 4-2: Conceptual stress profiles in undisturbed and raveled granular soils with arching phenomenon

The negative normalized values encountered in CPT-55 (figure 4-1) was not an isolated incident, ruling out cone sensor calibration error as a possible source of the anomaly. When looking more closely at the raveled Q_{tn} curve in Figure 4-1, there are some depths in which the measured cone tip resistance is approaching zero, but the resulting Q_{tn} value is still positive. The current accepted practice of identifying raveled soils is encountering a layer of q_c values below or near 10 TSF, as suggested by Foshee and Bixler (1994). This criterion may not yield accurate results if the encountered raveled layered is at a shallow depth and may be stiffer than the measured values suggest—as shown in the normalization procedure.

Therefore, by analyzing the normalization equation and observing data trends with depth, a critical depth can be determined at which the Q_{tn} equation (1) will yield negative results for various values of q_c. The critical depth analysis was performed by first assuming a constant q_c

value with depth. Soil saturated unit weights ranging from 110 to 125 lb/ft^3 were used to estimate the vertical effective and total stresses used in equation (2), and were based on the typically encountered values in central Florida residual sandy soil (Professional Services Inc., 2014). The resulting "critical depths" for each input q_c value were plotted and trends were quickly developed. As expected, the critical envelopes created for each estimated saturated unit weight, followed a linear trend, presented in Figure 4-3. These lines represent the envelope of which the measured q_c value obtained from CPT, will be yield either a positive or a negative value of Q_{tn}. Since most q_c data in the raveled zones are between 0 and 10 TSF, a log-scale was used for the x-axis. Depth was also presented in log-scale then to keep linearity in the envelopes.

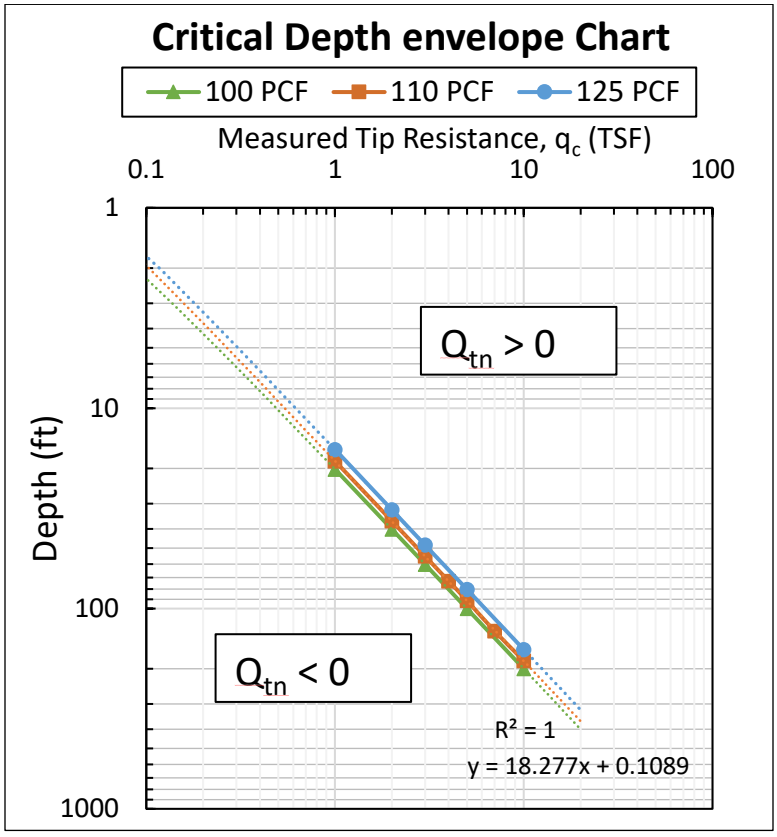

Figure 4-3: Critical depth and q_c envelopes which will yield negative Q_{tn} values.

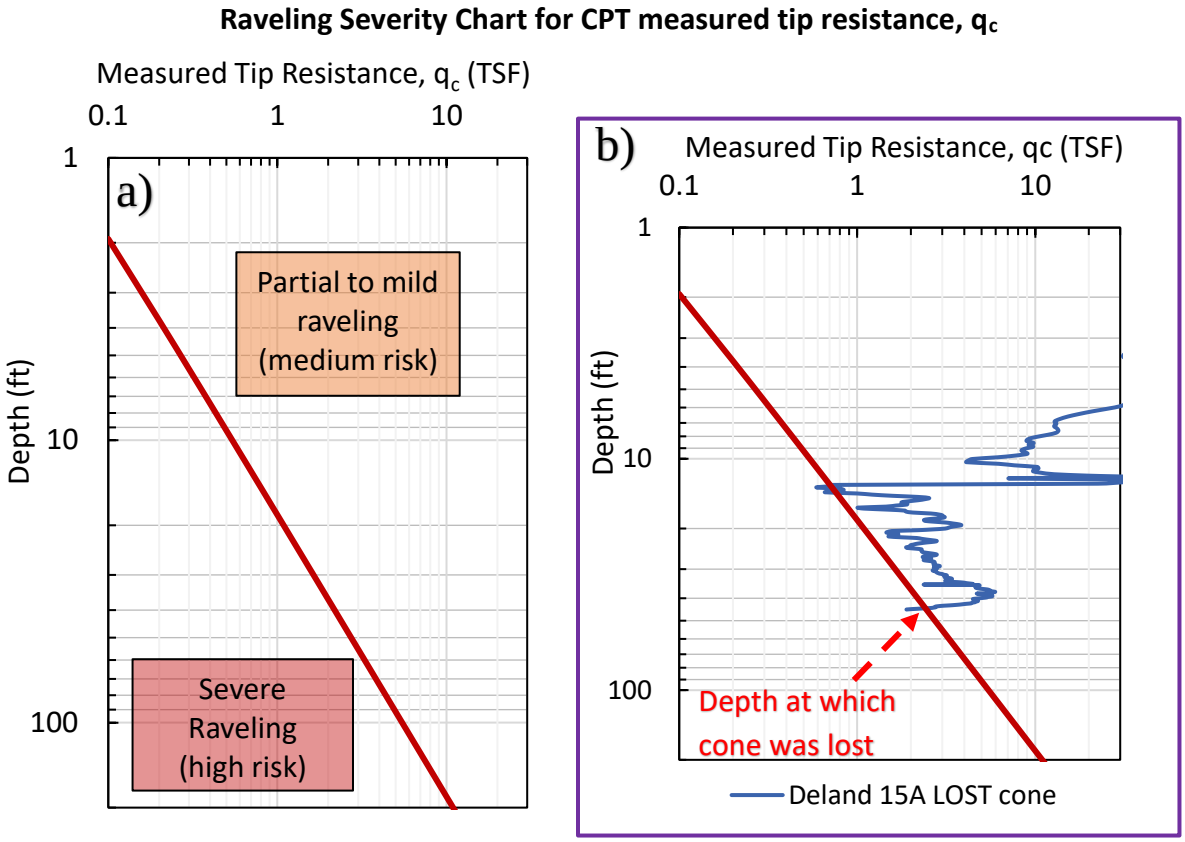

Figure 4-4: (a) CPT-based raveling severity chart for q_c. (b) example of plotted q_c curve from sinkhole site showing critical depth which cone was lost due to severe raveling.

The updated raveling identification criteria presented in chapter 3.7 of this thesis was used to set the q_c bounds presented in figure 4-4. The three envelopes for each assumed soil unit weight were compressed to form the single red line shown in Figure 4-4. This chart can be used to further classify encountered raveled soils based on their severity of raveling. Over time, the erosion and soil grain migration will weaken the overburden soils. Assuming a steady rate of erosion with respect to the many years it may take to form a sinkhole, we can declare that soil showing more severity of raveling, is more mature in sinkhole formation, therefore may be at a larger risk of collapse in the future. Soil that fit this characteristic will be found under the critical envelope line,

when q_c is plotted with depth from a single CPT. Figure 4-4b helps with verification of the proposed chart. In this figure, a CPT performed at the Deland 15A sinkhole site is plotted on the Raveling Severity chart. This specific CPT is unique in the fact that the test was terminated prematurely due to loss of the cone tip. During penetration, the cone sensor and pushing rods fell abruptly into the ground; not able to ever be recovered. Since this test was performed within 25 feet of a collapsed sinkhole, the abrupt fall of CPT rods was suspected to be due to penetration through the sinkhole void. However, a subsequent test performed within a few feet of the lost cone – and performed with much greater caution—measured resistance values, although extremely small, past the depth at which the previous cone was lost. This suggests that although there is no 100% air or water void at these depths, the soil within this zone is so raveled that it lacks any sufficient strength characteristics. The cone in the first test was lost at a depth of 42 feet, coincidently right as the q_c curve crosses the raveling severity envelope (shown in Figure 4-4). Although the q_c curve crosses the envelope before this point at a depth of approximately 13 feet, the curve quickly comes back to the "partial to mild raveling" section of the chart, suggesting that the thickness of severe raveling may also be indicative of sinkhole risk. Although strong correlation between the proposed raveling severity chart and a "severe" case CPT from an active sinkhole site was identified, this chart should still be used with caution as a tool for assessing sinkhole potential at central Florida specific sites based on a single CPT-q_c curve.

4.2.2 Area-based method (2D subsurface imaging)

If many initial CPTs show signs of severe raveling, and especially if the subsurface exploration tests are for design of a shallow foundation structure, then additional clusters of CPTs may be performed to identify the boundaries of the sinkhole anomaly. By viewing and comparing

clusters of CPT data within relatively proximity to each other, trends in soil stratigraphy can be more quickly established over a specific area within a project site. Since CPTs provide a great amount of data with depth, by combining multiple CPTs performed in a line, a high resolution 2D profile can be quickly developed to map the encountered bedrock elevations or the severity/thicknesses of raveled zones. Using CPT 2D imaging can also identify the pinnacles and "valleys" of the limestone surface, which are believed to be formed due to subterranean groundwater erosion and may be related to sinkhole formation.

In this study, 2D images of suspected sinkhole formations were created for the Wekiva parkway project site, presented in chapter 4.4. The images were developed by first creating matrices for each CPT performed in each cluster; consisting of q_c versus penetration depth. A MATLAB surface plotting code was then used to create the profiles based on multiple CPTs performed on a line. The surface plot uses linear interpolation between each CPTs' q_c value measured at the same depth. The linear interpolation creates a "staggered" look in the plots and is most likely not the most accurate representation of the soil profile. However, the resulting profiles (shown in Chapter 4.4) offer further information on the connectivity of the raveled zone as well as trends in over burden soil strengths, that an isolated CPT cannot provide. Measured tip resistance (q_c) was used since this technique was only imposed to view trends in soil stratigraphy within a certain area of a project site. If using this technique to compare the severity of raveled zones from one site to another, Normalized tip resistance (Q_{tn}) should be implemented instead.

One of the limitation of CPTs, discussed in earlier chapters, is its inability to penetrate through very dense layers. The maximum density of penetrable soils decreases greatly when attempting to push the CPT tip through hard layers directly below a layer of very loose soil (such

as raveling). Structural buckling can occur in the slender pushing rods due to the lack of horizontal support within the raveled sections. Therefore, CPTs are often terminated at the slightest sign of drastic increase in q_c after the raveled zone is encountered. This could result in misinterpretation of stratigraphy, suggesting the bedrock is starting at a certain elevation when it could just be penetrating through a thin layer of dense clay or lime-silts. Because of this limitation, it is imperative that SPTs be performed within the CPT clusters to understand the general stratigraphy and soil types within the project site. For the 2D subsurface profiles created at the Wekiva site (chapter 4.4) the CPTs were assumed to terminated at the limestone bedrock, and that the encountered bedrock is competent and null of any voids or cavities. We know this is not the case for karst terrain in Central Florida. However, the main purpose of the 2D profiles are to identify trends in the residual fine-grained soils (i.e. raveling), not the bedrock properties.

4.3 Index for Sinkhole Hazard Assessment

The proposed charts and methods presented earlier in this thesis provide tools for estimating the severity or risk of sinkhole forming soils encountered within a project site. However, these procedures lack a quantitative value in which comparison between other project sites can occur. Therefore, an investigation of the current, and newly proposed index, system for characterizing sinkhole risk in central Florida was performed and discussed upon in the next chapters. These indices were both developed using the measured cone resistance (q_c) values and stratigraphy estimations from a single CPT. The resulting indices allow geotechnical engineers to compare a single point-based CPT test, or when grouped with nearby CPTs, can be mapped to pinpoint the expanse of a forming sinkhole on a spatial (latitude vs longitude) map.

4.3.1 Raveling index (RI)

The Raveling Index (RI), suggest by Foshee and Bixler (1994), can be a useful tool to evaluate the sinkhole risk by using a CPT. The index is defined as the thickness of the raveled soil layers divided by the depth to the top of the raveled zone. This ratio gives a relative indication of the degree of erosion which has occurred in the overburden sandy soils encountered in Central Florida. Raveling index equation is shown below (3) and further details regarding development index can be found in chapter 3.3 of this thesis.

$$RI = \left(\frac{t_{ravel}}{t_{overburden}}\right) \quad (3)$$

Although useful, this index has numerous limitations which inhibit its ability to be used for a site to site comparison. The two major limitations are presented below:

- *No consideration of q_c spikes:* Since the Raveling index is a simple ratio of estimated layer thicknesses, there is no consideration for the actual average value of q_c within the raveled zones or the over burden layers. As shown in chapter 3.4.2.2, raveling soil layers may still produce isolated "spikes" in the q_c curve as the cone encounters suspended phosphates or pockets of denser material. Although these spikes may not increase the total strength of that particularly raveled soil layer by much, the presence of such material still can indicate the progression and severity of the raveling phenomena.
- *Not sensitive for depth of encountered raveling:* The raveling index provides a value correlated to the % of overburden that has been raveled. Therefore, it is common to get a value for RI for a variety of different encountered soil raveling thicknesses which may result in various sizes of sinkholes. For example, an encountered 2-foot-thick raveled zone with 10 feet of competent, overburden soils will produce a RI value of 0.2. The resulting

sinkhole in this case, if collapse occurs, may only be a few feet in diameter. If another site has an encountered raveling zone of 10 feet thick, with 50 feet of overburden soil, the resulting RI value will also be 0.2, but resulting sinkhole will most likely be of a much greater size.

With these limitations in mind, a new sinkhole-risk related index was developed to be used in congruent with CPTs performed in central Florida.

4.3.2 Sinkhole Resistance Ratio (SRR)

A proposed update to the raveling index was developed in the form of a resistance ratio. Coined by the authors as the Sinkhole Resistance Ratio (SRR), shown in equation (4); the larger the SRR, the less likely there is of sinkhole formation resulting from that CPT performed. The lower the SRR, the more risk there is of sinkhole occurrence within the encountered stratigraphy.

Sinkhole Resistance Ratio (SRR),

$$SRR = \left(\frac{t_{over}}{t_{ravel}}\right)\left(\frac{q_{over}+q_{ravel}}{100\sigma'_{vo}}\right) \quad (4)$$

Where: q_{over} = Average measured cone resistance in overburden, competent soils (TSF)

q_{ravel} = Average measured cone resistance in raveled zone (TSF)

t_{over} = Depth to encountered raveled zone (i.e. thickness of overburden soil) (ft).

t_{ravel} = Thickness of raveled zone (ft)

σ'_{vo} = Effective vertical stress created from overburden soils (TSF)

To account for the uncertainty of determining the exact depth at which the raveling zone may start (i.e the transition or partially raveled soils), the average values for q_c are used in analysis for over burden and raveled soils. Stability analysis of subterranean using finite element modeling

suggests that an increase in both the overburden soil and the raveled soil strength, will decrease the likelihood of collapse. Therefore, both factors are included in the numerator of equation (3). Likewise, the larger the competent overburden soil thickness is, the greater possibility of arching to support the loose soils underneath, thus delaying the possibility of collapse. Adversely, the larger the encountered raveled thickness, the greater risk of collapse, therefore this term is in the denominator. The vertical effective stress calculated at the top of the raveled zone is meant to create a normalization with depth. The values of stress in TSF is relatively small (1 – 3) compared to the measured tip resistance values (10 – 300), therefore this parameter has little influence on the SRR and is primarily used as a normalization factor. However, not only is it necessary to create a dimensionless SRR number, but the deeper the raveling void is encountered, the greater the calculated σ'_{vo} will be, thus decreasing the value of SRR. Deeper voids have a larger potential of forming a large diameter sinkhole on the ground surface, as proven in FEM and in the case history of sinkhole occurrences. Figure 4-5 presents an example calculation from a CPT performed at US27 Polk county sinkhole.

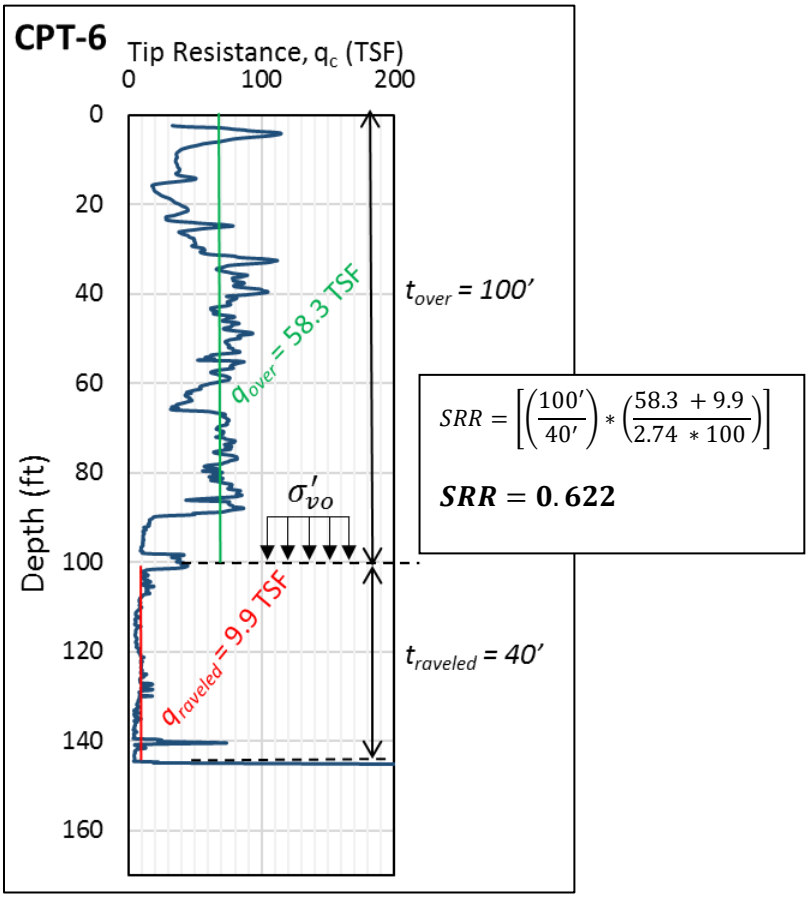

Figure 4-5: Example of how to obtain SRR from CPT.

To obtain the vertical effective stress at variable depths, a correlation equation was used to determine the estimated soil saturated unit weight of the stratigraphy at each depth the CPT records data. The correlation equation (5) is empirically based and suggested by Robertson and Cabal (2010). Caution should be used when using this correlation to unit weight with regards to the type of this equation is calibrated on.

Saturated soil unit weight:

$$\gamma_{sat} = \gamma_w[0.27[\log(R_f)] + 0.36\left[\log\left(\frac{q_c}{P_a}\right)\right] + 1.236] * \frac{G_s}{2.65} \quad (5)$$

Where: γ_w = unit weight of water [62.4 lb/ft^3]

R_f = Friction ratio obtained from measured CPT data

q_c = measured tip resistance (TSF)

P_a = atmospheric pressure (TSF)

G_s = specific gravity of soil

Using this correlation equation, we assume quartz-based soil having a specific gravity of 2.65. Also, the average atmospheric pressure in Central Florida is approximately 30 mmHg; which corresponds to 0.04 TSF, used in equation (5).

By applying this equation at each depth increment from the CPT data, we can develop γ_{sat} vs depth charts allowing us to see how soil density changes with depth. Each CPT from the wekiva parkway site was input and unit weight curves were developed, shown in Figure 4-6. Apparent from the figure, there exists a large amount of scatter within the CPT tests, however a general trend also can be seen if the outlier (spikes) are ignored. This trend is shown by the dotted red line the figure. We see that the estimated saturated soil unit weights range from 90 to 130 TSF within the depths of 0 to 60 feet. Then after approximately 60 feet in depth, the scatter becomes too large to recognize any trends. As one would expect, 60 feet is the typical depth at which the raveling soils start, suggesting that equation (5) is not calibrated correctly for these disturbed zones. Shown in the right side of Figure 4-6 is the calculated vertical effective stress versus depth. This plot shows a much more consistent trend within the CPTs at Wekiva, even though it was created using the saturated unit weights obtained from equation (5). However, at approximately 60 feet in depth, the effective stress of some CPTs remains constant as depth increases, which corresponds with the very low values of soil unit weight. A depth to water table of 10 feet was used for calculation of the effective vertical stress for each CPT, which is the typical depth provided in the SPT boring logs.

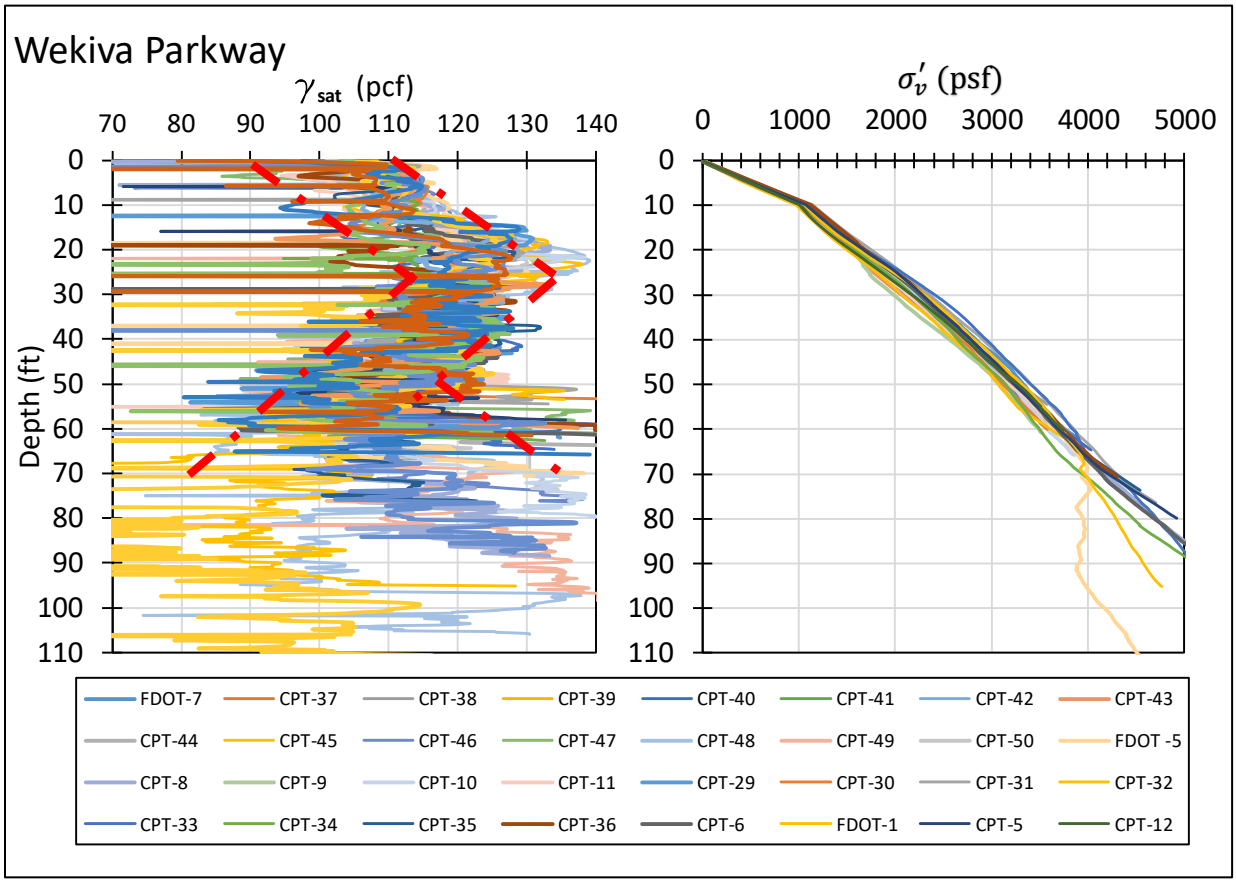

Figure 4-6: Soil saturated unit weights calculated using equation (5) and subsequent vertical effective stress with depth for Wekiva CPTs.

4.4 Case Study (Wekiva site)

An assessment of sinkhole formation risk was performed for the Wekiva Parkway SR 46 connector site, discussed in chapter 3.5.1, using the CPT-based indices and imaging methods discussed earlier in this chapter. The risk assessment was performed on three specific areas within the Wekiva site, in which clusters of CPTs were performed and additional mitigation techniques were decided upon by FDOT engineers due to indication of raveled soils from the initial subsurface exploration.

Figure 4-7: Mitigation zone layout at the Wekiva Parkway study site

A total of 55 CPTs were used for this assessment and values for Raveling index and the proposed Sinkhole Resistance Ratio numbers were calculated and compared for each test. Each CPT was performed on virgin ground, prior to any construction of the roadway or bridges shown in the Wekiva parkway CPT layouts in this chapter. 2-D profiles of CPT tip resistance values (q_c) were created at each CPT cluster, to view the estimated expanse of the soft soil anomalies and to determine if it fits the characteristics of a forming sinkhole. The suspected raveling profiles were developed using multiple CPTs performed on a line. Distance between the CPTs were determined by the given latitude and longitude coordinates of each. Ground surface elevation of each test was

not provided; therefore, the q_c profiles are presented as penetration depth in the y-axis. Topography maps of the project area show very slight ground surface elevation change, and since each test is performed within a spatial distance of less than 300 feet, it is safe to assume any elevation change will be relatively small when compared to the penetration depths of each test (60-120 feet) The three areas analyzed for this case study are presented in Figure 4-7.

4.4.1 Zone 1 – Geotextile area

Zone 1 consists of 20 CPTs and 2 SPTs performed for a planned bridge approach single lane road next to a small natural pond. Tests performed within proximity to the water feature have the largest layers of suspected raveled soils. The calculated Raveling Indices for this zone ranged from 0.11 to 0.92, as shown in Table 3. The resulting SRR numbers for this zone ranged from 5.23 to 0.34. Two interesting facts arise when comparing the two indices from this zone: One being that the CPT corresponding to the largest RI calculated (CPT 45) is different from the CPT corresponding to the smallest SRR value (FDOT-5), and two, that there are several instances where the calculated RI values are the same number. This is explained when looking at the q_c values for the two tests. Although CPT-45 has a thicker raveled zone, the average value for q_c in both the overburden and the raveled layers are larger than those in FDOT-5. The smaller q_c values within the raveled zones suggest further progression of internal erosion. The smaller q_c values within the over burden soils suggests a larger presence of transitional raveling in this layer, or suggests the lack of soil arching stresses which would increase the stability of the soft soil underneath. Both cases increase the risk of sinkhole formation but are not included in the Raveling Index formula.

Figure 4-9 shows the subsurface stratification of line R-R' using the CPT q_c values. From this figure, we see a lack of apparent "bowl" shape, usually indicative of a forming sinkhole void.

Surface contouring of the calculated RI and SRR values within this zone also does not provide any clear indication of concentrated areas with more severe RI or SRR values. However, the encountered soft soil layers do seem to connect in some form, as shown from CPT-40, 42, and 45. This information can be used as a tool to establish risk of future sinkhole formation for this project.

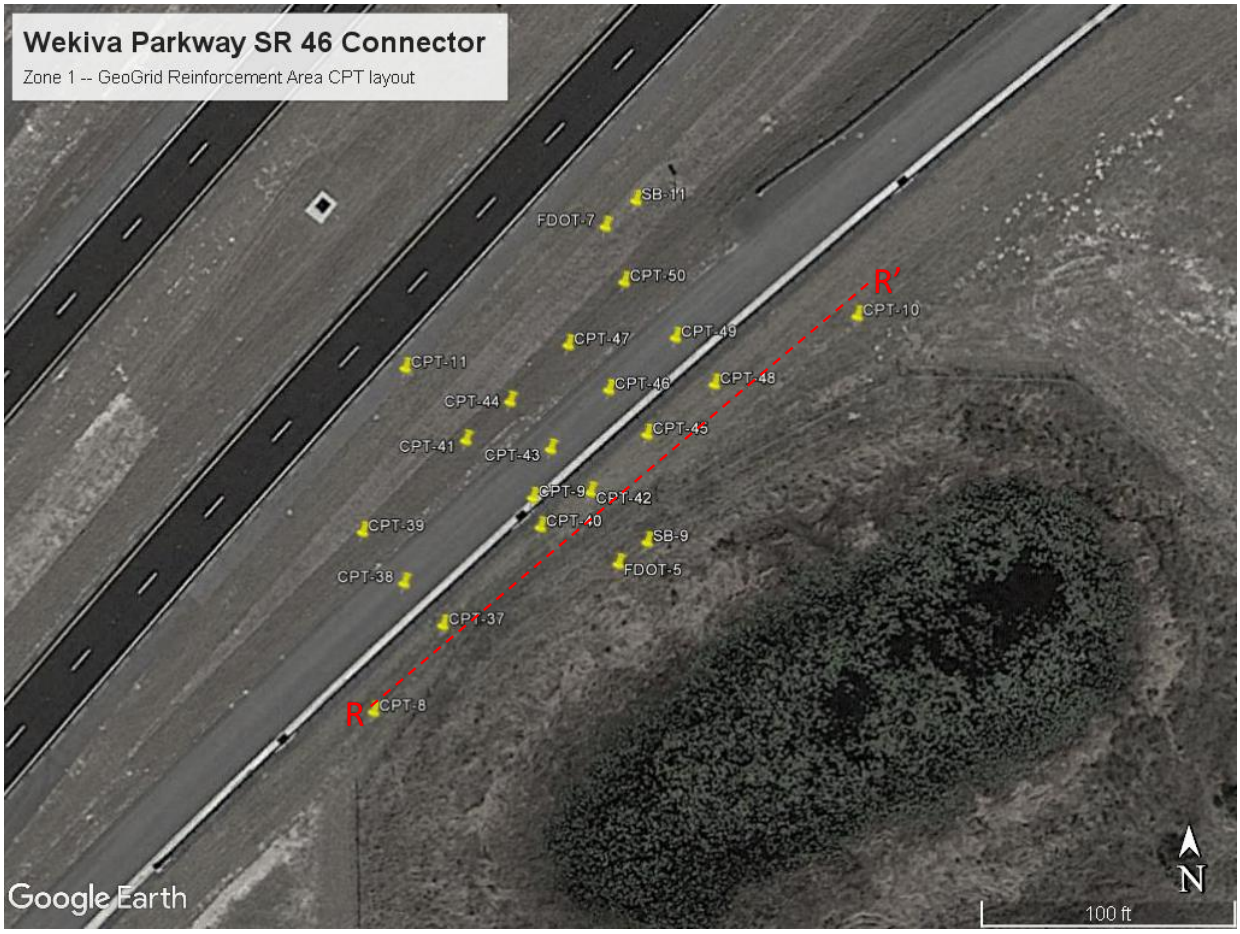

Figure 4-8: CPT cluster and Profile line for Zone 1.

Table 3: Zone 1 raveling characteristics from each CPT

Zone 1 - Geogrid Area	*Thickness (ft)*		*Measured q_c (TSF) average*		σ_v' *(TSF)*	RI [4]	SRR [5]
CPT	*Overburden*	*Raveled*	*Overburden*	*Raveled*			
CPT-45	48.9	45.1	53.24	19.18	1.589	0.92	0.49
FDOT-5	57.3	52.3	46.37	9.46	1.784	0.91	0.34
CPT-10	43.8	21.7	67.42	14.68	1.489	0.49	1.12
CPT-42	51.0	25.1	69.00	15.13	1.682	0.49	1.02
CPT-47	45.0	13.5	66.16	14.94	1.469	0.30	1.85
CPT-49	45.3	13.0	64.72	12.82	1.530	0.29	1.77
CPT-44	47.7	13.1	59.30	11.87	1.555	0.27	1.67
CPT-9	48.4	12.5	50.86	14.96	1.506	0.26	1.70
CPT-8	52.2	11.6	55.34	35.65	1.665	0.22	2.45
CPT-41	50.9	11.3	50.88	15.99	1.594	0.22	1.88
FDOT-7	46.6	10.2	78.23	12.20	1.602	0.22	2.59
CPT-40	48.6	10.0	59.09	17.83	1.583	0.21	2.36
CPT-46	44.0	8.7	50.16	11.65	1.456	0.20	2.14
CPT-50	45.0	8.4	80.17	12.71	1.512	0.19	3.30
CPT-43	47.4	8.5	51.43	13.75	1.534	0.18	2.36
CPT-39	43.5	7.7	76.90	14.66	1.486	0.18	3.47
CPT-37	44.3	6.1	46.66	14.81	1.436	0.14	3.12
CPT-11	54.0	6.7	70.70	14.67	1.699	0.12	4.03
CPT-38	45.3	5.1	74.73	14.63	1.531	0.11	5.20
CPT-48	42.8	4.6	59.23	23.25	1.466	0.11	5.23

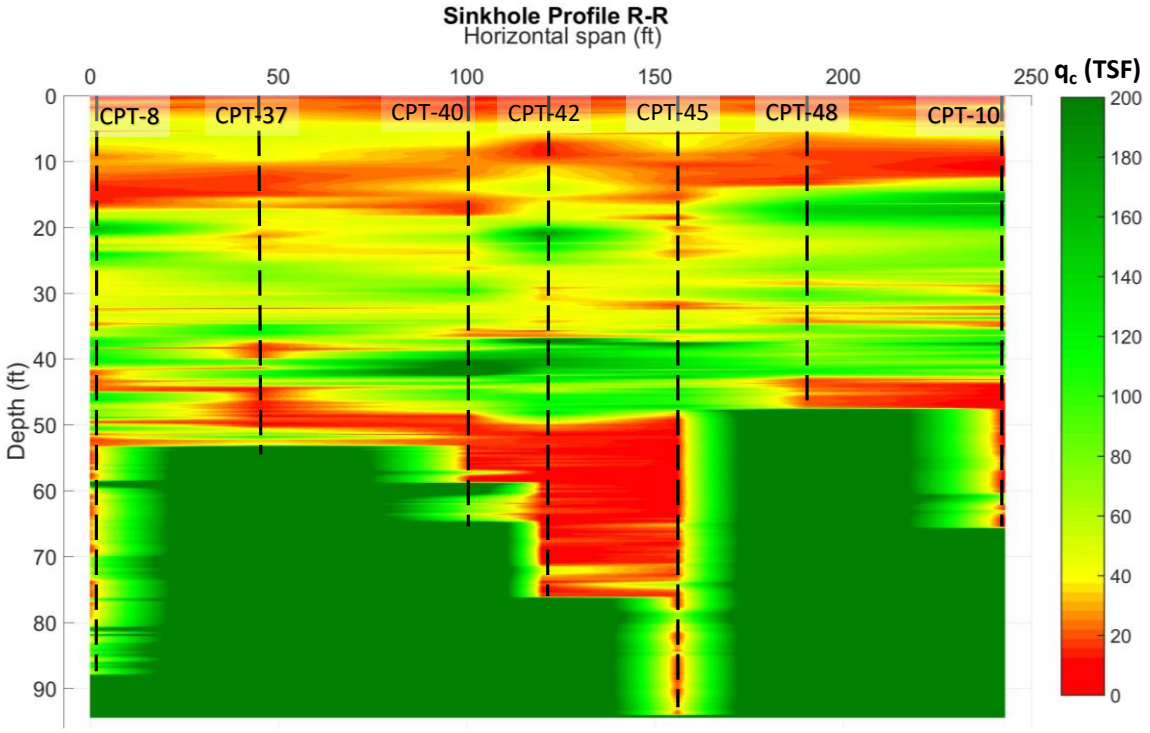

Figure 4-9: Raveling soil profile for line R-R' under Zone 1.

4.4.2 Zone 2 – Grouted area

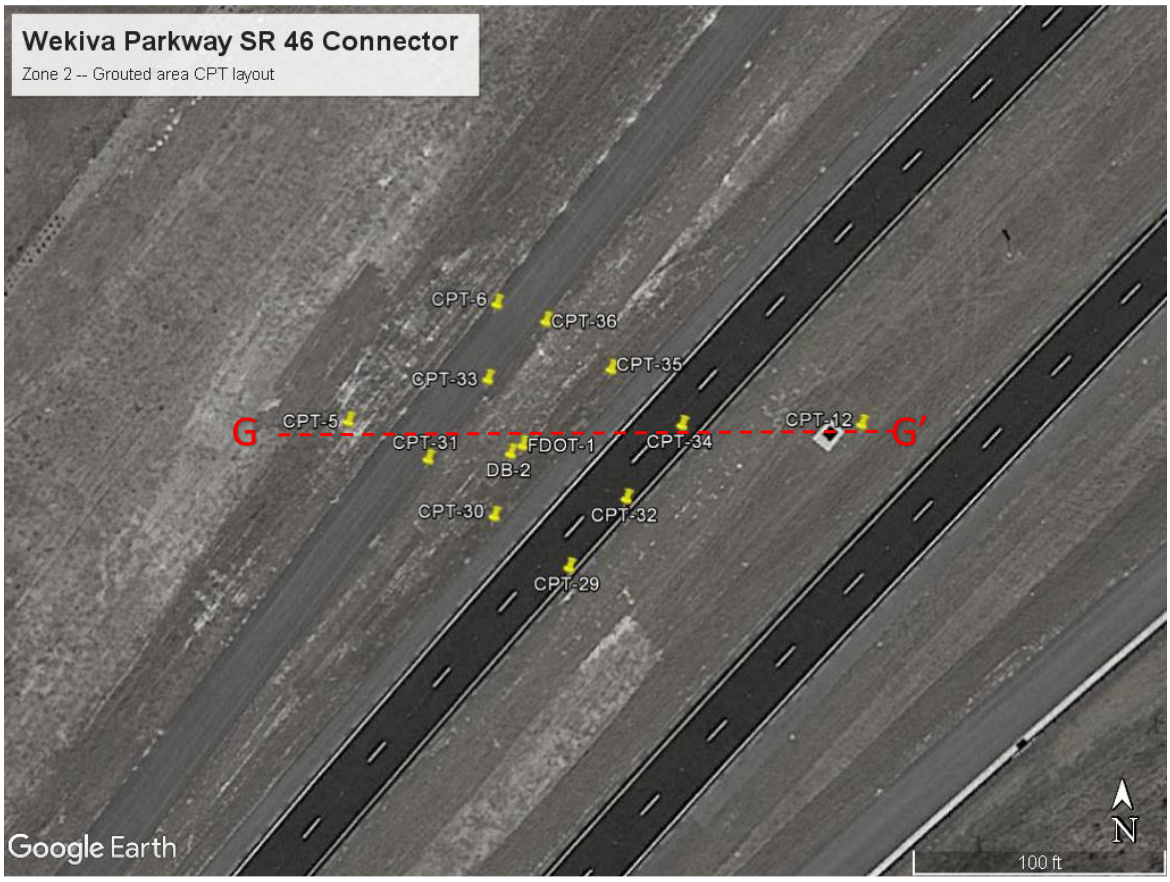

Figure 4-10: CPT cluster and profile line for Zone 2.

A total of 12 CPTs were performed within approximately 0.27 acres surrounding a SPT boring (DB-2) that showed extensive ranges of WR conditions. Many CPTs within this cluster showed large zones of raveling, with concentration of worst case tests in the center. Because of the encountered raveling and the planned heavy-traffic lanes above, cement grouting was performed to mitigate future sinkhole collapse.

Analysis of this zone suggests that grouting was a necessary precaution. Not only are there severe values of RI and SRR within this cluster, but grouping and imaging of CPT test data shows

a “bowl” shape of limestone bedrock, suggestive of a sinkhole void (Figure 4-11). Surface contouring of both RI and SRR strongly correlate with Figure 4-11, showing that the “worst-case” soft-soil anomalies are located within the center of the cluster and become less severe as it expands radially away (presented in Figure 4-12). Also, shown in Figure 4-11 is an increase in q_c measured in the overburden soils above the thickest raveled zone (see dashed ellipse). This increase in q_c may be an indication of soil arching occurring out of plane of the figure. Although not certain, this trend is apparent in many subsurface profiles where the CPT encounters relatively thick layers of very low tip resistant soils.

Table 4: Zone 2 raveling characteristics from each CPT

Zone 2 - Grouted Area	***Thickness (ft)***		***Measured q_c (TSF) average***		σ_v' ***(TSF)***	**RI [4]**	**SRR [5]**
CPT	*Overburden*	*Raveled*	*Overburden*	*Raveled*			
FDOT-1	52.49	42.65	85.83	7.45	1.711	0.81	0.67
CPT-33	55.61	41.01	105.36	32.39	1.716	0.74	1.09
CPT-31	49.05	22.64	77.98	17.53	1.720	0.46	1.20
CPT-5	46.75	21.16	81.18	21.80	1.723	0.45	1.32
CPT-30	41.83	16.73	68.25	14.95	1.727	0.40	1.20
CPT-6	53.31	18.54	71.59	16.27	1.730	0.35	1.46
CPT-35	49.87	15.42	76.38	21.41	1.733	0.31	1.82
CPT-34	50.36	15.42	62.04	9.23	1.737	0.31	1.34
CPT-29	50.52	10.18	72.60	13.36	1.740	0.20	2.45
CPT-32	47.24	8.37	65.79	15.66	1.743	0.18	2.64
CPT-12	51.51	8.86	83.36	21.43	1.746	0.17	3.49
CPT-36	54.63	9.35	63.21	18.24	1.750	0.17	2.72

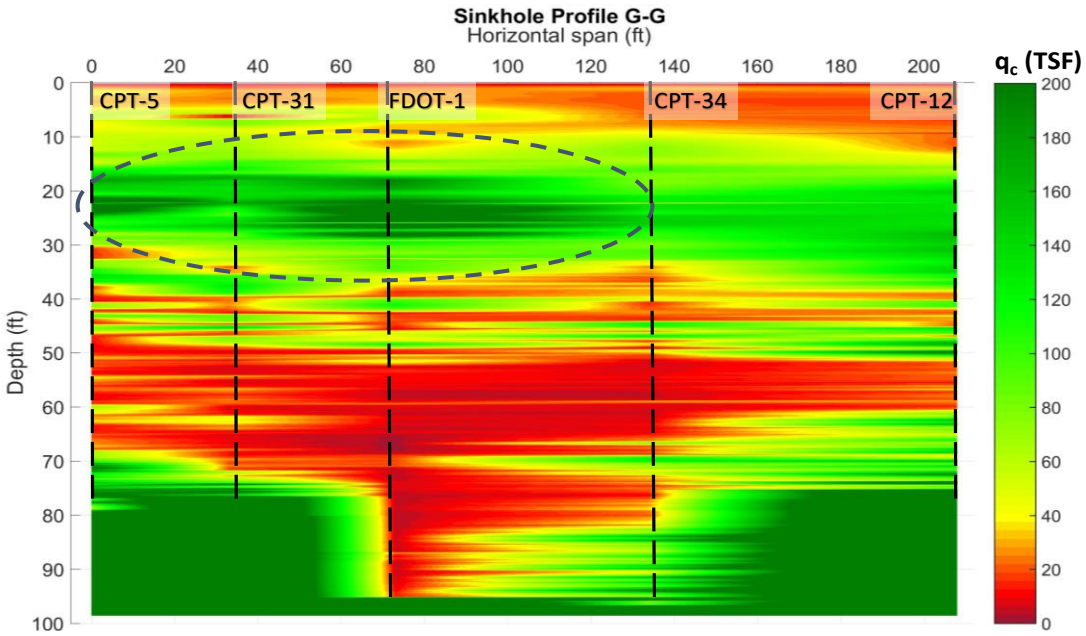

Figure 4-11: Raveling soil profile for line G-G' under Zone 2

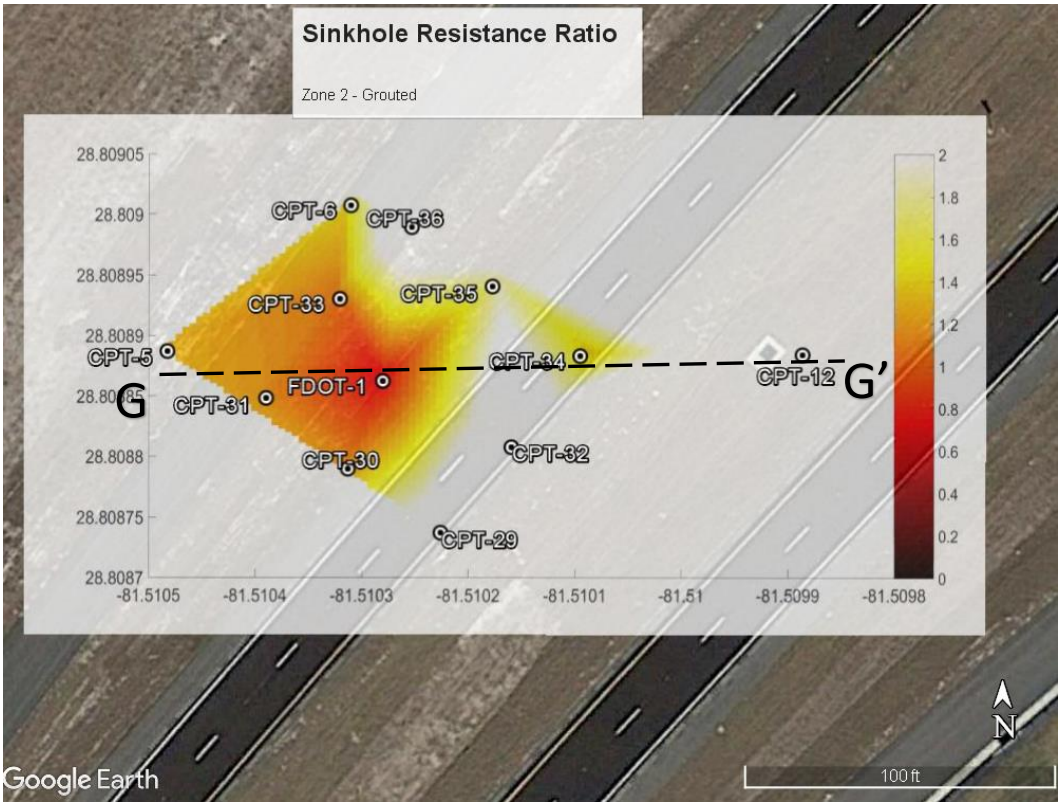

Figure 4-12: Surface contouring of SRR from Zone 2 CPTs

4.4.3 Zone 3 – Bridge area

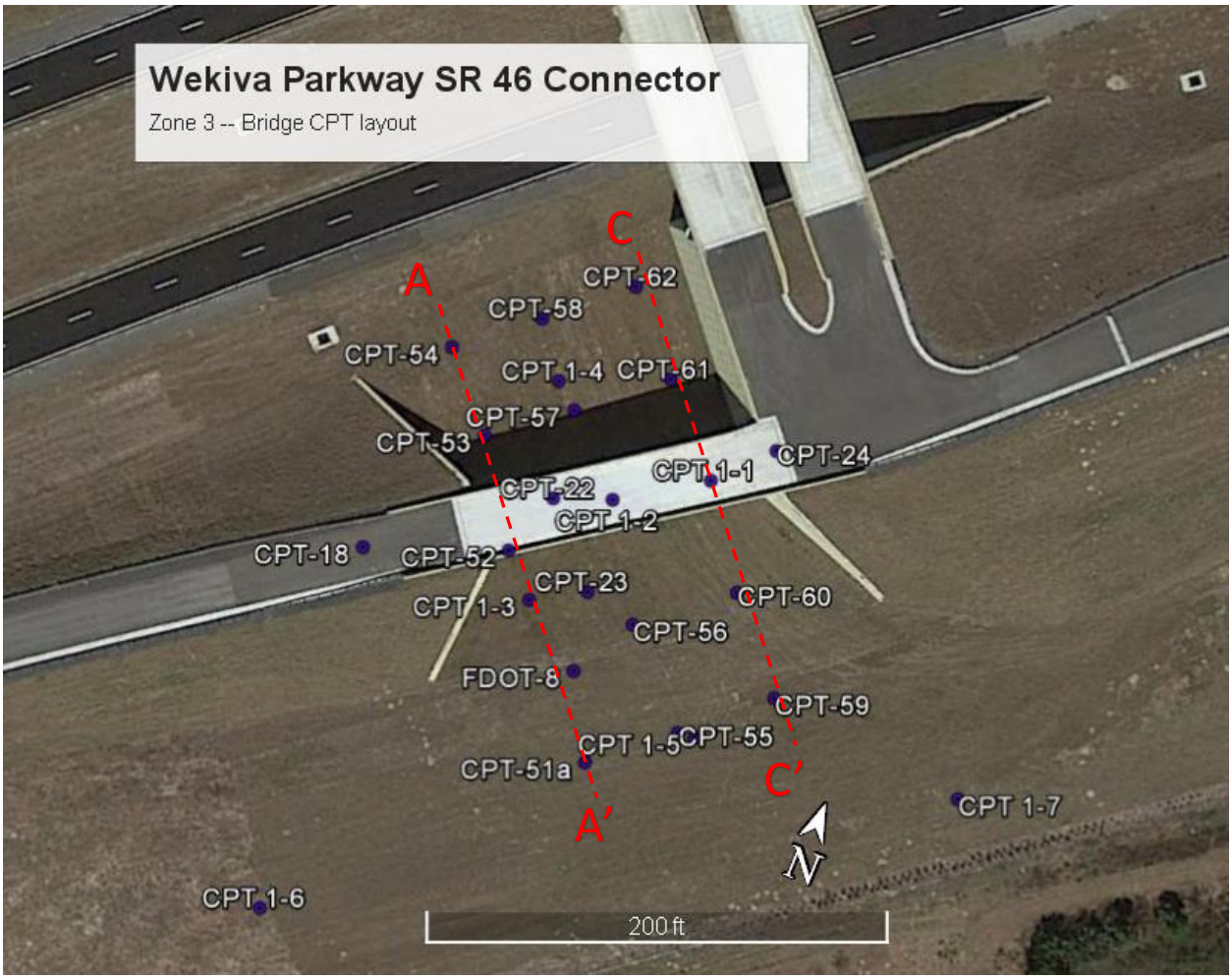

Figure 4-13: CPT cluster and profile lines for Zone 3

Zone 3 consists of a cluster of 23 CPTs and 4 SPTs performed in an area with a planned bridge approach earth embankment. Due to the extensive raveling encountered in these tests, the original earth embankment design was changed to a single-span bridge, supported on a deep pile foundation. After grouting the anomaly in zone 2 had significantly exceeded the estimated costs,

FDOT engineers came to the conclusions that a complete redesign of this bridge approach would be the most economical and safest solution.

Table 5 shows the raveling characteristics and calculated values of RI and SRR for each CPT within zone 3. Similar trends can be identified in this zone that were noticed in the previous 2 zones assessed. The raveling indices range from 0.92 to 0.11 and the general decreasing trend of RI seem to correlate with the increasing SRR values (as shown in Table 5). However, in this zone, there are several cases where a CPT produces a SRR value of much less concern than the respective RI produces. Such an example can be seen in CPT 1-4. The RI calculated for this test is 0.39, which is above the average for this zone. The respective SRR calculated, however, is 3.70, which is clearly does not follow the trend of increasing SRR as RI increases (seen in the color representation of cells [4] and [5]. Much like zone 1, this is because the measured tip resistance values in CPT 1-4 are larger than other tests with the same encountered raveling thicknesses (i.e. CPT-62).

Two created subsurface q_c profiles from Zone 3 area presented in Figures 4-14 and 4-15. Figure 4-14 is the representation under line A-A, and shows the most significant change in encountered limestone depth and raveled soil severity. Figure 4-15 is the subsurface profile under line C-C', and shows much less variation in soil stratigraphy, although only approximately 90 feet away from line A-A'. This large variation in encountered soil strength and stratigraphy is the perfect example of why a thorough site investigation is needed for projects within Karst Terrain.

Table 5: Zone 3 raveling characteristics from each CPT.

Zone 3 - Bridge Area	*Thickness (ft)*		*Measured q_c (TSF) average*		σ_v' *(TSF)*	RI [4]	SRR [5]
CPT	*Overburden*	*Raveled*	*Overburden*	*Raveled*			
CPT-51a	55.94	51.67	99.35	13.60	1.86	0.92	0.66
FDOT-8	68.41	54.46	134.51	25.84	2.14	0.80	0.94
CPT-23	67.42	46.26	129.55	14.13	2.17	0.69	0.96
CPT-55	72.83	40.69	121.94	9.60	2.41	0.56	0.98
CPT 1-1	44.78	21.82	133.22	21.22	1.37	0.49	2.31
CPT 1-2	51.67	21.66	82.42	19.79	1.73	0.42	1.41
CPT-62	37.73	14.93	128.55	16.62	1.40	0.40	2.62
CPT 1-4	43.14	16.74	165.77	26.43	1.34	0.39	3.70
CPT 1-6	43.80	15.26	86.73	13.72	1.36	0.35	2.12
CPT-24	42.32	13.95	112.70	18.80	1.34	0.33	2.98
CPT-53	48.72	14.60	95.80	8.01	1.65	0.30	2.11
CPT 1-3	54.30	16.24	115.59	33.92	1.74	0.30	2.87
CPT 1-7	35.76	9.68	119.11	17.17	1.42	0.27	3.55
CPT-58	37.57	9.35	112.64	17.72	1.33	0.25	3.95
CPT-54	39.21	9.51	122.96	21.39	1.43	0.24	4.15
CPT-61	42.65	10.01	104.91	10.93	1.48	0.23	3.32
CPT-52	58.23	12.31	104.48	14.68	1.95	0.21	2.88
CPT-18	50.52	9.68	80.84	24.81	1.69	0.19	3.26
CPT-56	65.94	12.14	129.68	25.32	2.23	0.18	3.78
CPT-22	52.49	7.71	88.80	27.30	1.70	0.15	4.64
CPT-60	51.02	7.21	115.04	17.54	1.73	0.14	5.42
CPT-57	42.32	4.76	123.07	13.62	1.49	0.11	8.13
CPT-59	58.23	6.40	100.86	22.35	1.94	0.11	5.77

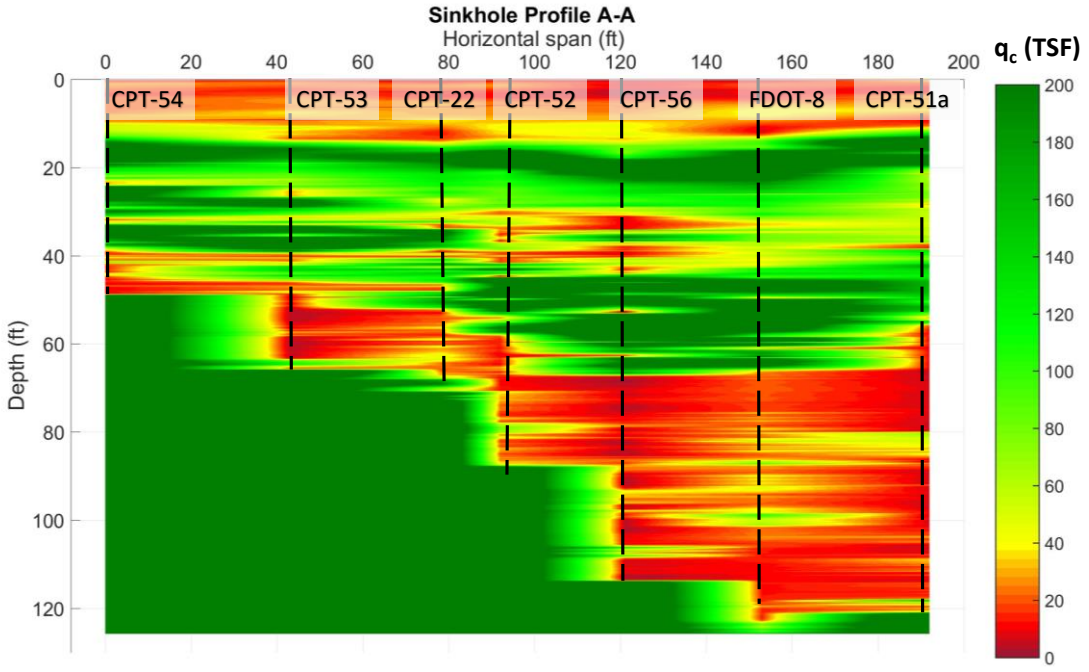

Figure 4-14: Raveling soil profile for line A-A' under zone 3

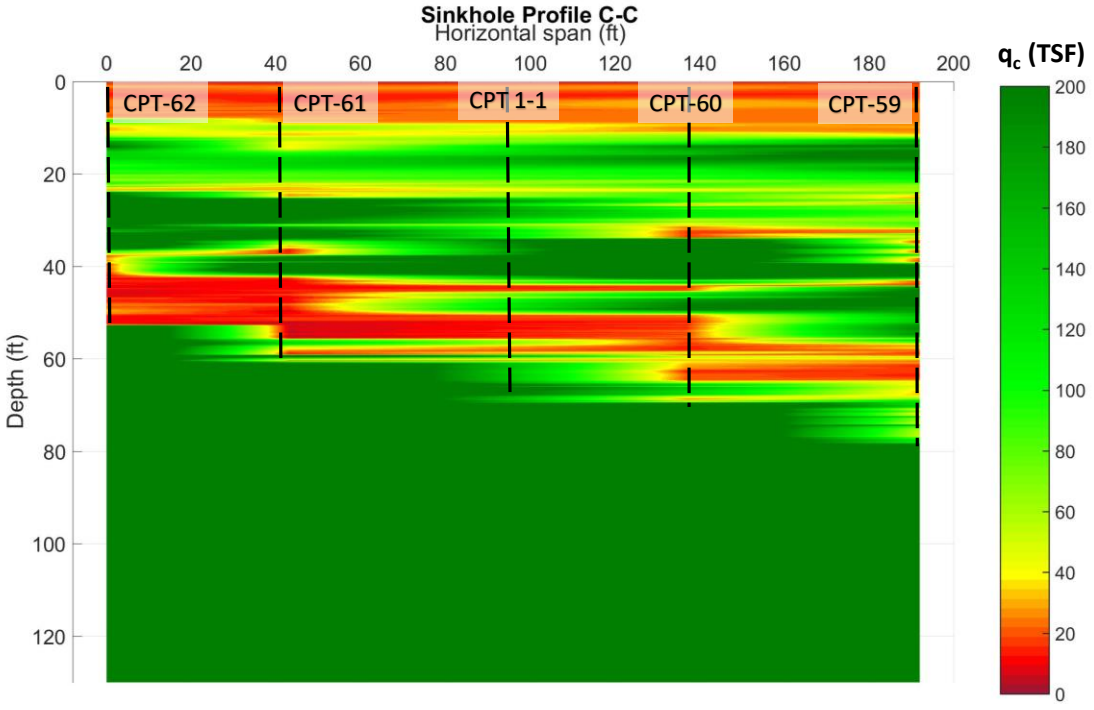

Figure 4-15: Raveling soil profile for line C-C’ under zone 3

4.5 Conclusions

This chapter presented specific tools which can be used to analyze CPT results for assessment of sinkhole risk. The point based method can be used to estimate how severe the encountered raveling is and how much soil may simulate a void. This technique requires assumptions of soil unit weight to correct the measured q_c and R_f for overburden stresses. The theory of soil arching stresses is also applied to this analysis; assuming the granular material above the void forms a structural arch to transmit the overburden stresses around the weaker layer. Although many assumptions were needed for development of the CPT-based raveling severity chart, the resulting chart predicted with great accuracy the depth at which a CPT sensor fell of the cone rods due to the extremely low-resistance soils it was penetrating through.

Subsurface imaging was also presented as a tool for sinkhole risk assessment by viewing multiple CPTs along a profile line in a suspected sinkhole anomaly. This technique can help identify areas with large variation in soil stratigraphy and resistance values which suggests the encountered soil in that area may be disturbed from its original formation. Although only basic linear interpolation was performed for the subsurface profiling in this study, trends in the limestone interface and the raveled soils can still be identified and used to estimate the expanse of subterranean anomaly. These profiles can then be accumulated for each area to approximate the best mitigation technique or to estimate the amount of mitigation needed to safely cover the problematic soils.

Also in this chapter an update to the currently used Raveled Index was proposed. The coined “sinkhole resistance ratio” includes the influence of tip resistance values with the encountered thicknesses of the raveled and the competent overburden soils from CPTs.

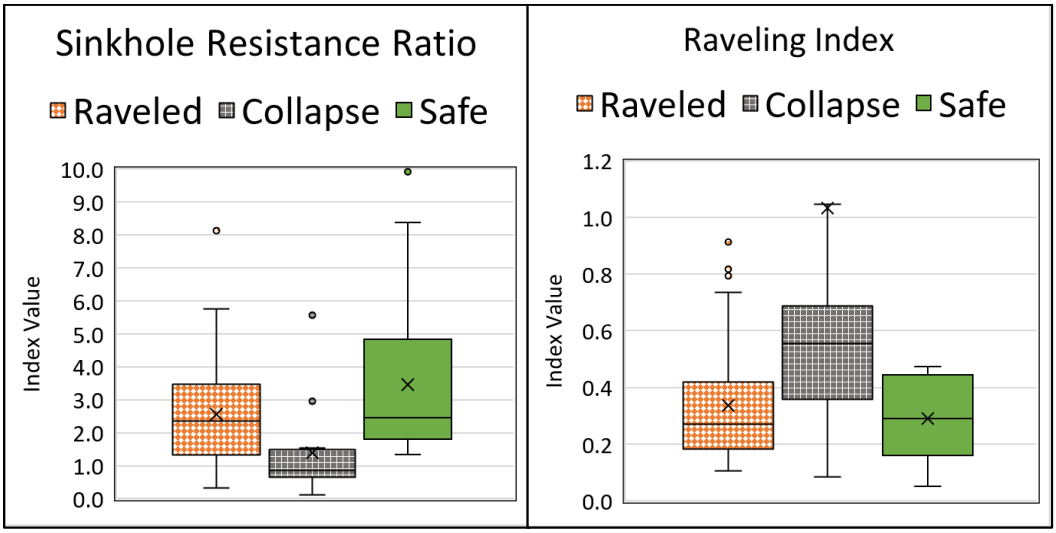

Figure 4-16: Box and whisker plots comparing SRR and RI values for raveled, collapse, and "safe" CPTs performed at both Wekiva and the central Florida collapse sites.

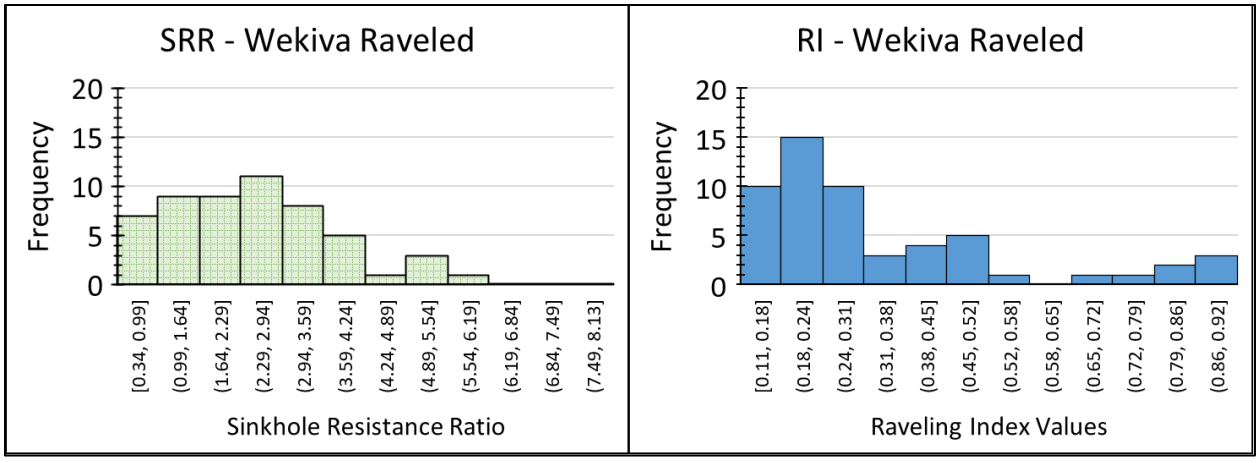

Figure 4-17: Histograms comparing SRR and RI values for raveled CPTs performed at Wekiva project

The resulting index value provides the relative resistance to sinkhole formation from each CPT; that is, the higher the SRR, the less risk of sinkhole formation from the single CPT. The two indices were compared for all CPTs at both the Wekiva parkway project and the sinkhole collapse study sites, shown in Figure 4-16. When comparing the two groups of data, it is apparent that the

sinkhole collapse site indices are more severe than those at calculated from the Wekiva CPT raveled and “safe” data. This is expected since, despite the evidence of raveled soil, no collapse or subsidence has been recorded at the Wekiva parkway study site. The box and whisker plots in Figure 4-16 also suggests that the SRR index better represents the risk of sinkhole due to raveling collapse since upper and lower quartiles of data in the “safe” SRR values does not coincide with same range from the CPTs within the collapse sites. Adversely, the box and whisker plots showing the Raveling Indices from collapse and “safe” CPTs shows a large overlap of data between the two. Figure 4-17 shows a comparison of SRR and RI values at wekiva from the raveled CPTs in a frequency histogram chart. Although limited by the number of CPTs and subsequent values for each index (55 tests), we see that the SRR histograms seem to be more normally distributed. The distribution of SRR values will allow for a more accurate confidence interval to be set in future works, creating a method of comparing future CPT tests which may be performed at or near the Wekiva parkway project.

CHAPTER 5: SUMMARY AND CONCLUSIONS

As discussed in the previous chapters, the work performed in this thesis was aimed in addressing sinkhole detection and risk assessment in central Florida's karst terrain. Particularly, the main interest was to produce and evaluate methods in which CPTs can be implemented to better understand the risk, or severity, of any subterranean sinkhole formation. These techniques can provide central Florida engineers a valuable tool when assessing sinkhole formation risk during site characterization or when determining what type of mitigation action should be performed for soil improvement—if any at all.

The following is a summary of the methodology and resulting assessment tools presented throughout the study.

In the literature review, central Florida's geologic history and resulting characteristics are explained. The review also includes an extensive description on the mechanism and formation of the different types of sinkholes commonly found in the central Florida region. A brief background on Cone Penetration Testing is also presented with focus on the lack of current research performed on CPT data within Karst terrain. CPTs, when used properly in conjunction with SPTs, are a much more reliable and quicker test and can aid in site characterization while decreasing the time needed for drilling. Although severely limited by soil density, CPTs are ideal for detecting discrete soil horizons in central Florida's silty and clayey fine sand over burden. The ability to detect slight changes in soil density with depth allow for a more accurate representation of soil stratigraphy from each test. Further analysis can then be performed to estimate the encountered soil type using SBT charts produced by past and current researchers. These charts, however, should be used in caution especially when testing in residual soils

underlain by karst bedrock with large amounts of groundwater flow. The assumption that soil density increases with depth is not always the case in karst landscapes due to the internal erosion of overburden soils from the natural recharge of water into the deeper aquifers. That is why this study aims to develop methods to identify the eroded (raveled) soils which may cause potential excessive settlement or collapse in the future.

Within chapter 3, the raveling mechanism and criteria is explained in detail. Also, briefly presented in this chapter is the current method used by Central Florida engineers to evaluate the potential of sinkhole formation from a single CPT q_c curve; termed the raveled index by Foshee and Bixler in 1994. The methodology of collecting and preparing the CPT data in this study is presented as well as a description of the geology of the four sites studied. Since comparison between different sites is needed for this study, a normalization procedure was presented and followed based on the current CPT research literature. The normalization of measured tip resistance values (Q_{tn}) correct for overburden stresses, allowing raveled soils encountered at varying depths to be compared to one another. Also presented was a method of normalizing friction ratio (F_R) and the subsequent "spiking" anomalies found when doing so in raveled soils, inhibiting data analysis of such F_R values. Therefore, measured sleeve friction (f_s) values were used to develop an updated criterion of raveled soils based on the measured characteristics from known sinkhole sites. The results of filtering and correlating the CPT database of sinkhole active sites within similar geologic formation is summarized in the CPT-based raveling chart (Figure 3-18). This chart can be used to identify CPTs which encounter significant layers of raveled soils. By plotting all the CPT data on the proposed raveling chart, engineers can see how much of the subsurface soil is raveled and use this information to establish a hazard potential of sinkhole.

Another subsequent finding from the CPT sinkhole database processing is the strong correlation of negative sleeve friction values in raveled material. Although not fully characterized by this study, this finding should be further investigated to determine the exact cause, and resulting meaning, of any measured negative sleeve friction values obtained at depths where raveling is suspected to be occurring.

Chapter 4 presents several additional tools which can be used to analyze CPTs and aid in characterizing sinkhole potential. Techniques include a 1D assessment using a single CPT, a 2D subsurface profiling system to view any subterranean raveling formations as well as identify soil stratigraphy which may be indicative of sinkhole formation, and two indices which can be calculated to compare several CPTs within the same site or within various sites.

The 1D assessment uses the same normalization equation presented in chapter 3 to correct for the vertical effective stresses. Based on the assumption that the granular soil is in equilibrium, the measured tip resistance from CPT (q_c) should be greater than the effective vertical and horizontal stresses. Therefore, when the resulting normalized tip resistance values (Q_{tn}) is negative, then that means the soil penetration resistance is smaller than the effective vertical stress felt at that depth within. This occurrence can be explained by the theory of soil arching in granular material first presented by Terzaghi in 1943. Soil arching occurs when granular material above a void transmits the vertical stresses horizontally through the soil around the void. This occurrence creates an increase in horizontal stress above the void, then an inverse profile of decreasing horizontal stress as the depth within the void increases. A chart was developed based on this principle to create a relationship between measured tip resistance values (q_c) and their corresponding critical depths at which the vertical stresses created from the overburden soils

would be a larger value. This chart (Figure 4-4) can be used to further characterize any encountered raveled soils using the criteria mentioned in the previous chapter. The characterization of raveled material using the 1D technique was validated by not only SPT borings showing severe signs of raveling, but also a case when a CPT probe fell off the pushing rods due to the lack of support underneath the penetrated soil. This CPT was performed within feet of a collapsed sinkhole, therefore the drastic decrease in tip resistance was concluded to be due to the severely raveled soils in which caused the nearby cover collapse sinkhole.

Further assessment tools for sinkhole risk presented in chapter 4 are two indices which provide a quantifiable way of comparing soil raveling per test or per site. These indices can then be correlated to sinkhole formation risk with further investigation of possible sinkhole mechanism parameters (i.e groundwater recharge rates). Limitations of the current Raveling Index are presented in this section and details on how to update the index is cumulated to what was coined as the Sinkhole Resistance Ratio. The SRR provides a relative value for resistance against sinkhole formation from that particularly tested CPT q_c-curve. Unlike the raveling index, the SRR is a function of the average tip resistance within the overburden and the raveling soils. The SRR formula was developed by modeling underground voids using FEM, and by comparing results of physical sinkhole formation modeling, to determine what soil parameters are the most crucial to sinkhole stability collapse. It was determined that an increase in the strength of both the raveled and the overburden soil will increase the stability of the underground void. Also, the deeper void is encountered, the larger the resulting collapse would be if stability is breached. These findings are reflected in the SRR formula (page 70).

A complete assessment using the previously discussed tools was then performed to view and characterize the sinkhole anomalies encountered within three zones at the Wekiva Parkway SR 46 connector project. Although sinkhole mitigation techniques were already performed at these locations, the presented assessment helps to validate the suspected sinkhole anomalies as well as the procedures used for mitigation. Resulting indices calculated from the active sinkhole collapse sites can then be compared to new sites in karst geology to help establish a risk of future sinkhole. A comparison of RI and SRR values between the Wekiva parkway and the central Florida sinkhole sites suggests that the sinkhole activity encountered at the Wekiva parkway site is not as severe as the initial mitigation procedures may infer. This finding is based strictly on the encountered soil stratigraphy with no hydrogeological factors included in the evaluation. As mentioned in chapter 1, sinkhole risk is a multidisciplinary field and cannot be fully characterized by viewing a single aspect. An additional investigation on groundwater movement is currently underway to characterize sinkhole risk based on groundwater movement data to be incorporated with the CPT-based risk assessment procedures. However, the results from this study still can aid when estimating the current sinkhole risk for a project site in Central Florida.

5.1 Limitations

Limitations encountered while performing this study include:

1. Cone penetration testing data collected was performed over a 7-year span. Therefore, proper calibration of the cone or validation of the testing procedure could not be verified by the researchers.
2. Survey elevations were not provided for each CPT; therefore, all data was presented as penetration depth and assumptions of constant ground elevation had to be made when creating the 2D subsurface images.
3. Detailed descriptions of the sinkhole collapse sites were not provided. This includes lack of information regarding: exact location of every CPT and SPT performed with respect to the sinkhole; specifics regarding the sinkhole repair procedure performed at each site; and other general details such exact sinkhole coordinates, precipitation data, exact size and depth of formed sinkhole.
4. More SPT borings can provide a stronger verification of suspected raveled zones. Although results were well correlated with the sinkhole occurrence sites, CPTs cannot provide an actual soil sample, used to verify loose raveled sand, therefore CPT analysis should always include ATLEAST one SPT for ground truthing.
5. CPT-based raveling chart is calibrated only for one geologic formation in Central Florida. Although this formation spreads through the majority of the urbanized areas within central Florida, further investigation should be performed in other geologic formations to either validate, or update, this study's results.

5.2 Recommendations for Future Research

The following recommendation may be useful for future studies:

1. CPTs equipped with a piezocone (CPTu) may provide valuable information on stratigraphy within karst geology. Sinkhole formation is strongly related to recharge rate and groundwater flow through soil, therefore CPTu testing may provide valuable information regarding raveling severity and subsequent sinkhole risk for site characterization.
2. Laboratory testing using a CPT cone with controlled soil types and densities can help calibrate or validate the results of this study. Especially for the normalization protocol and to test the theory of soil arching stresses being detected in the CPT q_c data.
3. CPTs performed over a span of time in the same spot may add valuable information regarding rate of erosion and growth of sinkhole formation. The resulting subsurface images and raveling and resistance ratios can then be viewed over time to estimate progression and better establish a risk of potential sinkhole collapse.
4. Analysis of additional types of subsurface testing, or modifications of CPT, may be worth investigating for further means of identifying and characterizing premature sinkhole raveling zones. Such tests include: pressure-meter tests (PMTs), dilatometer tests, or CPTs equipped with soil grain-size viewing cameras. These tests may be able to further verify the loose/disturbed hawthorn group of soils by performing soil strength tests at static depths.
5. Monitoring of groundwater trends within sinkhole active sites can better characterize the rate of erosion or seepage forces which induce raveling of the sandy residual soils. Laboratory tests to determine the critical shear stress causing soil particle detachment

should be performed on *undisturbed* soil samples to establish the sites susceptibility to sinkhole formation. This investigation will aid in creating a database of sinkhole soil properties throughout central Florida.

LIST OF REFERENCES

ASTM Standard D5778. (2012). Standard Test Method for Electronic Friction Cone and Piezocone Penetration Testing of Soils. West Conshocken, PA, United States: ASTM International.

Beck, B. F., & Sinclair, W. C. (1986). *Sinkholes in Florida.* Orlando: U.S. Geological Survey.

Bloomber, D., Upchurch, S. B., Hayden, M. L., & Williams, R. C. (1988). Cone-penetrometer exploration of Sinkholes: Stratigraphy and soil properties. *Environmental Geology* , 99-105.

Bullock, P. J., & Dillman, A. (2003). Sinkhole Detection in Florida Using GPR and CPT. *Presented at the 3rd International Conference on Applied geophysics, Hotel Royal Plaza.* Orlando.

Craig, W. (1990). Collapse of cohesive overburden following removal of support. *Can. Geotech Journal*, 355-364.

Department of Geological Sciences & Engineering. (2006). Subsurface Exploration Using the Standard Penetration Test and the Cone Penetration test. *Environmental & Engineering Geoscience*, 161-179.

Douglas, B. J., & Olsen, R. S. (1981). Soil Classification Using Electric Cone Penetrometer. *Symposium on Cone Penetration Testing and Experience, Geotechnical Engineering Division, ASCE.* St. Louis, Oct. 1981.

Edward D. Zisman, a. D. (2013). If It's Weight of Hammer conditions, it must be a sinkhole? *13th Sinkhole Conference* (pp. 45-52). Carlsbad, New Mexico: National Cave and Karst Research Institute.

FGS. (2001). *Text to accompany the Geologic Map of Florida.* Tallahassee: Florida Geological Survey.

Fischer, J. J., & Fischer, J. A. (2015). Concepts For Geotechnical Investigation in Karst. *14th Sinkhole Conference* (pp. 549-557). Rochester: NCKRI Symposium 5.

Florida Geological Survey. (2001). *Text to Accompany the Geologic Map of Florida.* Tallahassee, Florida: Florida Geological Survey.

Florida Office of Insurance Regulation. (2010). *Report on Review of the 2010 Sinkhole Data Call.*

Foshee, J., & Bixler, B. (1994). Cover subsidence sinkhole evaluation of State Road 434, Longwood Florida. *ASCE Journal of geotechnical Engineering*, 2026-2040.

Gray, K. M. (1994). *Central Florida Sinkhole Evaluation.* Deland, FL: Florida Department of Transportation.

Kim, Y., Xiao , H., Wang, D., Choi, Y. W., & Nam, B. H. (2017). Development of Sinkhole Hazard mapping for Central Florida. *ASCE Geofrontier*. Orlando.

Meyerhof, G. G. (1956). Penetration Tests and bearing Capcity of Cohesionless Soils. *Soil Mechanics Foundation Division, ASCE*.

Moss, R., Seed, R., & Olsen, R. (2006). Normalizing the CPT for Overburden Stress. *Journal of Geotechnical and Geoenvironmental Engineering*.

Olsen, R. S., & Malone, P. G. (1988). Soil classification and site characterization using the cone penetrometer test. *Penetration Testing* , 887-893.

Perez, A., Nam, B., Chopra, M., & Sallam, A. (2017). Understanding of Florida's sinkhole hazard: A hydrogeological laboratory study. *ASCE Geofrontier.* Orlando.

Professional Services Inc. (2014). *Sinkhole and Engineering Evaluations Wekiva Parkway and State Road 46 Connector Road Interchange.* Orlando, Florida: Florida Department of Transportation.

Professional Services Industries, Inc. . (2014). *Sinkhole and Engineering Evaluations Wekiva Parkway and State road 46.* Orlando.

Riaund, J.-L., & Miran, J. (1992). *The Cone Penetrometer Test.* Washington, D.C.: FHWA.

Rizzo, R., & Dettman, M. (2017). Sinkhole Early Detection System. *Geofrontiers.* Orlando: ASCE.

Roberston , P., & Cabal, K. (2010). Estimating soil unit weight from CPT. *2nd Internation Symposium on Cone Penetration Testing.* Huntington Beach, CA.

Roberston, P. (1990). Soil Classification using the Cone Penetrometer test. *Can. Geotech. J.*, 151-158.

Robertson, P. K. (2010). Soil Behaviour type from the CPT: an update.

Robertson, P. K. (2016). Cone Penetration test (CPT)-based soil behavior type (SBT) classification system - an update. *Can. Geotech Journal*, 1910-1927.

Robertson, P. K., & Wride, C. E. (1998). Evaluating cyclic liquefaction potential using the cone penetration test. *Canadian Geotech Journal*, 442-459.

Rupert, F., & Spencer, S. (2004). Florida's Sinkholes. *Poster 11*. Tallahassee, Florida: Florida Geological Survey, Department of Environmental Protection.

Sanglerat, G. (1972). *The Penetrometer and Soil Exploration.* Amsterdam: Elsevier Scientific .

Schmertmann, J. H. (1978). *Guidelines for Cone Penetration Test, Performance and Design.* Washington D.C.: FHWA.

Shamet, R., Gray, K., & Nam, B. (2017). Sinkhole Risk Evaluation by Subusrface Cone Penetration Test. *Geofrontier* . Orlando: ASCE.

Shamet, R., Nam, B., Soliman, M., & Rajabi, A. (2017). Sinkhole risk evaluation: Detection of raveled soils in Central Florida's karst geology using Cone Penetration Testing. *ASCE Georisk.* Denver: American Society of Civil Engineers.

Sheets, R. A. (2002). *Use of Electrical Resistivity to Detect Underground Mine Voids in Ohio.* USGS Numered Series.

Sinclair, B. F. (1986). *Sinkholes in Florida.* Orlando: The Florida Sinkhole Research Institute.

Sowers, G. (1996). Building on Sinkholes: Design and construction of foundations in karst terrain. *ASCE*, New York.

Terzaghi, Peck, & Mesri. (1943). *Soil mechanicas in engineering practice.* New York: John Wiley & Sons, Inc.

Tihansky, A. B. (1999). *Sinkholes, west-central Florida.* United States: U.S. Geological Survey Cirvular 1182, p. 121-140.

Tu, T. (2016). *Sinkhole Monitoring Using Groundwater Table Data.* Retrieved from Electronic Thesis and Dissertations: http://stars.library.ucf.edu/etd/5236

Weary, D. J., & Doctor, D. H. (2014). *Karst in the United States: A digital map compilation and database: U.S. Geological Survey Open-File Report* . https://dx.doi.org/10.3133/ofr20141156.

Wilson, L. W., & Beck, F. B. (1992). Hydrogeologic Factor Affecting New sinkhol Development in the Orlando Area, Florida. *National Ground Water Association* (pp. 918-930). Blackwell Publishing Ltd.

Xiao, H., Kim, Y., Nam, B., & Dingbao, W. (2016). Investigation of the impacts of local-scale hydrogeologic conditions on sinkhole occurence in East-Central Florida, USA. *Environmental Earth Sciences.*

Zhou, W., & Beck, B. F. (2008). Management and mitigation of sinkholes on karst lands: an overview of practical applications. *Environmental Geology*, 837-851.